# Watershed Assessment Model (WAM) : Calibration and Uncertainty and Sensitivity Analyses

## Task 1.1: WAM Simulated Existing Conditions Characterization Report and Model Validation Report - Final

Soil and Water Engineering
Technology, Inc.

September 4, 2015

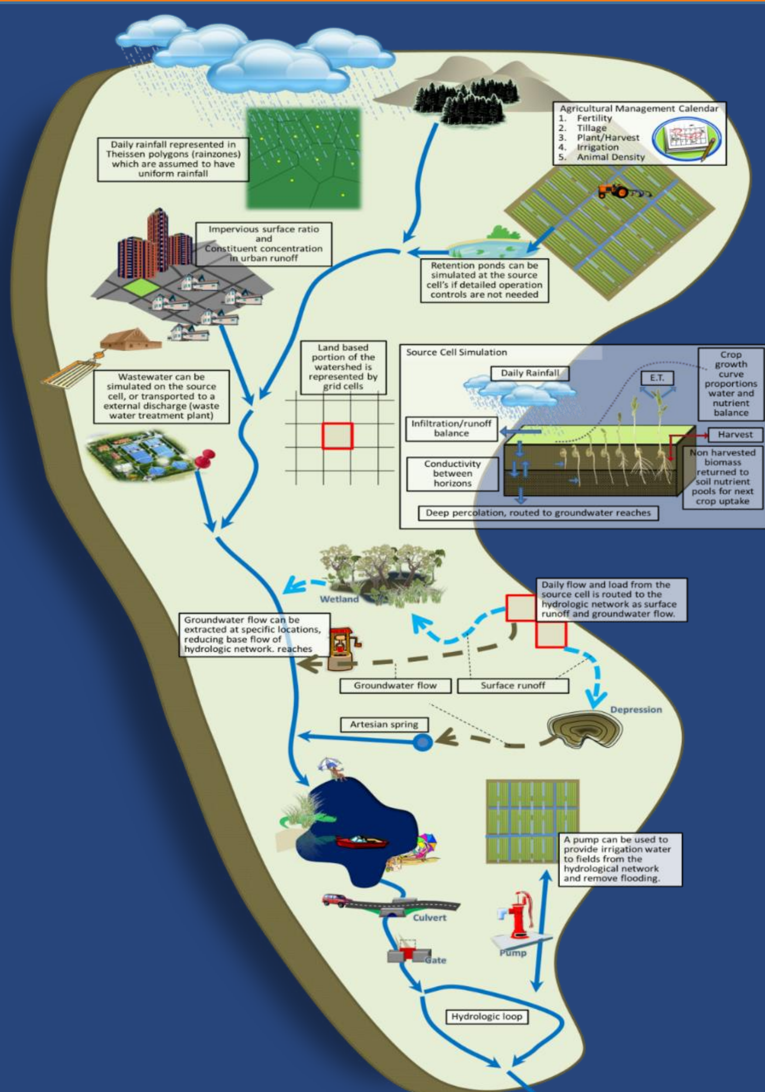


FDACS Contract No. 022589

# Table of Contents

# Table of Tables



# Table of Figures

# 1 Introduction and Background

## 1.1 Introduction

The ecological health of Lake Okeechobee and its associated influence on downstream waterbodies, such as coastal estuaries and the Everglades, has been the focus of much research and management activities for decades. Phosphorus loads to the lake are the primary concern because they have been identified as the dominant cause of increased eutrophication within the lake. However, total nutrient loads and excessive freshwater releases from the lake to coastal estuaries are also a concern. The phosphorus sources and potential abatement strategies to meet phosphorus reduction targets for Lake Okeechobee are summarized in the December 2014 adopted Basin Management Action Plan (BMAP). The Watershed Assessment Model (WAM) was an integral tool used for the development of the load estimations described in the BMAP, and moving forward will be used to help assess the cost benefits of alternative abatement strategies.

To enhance the WAM tool for future use, Soil and Water Engineering Technology, Inc. (SWET) was contracted by the Florida Department of Agriculture and Consumer Services (FDACS) (Contract #021095) to address the following objectives: 1) to update and recalibrate WAM to existing conditions using the latest land use, soils, hydrography, control projects, and weather databases; 2) to complete detailed sensitivity and uncertainty analyses to verify and quantify the functionality of the model and to identify potential model enhancements to improve its predictive capabilities; 3) and to complete a goodness of fit assessment for a representative sub-watershed to validate its utility. This report describes the work completed under Task 1, entitled "WAM Simulated Existing Conditions Characterization Report and Model", of the above referenced contract, which includes a brief background of the WAM model and the results of the Task 1.

## 1.2 Background

WAM was developed to evaluate the impact of alternative land uses and management practices associated with the implementation of best management practices (BMPs) and nutrient load reduction projects for the Lake Okeechobee Watershed (LOW). It is a process-based model that can be used to perform hydrological and water quality analysis to:

- Simulate flows and nutrient loads for existing land uses, soils, and land management practices.
- Analyze the hydrological and water quality impacts on streams and lakes for management scenarios, such as land use changes, implementation of BMPs or the addition of regional stormwater treatment areas (STAs).
- View and analyze the simulated flow and concentrations for every source cell and stream reach within the LOW under the ArcGIS platform.
- Prioritize geographical areas where BMP efforts are to be focused.

The South Florida Water Management District (SFWMD), the Florida Department of Environmental Protection (FDEP), and the Florida Department of Agriculture and Consumer Services (FDACS), hereinafter collectively referred to as the Coordinating Agencies, have identified WAM as the best tool for performing such analyses in the LOW.

Some examples of WAM applications include:

- Evaluation of various phosphorus (P) and nitrogen (N) control programs within the LOW.

- Evaluation of total phosphorus (TP) and total nitrogen (TN) load reductions under agricultural BMPs, which were included in the 2011 Lake Okeechobee Watershed Protection Plan (LOWPP).
- Simulation of existing and pre-drainage flows, concentrations, and loads for the Lake Okeechobee Pre-drainage Characterization Project, which was contracted by the SFWMD to SWET.
- Refinement of existing loads, project load reductions, and monitoring locations, associated with the Lake Okeechobee BMAP, which was developed by the Coordinating Agencies in collaboration with the local stakeholders.
- Assessment of temporal and spatial loading patterns for inclusion in the BMAP refinement process.

The Coordinating Agencies invested in improving the tool through the WAM Enhancement and Application in the Lake Okeechobee Watershed Project (2009). This report is the result of Task 1: WAM Simulated Existing Conditions Characterization Report and Model Validation Report.

## 1.3 Objectives

The primary objective of Task 1 is to update the earlier application of WAM to the Lake Okeechobee sub-watersheds north of Lake Okeechobee. The WAM Enhancement and Application in the Lake Okeechobee Watershed Project (2009) used a rainfall period of record (POR) between 1998 and 2007 for model calibration. This model was rerun without calibration for the extended period of record of 1975 through 2010 (HDR, 2012). In the intervening period, a number of datasets have received significant updates. These updates were obtained from the SFWMD and incorporated into WAM. These datasets include land use, hydrography (AHED), topography from LIDAR (Light Detection and Ranging), drainage boundary, rainfall, flow, hydraulic structure, and TP and TN concentration data. The main focus of the reported work was to extend the POR through the end of 2013 using the latest available rainfall, temperature data, and other meteorological data. Simulations using WAM were conducted on the updated existing conditions for all of the basins north of Lake Okeechobee located in the following sub-watersheds:

- Fisheating Creek
- Lake Istokpoga
- Indian Prairie
- Upper Kissimmee
- Lower Kissimmee
- Taylor Creek/Nubbin Slough

The existing conditions used the 2009 SFWMD land use coverage, as updated in 2013, for the LOW. The model was also updated to the latest version of ArcGIS being used by the Coordinating Agencies (ArcGIS 10.2.2). Simulation data are reported and analyzed on a daily, monthly, annual, and five-year rolling average basis to determine flows, TP and TN concentrations, and P and N loads from each of the six (6) sub-watersheds north of Lake Okeechobee (see Figure 1). The model domains were modified to be consistent with the most current sub-watershed boundaries provided by the SFWMD. Shoreline reaches for all major lakes to separate flow and loads from source cells that directly discharge to the lake and other reaches draining to the lake have been added to the model as this information is useful for budget analyses.

The WAM outputs for the existing conditions were compared to actual measured data to provide a preliminary goodness-of-fit standard Nash-Sutcliffe Efficiency (NS) error statistics and five-year rolling average time intervals.  The model was run from 1975 through 2013; however, the validation period was limited to 2003 through 2013 because the existing land use conditions are most representative for this period. The results of the WAM simulations are summarized on a daily, monthly, annual, and five-year rolling average for flow, TP and TN concentrations, and TP and TN loads. In addition, a qualitative evaluation of the goodness-of-fit standard error analysis was completed that has resulted in the recommendation to the Coordinating Agencies that a recalibration of the model will be required to provide significant improvements to the simulations. The basis for this recommendation to recalibrate including success criteria and a discussion of the relative performance of the model for the additional period simulated against the previous calibration validation period will be described in greater detail below.  Upon concurrence by the Coordinating Agencies, SWET shall proceed with the recalibration process as further detailed under Task 3.

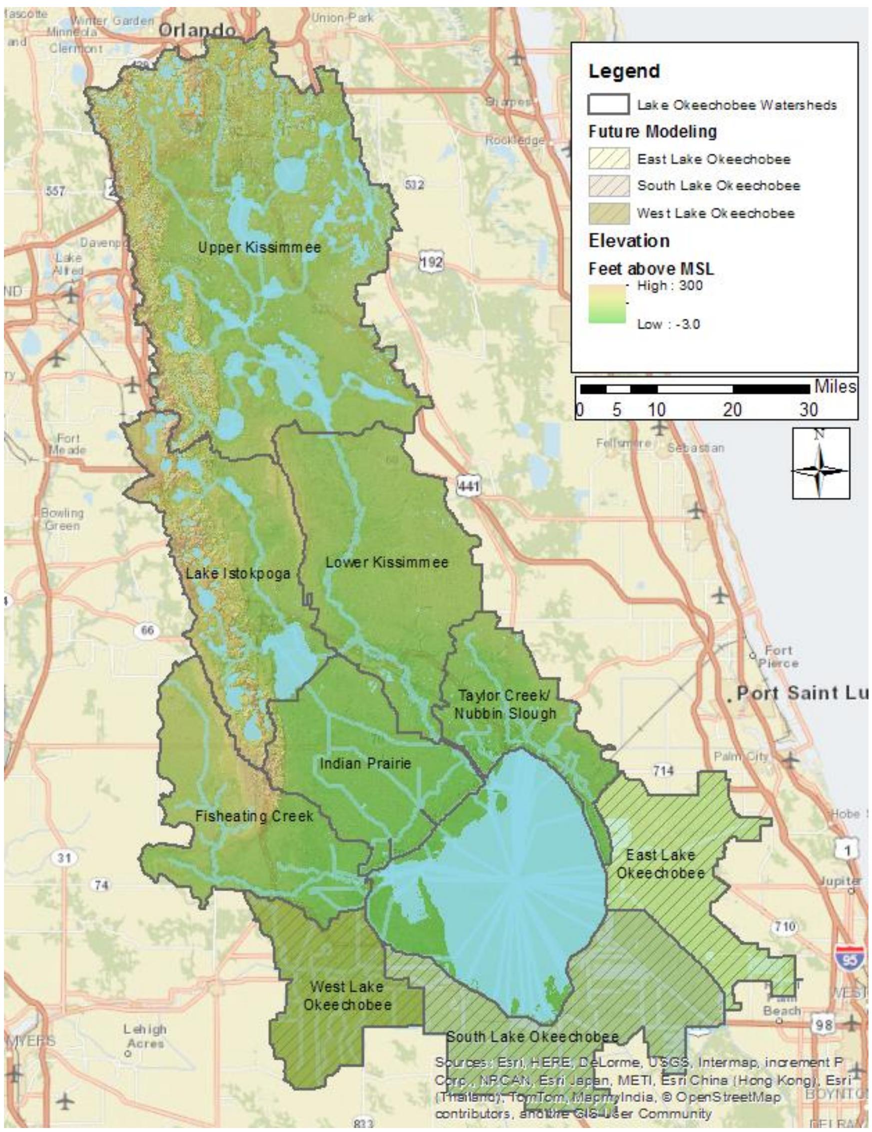


**Figure 1.  Location of the six Lake Okeechobee sub-watersheds that were modeled for the project.**

# 2 The Watershed Assessment Model

## 2.1 Model Approach

The WAM was chosen to simulate the water quantity and quality discharged from the project area because of its ability to simulate a wide variety of land uses and land use practices while taking into account the geographic and geologic features of the land. WAM uses a GIS grid-based representation to model the physical characteristics of the watershed. One of the first steps is the determination of the specific combination of land use, soil, rainfall, and wastewater service area for each cell in the watershed (Figure 2). These four datasets are overlain as part of the modeling process to identify the unique combinations of these inputs. These unique cell combinations characterize the specific conditions that occur on each cell within the watershed.

WAM then creates a spatial map and tabular list of every unique combination of the inputs. The concept of identifying unique cell groupings is critical because it greatly reduces the number of cell level simulations that are needed while still providing the detail of cell level simulated flow and constituent transport for every cell within the watershed.

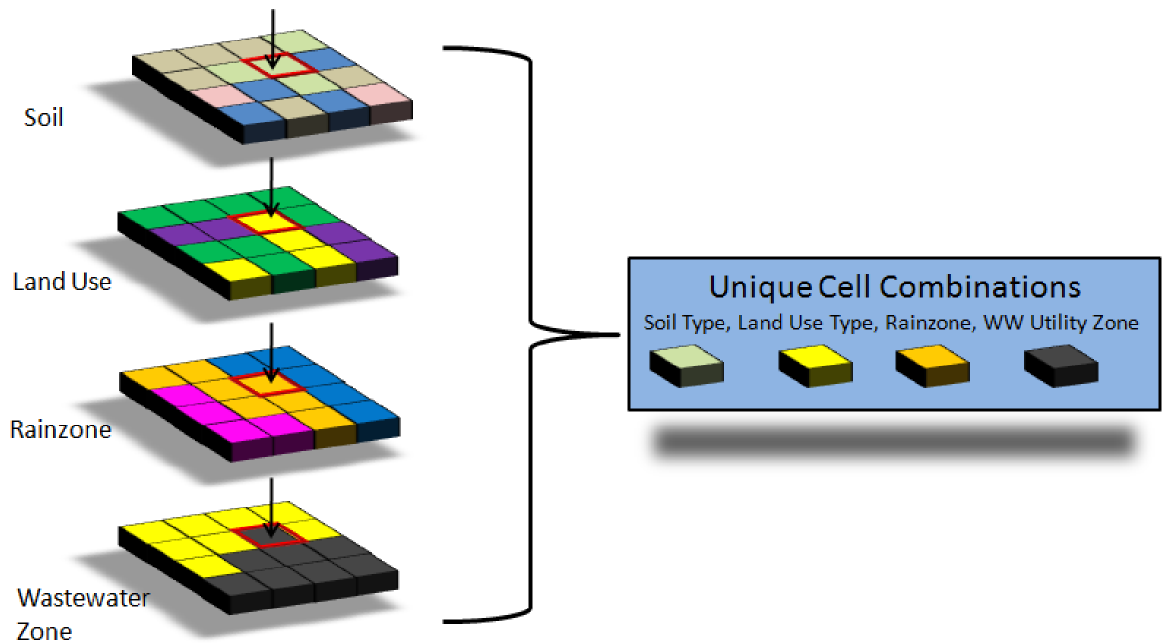


**Figure 2. Unique cell generation.**

## 2.2 Source Cell Modeling

The creation of unique cell groupings is also critical because it allows for the most appropriate field-scale sub-model to be used for each unique cell condition, more accurately simulating the daily runoff in terms of both water quality and quantity. Based on the soil and land use combination of the cell, the most appropriate field scale sub-model is selected to simulate that cell as shown in Figure 3.

The sub-models include Groundwater Loading Effects of Agricultural Management Systems (GLEAMS) (Knisel, 1993), the Everglades Agricultural Area Model (EAAMOD) (Bottcher et al., 1998;

SWET, 2008; Bottcher et al., 2012), and a special-case model written specifically for WAM. GLEAMS is used to simulate processes in areas that have well-drained soils while EAAMOD is used to simulate processes on high water table soils. The special case sub-model is used to simulate source cells that are not handled well by these other two sub-models, e.g. wetlands, mining, aquiculture, and open water. These sub-models are bundled into one Fortran program called BUCShell (BUC stands for Basin Unique Cell).

The individual field scale sub-models used are specifically designed to deal with the particular natural processes that exist between those land use and soils combinations. The daily flows and loads produced by BUCShell are stored in what are referred to as dayfiles and contain the amount of nutrients and water that are leaving each source cell on a daily basis.

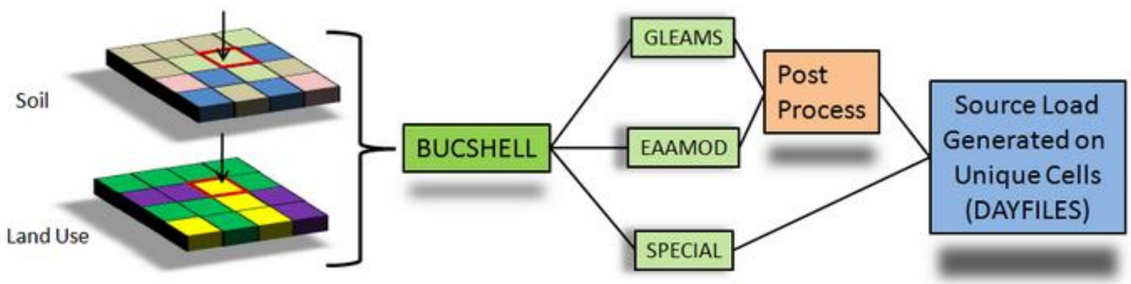


**Figure 3. Field scale model selection process**

## 2.2.1 GLEAMS

GLEAMS (Leonard et al., 1987 and Knisel, 1993) is a physically based model used to simulate processes affecting water quality on an agricultural field scale. It has been used extensively and is well documented. GLEAMS is divided into four separate models. These models include:

1. Hydrology
2. Erosion/sediment yield
3. Chemical (pesticide) transport (not currently available within WAM)
4. Nutrient transport

The hydrology component of GLEAMS simulates runoff due to daily rainfall using a modification of the NRCS curve number method, where ground recharge is calculated as rainfall minus ET/interception and the change in soil storage. Hydrologic computations for evapotranspiration, percolation, infiltration, and runoff are determined using a daily time step (Knisel, 1993). Two options are provided in the hydrology component to estimate potential evapotranspiration.

The Priestly-Taylor evapotranspiration estimation method (1972) using daily temperature and radiation data computed from mean monthly data is currently used by WAM. The other available option in WAM is the Penman-Monteith method (Jensen et al., 1990), however it requires additional data that are more difficult to obtain. Water routing through the soil profile is based on the storage routing concept which allows the downward movement of water in excess of field capacity water content from one layer to the next. Comprehensive detail is provided in Knisel (1993).

The erosion component in GLEAMS uses the universal soil loss equation (USLE) and the concept of continuity of mass to predict erosion and sediment transport under different topographic and cultural conditions. The erosion component considers overland, channel, impoundment, or any combination of these routes. Computation begins at the upper end of the overland slope. The overland flow may be selected from several possible overland flow paths. Its shape may be uniform, convex, concave, or a combination of these slopes. The processes of detachment and deposition are both considered, and each condition occurs based on the relationship between transport capacity of runoff water and sediment load.

The plant-nutrient component of the GLEAMS model considers both nitrogen (N) and phosphorus (P) cycles. For a detailed description of the GLEAMS input parameters see Knisel (1993). The N component includes: mineralization, immobilization, denitrification, ammonia volatilization, nitrogen fixation by legumes, crop N uptake, and losses of N in runoff, sediment, and percolation below the root zone. It also considers fertilizer and animal waste application. The P component includes: mineralization, immobilization, crop uptake, losses to surface runoff, sediment and leaching, and it also includes fertilizer and animal waste application. Tillage algorithms are included in the model to account for the incorporation of crop residue, fertilizer, and animal waste. Soil temperature and soil moisture algorithms are also included in the model to provide proper adjustments for ammonification, nitrification, denitrification, volatilization, and mineralization rates. Rainfall N and P are inputs for the model and may vary depending upon the study region. Initial soil TP, as an input in the land use parameter file, is a sensitive parameter in the model and is used to represent legacy P, which makes it an important calibration parameter. Initial soil TN is not as sensitive as TP because N will not accumulate within the soil.

The GLEAMS model provides outputs of soluble inorganic nitrogen (ammonium-N and nitrate-N) and phosphorus (soluble P) in runoff and leachate and sediment-attached organic and inorganic N and P in surface runoff. The GLEAMS model does not produce outputs of biological oxygen demand (BOD) or soluble organic N and P. Outputs of these constituents are derived within WAM as a function of total suspended solids (TSS) and from total nitrogen loads in runoff and leachate, respectively.

### 2.2.2 EAAMOD

The EAAMOD is a field-scale model developed by Soil and Water Engineering Technology, Inc. (SWET) for multi-layered soils with high water tables. Created in the early 1990s, the model grew out of a need to evaluate agricultural BMPs within the Everglades Agricultural Area (EAA) and other high water table soils in Florida. The model initially focused on water using a hydrography sub-model (WP) and P movement from histosols (flat organic soils) using the P sub-model (PMOVE), but was then expanded to all high water table soils and to handle N with the inclusion of the nitrogen sub-model (NUTMOD). Histosols require special consideration because of the aerobic mineralization releases of both P and N from organic matter due to drainage and the resulting nutrient impacts downstream. To adequately address this problem, EAAMOD simulates water control practices and the impacts of various cultural management scenarios on nutrient transport.

Percolation and runoff in EAAMOD is calculated using a vertical two-dimensional hydrologic model (WP). The flow model within EAAMOD uses the Dupuit-Forcheimer assumption (zero vertical hydraulic gradient) for two separate flow regimes in the field profile, specifically, above and below an impeding layer such as the spodic horizon in flatwoods soils and the marl cap rock in histosols. The impeding layer is generally highly localized, and while water locally perches above the layer it does not act as a confining layer. The model is conceptually represented in Figure 3.

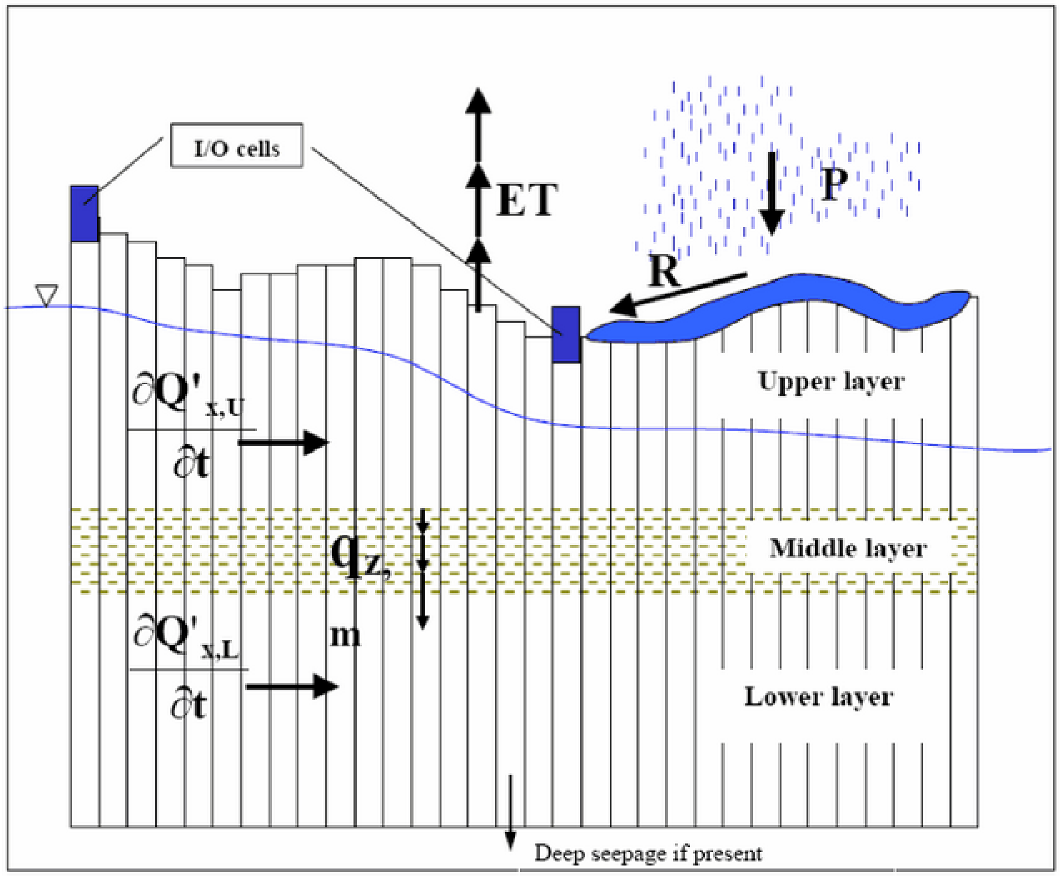


**Figure 4. EAAMOD digitization scheme for a general soil profile.**

The one-dimensional horizontal flow model provides the water table depth and horizontal flow for each cell across the field between drainage ditches. Flow through the spodic horizon is determined by solving the piezometric head distribution below the horizon and then using Darcy's Law across the impeding layer with the gradient across the horizon being the difference between the water table above it and the piezometric head below it. Water flow is simulated by using finite difference techniques with forcing functions representing pumped drainage/irrigation, culvert flow, rainfall and ET. Saturated horizontal flow above the mid- horizon is calculated by a fourth order Runge-Kutta method that solves the continuity equation for each cell using Darcy's Law within the saturated zone.

The water budget is calculated in the top zone of cell *i* by the following equation:

$$\Delta S(i) = Q(i+1) - Q(i) + R(i) - ET(i) - QS(i) + P(i)$$

Where:

$\Delta S$ is the change in water storage in the top zone (inches of air void/hr),

$Q$ is horizontal saturated flow (in/hr),

$R$ is rainfall (in/hr),

$ET$ is evapotranspiration (in/hr),

$QS$ is deep percolation through the middle restricting zone (in/hr), and

$P$ is the forced input or output (irrigation/drainage) (in/hr) for up to two cells, typically ditches.

The calculated flow is always for the left side of the cell indicated. Rather than using total water storage in a cell, the water profile algorithm keeps track of air void volume (S). Therefore a zero value for S would represent a saturated soil condition with no surface ponding. Surface ponding results in a value of S less than zero and typically would indicate that surface runoff is occurring, but could be a stagnant surface storage condition.

The air void volume, S, is calculated for each time step, $t$, by the following equation:

$$S(i,t) = S(i,t-1) + \Delta S(i,t) \cdot \Delta T$$

Where: $\Delta T$ is equal to $t$ (current time in hours) minus $t$-1 (previous time step in hours).

To represent actual water management in a field, a series of utility features within the model allow for controlled drainage through a pump, gravity flow through a culvert (bi-directional), flow over a weir, subsurface or surface irrigation, and variable crop ET parameters. Automatic scheduling of irrigation and drainage pump operation is available based upon desired ditch water levels or soil moisture deficit. The flow properties of the pump(s), culvert(s), or weir(s) for specific land use types can be specified by the user in the management section for High Water Table Soils.

Surface water is only allowed to flow to or from the first defined ditch/drainage outlet cell, but this cell may be located anywhere. For flooding, the water profile algorithm allows flows from the ditch to fill each successive cell to the level of the ditch until the time step's flow volume is depleted. The flow volume is limited by the flow rate to the ditch cell and conservation of mass within the ditch. This procedure continues until complete flooding occurs, at which time any subsequent flow due to a rise in ditch levels will be artificially applied to all cells. For surface runoff the procedure is reversed except that artificial ET is used to move the water from the field and move it to the ditch.

## 2.3 Hydrodynamic Routing

The daily outputs from each cell, which includes surface and groundwater flows and constituent concentrations, are simulated they are routed to the streams by the Basin Land Area to Stream Routing model (BLASROUTE). BLASROUTE is a Fortran program that routes the flows and loads based on the distance grids previously calculated and delayed using separate unit hydrographs and delay factors for surface and groundwater. The constituent loads are attenuated based on the landscape features encountered en route to the reach network. The routing process is a complex combination of transport, dispersion, and assimilation that, in most cases, will result in an attenuation, or decrease, in the constituent concentration. The source loads are transported to the reach network via surface and/or ground water.

The transportation path is based on the distance to the closest downhill hydrogeologic feature (reach, wetland or depression) which is identified from the Distance Grids that are calculated by WAM. The transportation path will influence both the time it takes for daily flows to be delivered to the reach network, as well as the attenuation rates that are applied to the constituent concentrations en route to the reach network, depending on the hydrogeologic features encountered. Figure 5 shows the conceptual routing schemes and flow distances that are calculated for each cell.

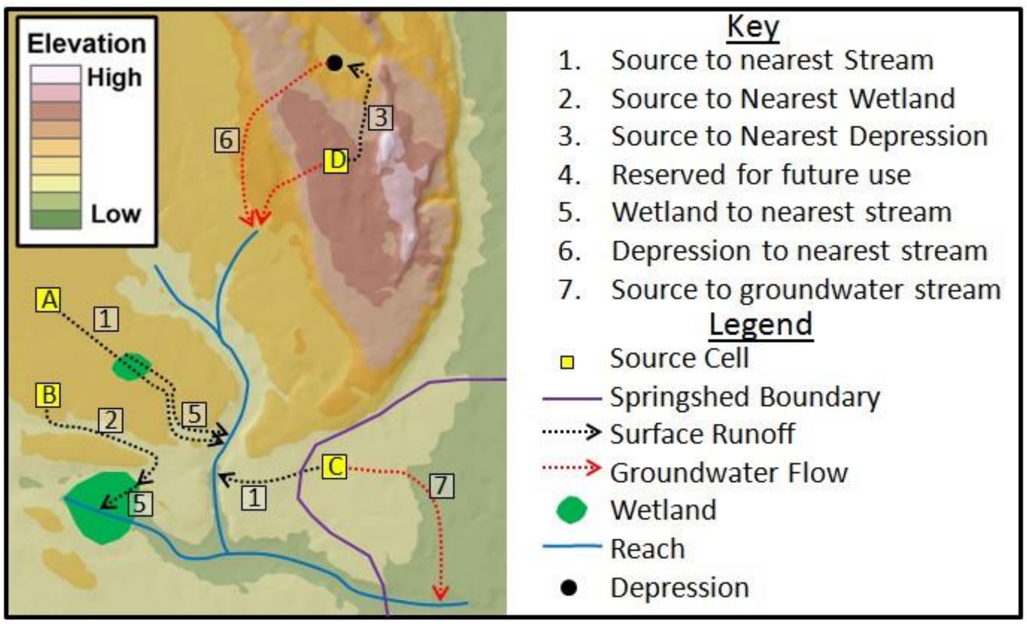


**Figure 5. Flow path routing for attenuation distance determination.**

WAM includes overland and in-stream attenuation algorithms that function on a daily time step starting at the source cell. From this starting point, nutrients are attenuated during both overland flow, when passing through wetlands, and within streams and canals before finally discharging to the lake.

Each numbered path shown in Figure 5 is represented by a GIS grid, which includes the distance of the paths. These distances are related back to the original source cell so that the model can extract the needed distance through a downstream geographic feature for each and every grid cell. Destination information is stored in a similar manner. When extracting the distance through a downstream wetland, for example, the type of wetland can also be extracted, which has an associated set of assimilation coefficients.

# 3 Data Gathering and Formatting

## 3.1 Required Input Spatial (GIS) Datasets

The required spatial datasets are:

- Basin boundary
- Sub-basin boundaries
- Topography
- Hydrologic network
- Land use
- Soils
- Rain gage locations
- Hydrologic structures
- Utility (wastewater) zones.
- Location of water and nutrient point sources (or sinks)
- Irrigation source specification

The specifics of each of these spatial datasets with respect to the entire Lake Okeechobee model domain are discussed below. In addition to these spatial datasets, a time series of recorded rainfall values at each rain station, daily temperatures, and other climate data required to run WAM is also discussed below. Prior to building a WAM scenario, a projection for the spatial data must be chosen. For this project the Florida State Plane East (in feet) was used. Other relevant coordinate system details are shown in Table 1.

**Table 1. Coordinate system selected for the model project.**

| NAD 1983 HARN State Plane Florida East (FIPS 0901) Feet | |
|---|---|
| Projection | Transverse Mercator |
| False Easting | 656166.67 |
| False Northing | 0 |
| Central Meridian | -81 |
| Scale Factor | 0.99994118 |
| Latitude of Origin | 24.33333 |
| Linear Unit | Foot |

## 3.2 Data Acquisition

### 3.2.1 GIS Datasets

Many of the spatial datasets used in the 2009 WAM modeling effort dated from the mid-2000's and have been superseded by newer datasets. In some cases, such as with land use, this reflects actual changes in the underlying data as development occurs or as some agricultural land uses are taken out of production. Some datasets, such as soils, have been updated as studies have been used to refine and further delineate specific soils types. Thus, while the general dataset types outlined in the 2009 report are still applicable, the actual datasets have changed. In many cases the available information is more consistent across the basin and a single feature class may suffice where before several disparate coverages had to be merged to provide an accurate representation. For example, a single topography dataset was provided by the SFWMD whereas for the 2009 project a number of datasets had to be merged to create a comprehensive dataset. Similarly, the hydrography used in 2009 was created from a number of sources; for this project a single hydrography dataset (part of SFWMD's ArcHydro Enhanced Database) covers the entire study area. In a number of cases data from the 2009 study could easily be adapted with only minor modifications (such as basin and subbasin coverages, rainfall stations, and hydrologic structures). However, in a number of other cases, such as soils, land use, hydrography, and the actual model domains, entirely new datasets needed to be incorporated.

The following listing of the spatial datasets indicate the provenance of the various feature classes. Details about the specific preparation, adjustments, and modifications to these input datasets for use within WAM are discussed in Section 3.4.

#### *3.2.1.1 Model Domain Boundaries*

Each model domain boundary serves as the domain for all of the input spatial datasets, with each GIS dataset (with two exceptions, discussed below) clipped to this boundary. The model domains are shown in Figure 6.

Each of the six model domains requires a basin boundary, which were defined to be the sub-watersheds as defined by the Coordinating Agencies. The dataset used was obtained from FDEP in January of 2015 and is named "LOW_Subwatersheds". The LOW includes four major tributary systems: Kissimmee River, Lake Istokpoga–Indian Prairie/Harney Pond, Fisheating Creek, and Taylor Creek/Nubbin Slough. These tributary systems and drainage networks are generally bound by the drainage divides of the major water bodies. The dataset represents the external boundaries of the LOW, the nine sub-watersheds which comprise the LOW, and the 69 basins which comprise the sub-watersheds as per the 2014 LOWPP Update and the Northern Everglades and Estuaries Protection Program (NEEPP). The three sub-watersheds located on the eastern, southern, and western boundaries of Lake Okeechobee are not part of the current modeling effort, but will be included in a future modeling effort. The basis for the boundaries was the technical work associated with the "Draft – Technical Support Document: Lake Okeechobee Watershed Performance Measure Methodologies" document dated February 2013 developed for revisions to the 40E-61 Works of the District Program, with minor modifications.

As mentioned above, the model domain boundaries are used to clip the input datasets such as land use or soils. Note that two datasets may contain data that lie outside of the boundary, which are the hydrologic network and the location of rain gages. These are discussed below. Additionally, during the modeling process the WAM interface uses the model boundary as a mask while creating grids (rasters) from the various input datasets.

#### *3.2.1.2 Subbasin Boundaries*

Subbasins are used by WAM to further subdivide the modeling domains discussed above in Section 3.2.1.1. The motivation for this is to separate surface water flow based on either natural or man-made flow paths on a finer scale than is possible at the sub-watershed level. Note that the terminology used here for a dataset input to WAM does not imply that these features are coincident with the subbasins defined within AHED. The subbasins used by WAM are generally much smaller than the basins that comprise the sub-watersheds.

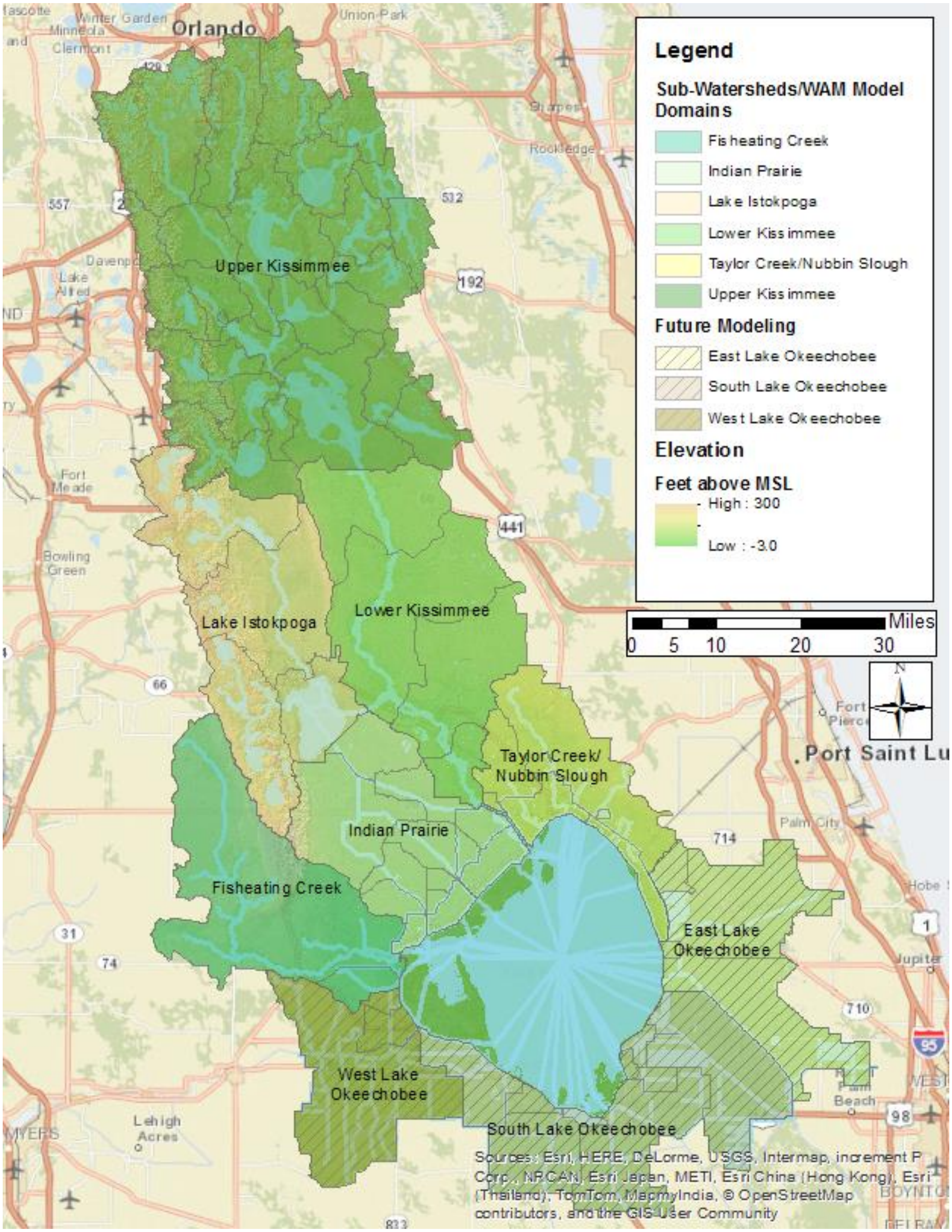


**Figure 6. Model domain boundaries for the WAM simulations, based on the sub-watershed boundaries defined by the Coordinating Agencies.**

For modeling purposes, the subbasin boundaries are those that reflect hydrologic divides or boundaries within the model domain/sub-watershed. In many parts of Florida subbasin boundaries can be created by artificial levees or berms, but are more typically due to natural topographic features, such as ridges. The subbasin data from the 2009 modeling effort was developed using the ArcHydro toolset, and was modified for this study to fit the updated six sub-watershed boundaries. In addition, the sub-watershed boundary dataset discussed in the previous section included a dataset named "LOW_Subwatersheds_Basins", which served to refine some of the WAM subbasin boundaries.

#### *3.2.1.3 Topography*

Topography datasets in the previous 2009 WAM modeling efforts were created by obtaining and merging Digital Elevation Model (DEM) data, LIDAR data, which became available in 2006 from the Kissimmee Basin Modeling and Operations Study (KBMOS). The datasets were derived from various sources of information including USGS 5-foot contours, SFWMD bathymetry and LIDAR (Earth-Tech, 2006).

For the current modeling effort, a continuous elevation raster that covers the entire study area was obtained from the SFWMD. This raster has 50-feet by 50-feet grid cells. The topography data are used by WAM during the modeling process to determine the directions of flow and distances to (and through) hydrologic features such as lakes, streams, canals, sloughs, riparian wetlands and depressions (see Figure 5). The topography dataset used for the study is shown in Figure 7.

#### *3.2.1.4 Hydrography*

The hydrography used for the current effort was based on modification of the latest hydrographic dataset obtained from the SFWMD together with the hydrography used in the 2009 WAM modeling effort and the 2012 update. The SFWMD maintains all hydrologic data in an ArcHydro Enhanced Database (AHED). This data was obtained in February of 2015. In addition to linear (e.g., stream) features (the "hydroedge" feature class), the AHED dataset includes water bodies, hydrologic structure locations, monitoring points, etc. In many locations, the AHED hydroedge feature class contains somewhat more detail than is necessary for developing a reach network for WAM. For example, disconnected hydrologic features such as isolated wetlands and lakes are included in the hydroedge network. WAM has a separate algorithm for routing water into these types of features and then into groundwater (or lost via evaporation), so hydroedge features of this type were not included in the WAM network. The reach network used in WAM is shown in Figure 8.

#### *3.2.1.5 Land Use*

The land use feature class ("LOW_LU_LOPP_09") (LOPP is the "Lake Okeechobee Protection Plan") used was obtained from the SFWMD in February of 2015. According to the metadata received with the feature class:

> *2009 Land Use for the Lake Okeechobee watershed and associated watersheds, for the LOPP. The boundaries are derived from the "current" version as developed for the Northern Everglades and ongoing Watershed Protection Plans, as of December 2012 (v2). The land use is composited from 2008/9 SFWMD, 2009 SJRWMD, and 2009 SWFWMD. The land-**use** FLUCCS code is used, except for the Avon Park area, where the land-**cover** FLUCCS code is used. Polygons for active and inactive dairies, as of 2009, were supplied by JGH and were superimposed on the WMD land-use*

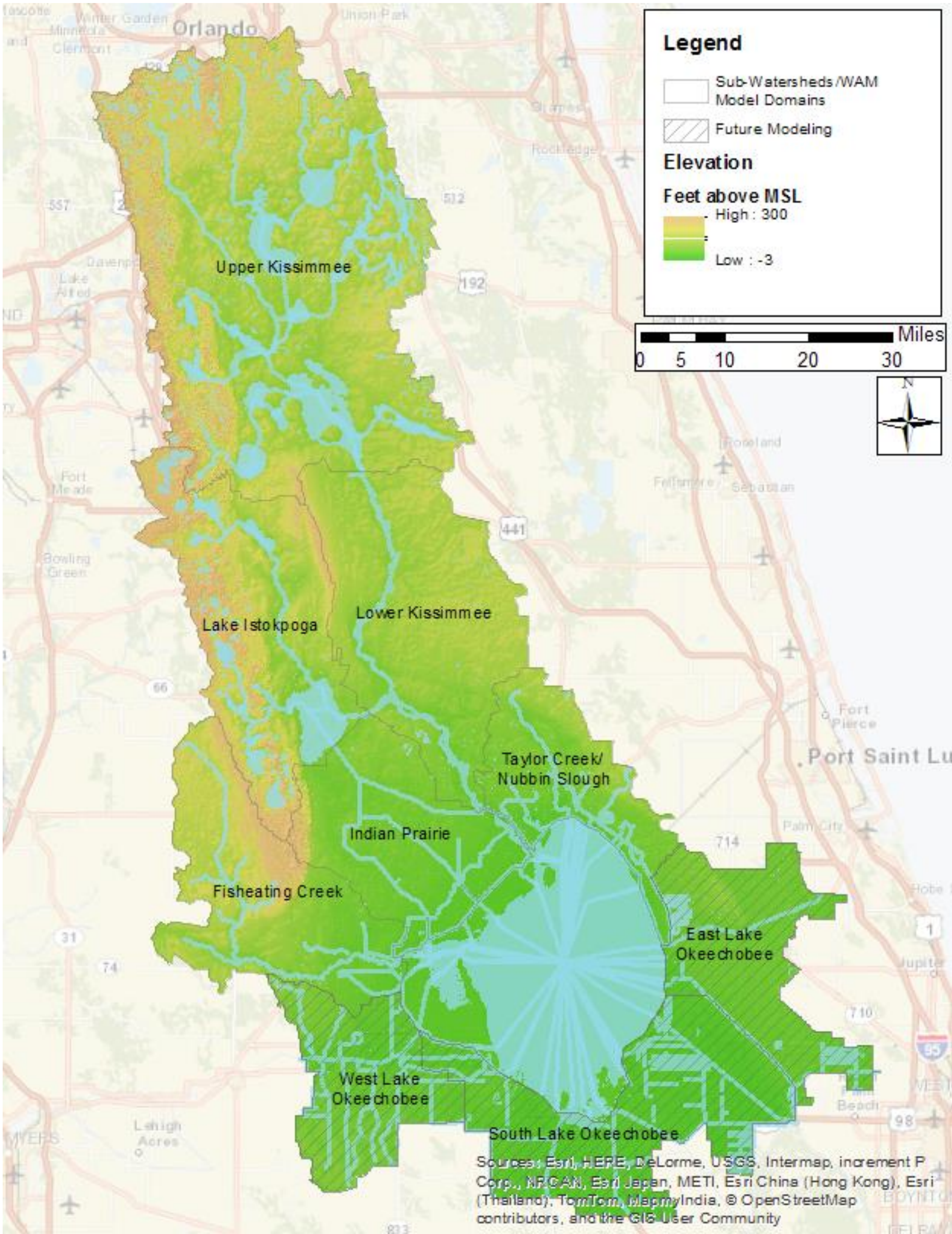


**Figure 7. Representation of the topography data used for the WAM simulations.**

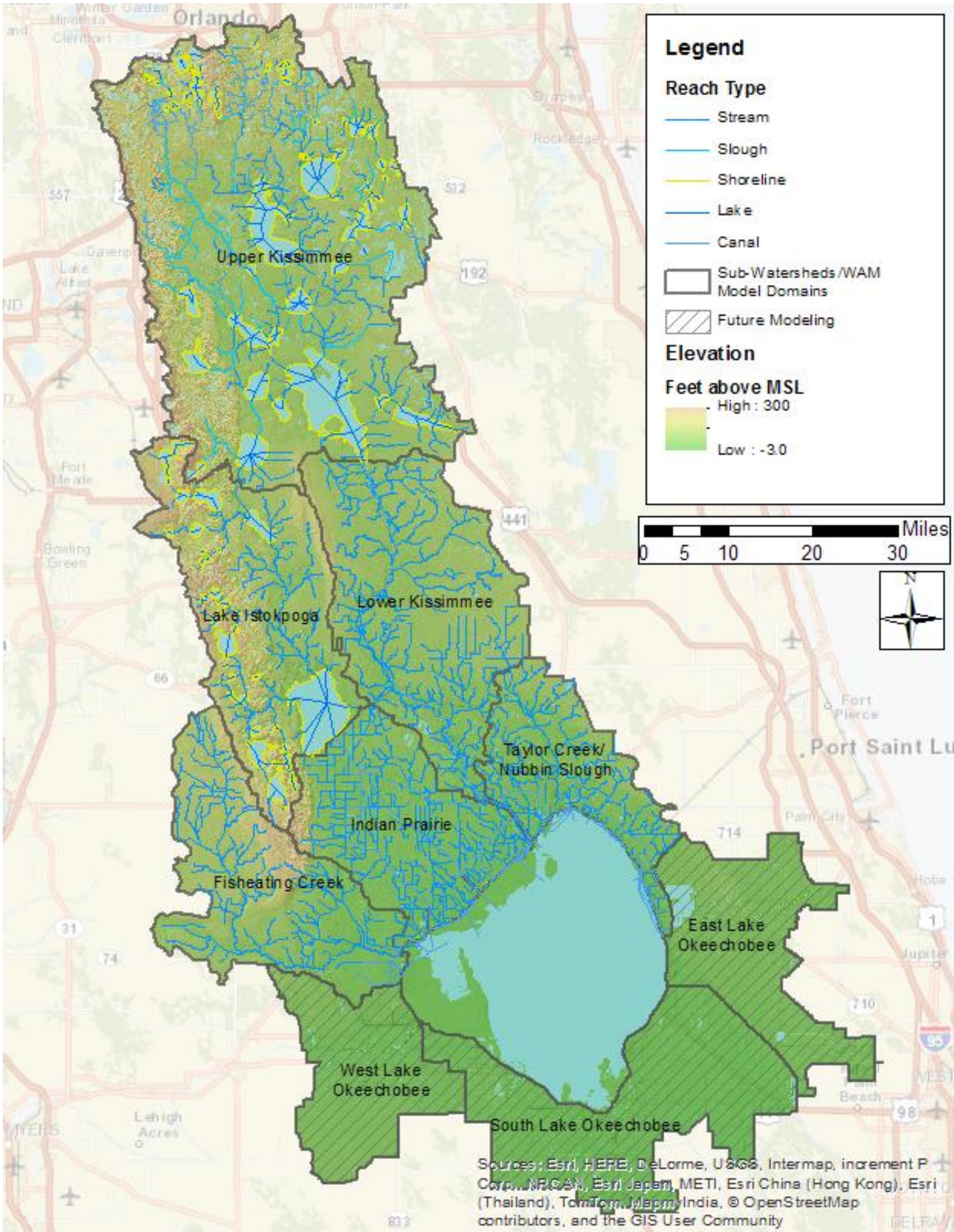


**Figure 8. The reach network developed for WAM.**

> *polygons. Most of this metadata is copied from the LOPP boundary or the LCLU documentation. *** From the SFWMD LCLU documentation -- This data set serves as documentation of land cover and land use (LCLU) within the South Florida Water Management District as it existed in 2008-09. Land Cover Land Use data was updated from 2004-05 LCLU by photo-interpretation from 2008-09 aerial photography and classified using the SFWMD modified FLUCCS classification system. Features were interpreted from the county-based aerial photography (4 in - 2 ft pixel) and updated on screen from the 2004-05 vector data. Horizontal accuracy of the data corresponds to the positional accuracy of the county aerial photography. The minimum mapping unit for classification was 2 acres for wetlands and 5 acres for uplands.*

The land use data received from SFWMD and currently incorporated into WAM is shown in Figure 9. Acreages for the predominant land use categories used by WAM is broken down by sub-watershed and summarized in Table 2.

The land use feature class is in the process of being updated to change the classification of some areas that were originally mapped as improved pasture but are more properly categorized as conservation areas. As these data become available from the Coordinating Agencies it will be substituted into the WAM land use layer.

#### *3.2.1.6 Soils*

The spatial distribution of soils is a required input to WAM and because of previous modeling efforts with WAM, the WAM database of soil parameters already contained data for 429 soil categories common to Florida. The existing database was used with a newly updated and compiled feature class of Soil Survey Geographic (SSURGO) data. The final soils information used in the project came from the U.S. Department of Agriculture, Natural Resource Conservation Service (NRCS) published SSURGO data for 2013 and 2014. These data were derived from each of the county soils feature classes downloaded from NRCS. The county-wide datasets were merged and then the final product was clipped to cover the entire study area. Section 3.4.2.2 discusses how the soils data from NRCS were imported into WAM. The soils dataset is shown in Figure 10.

#### *3.2.1.7 Rainfall Stations*

WAM uses a point feature class for rainfall stations that is used to generate a Theissen polygon raster that is used within the program to assign rainfall time series to each unique cell. Location of rainfall stations were included in the AHED dataset. For consistency, the same stations that were included in the 2009 WAM application and the 2012 update were used for the current work and are shown in Figure 11. With the exception of one station, all data was available from the SFWMD database DBHydro. The lone exception was a station (Frostproof) that lies within the South West Florida Water Management District (SWFWMD) boundary. All data were updated to include data through the end of 2013. This is discussed in more detail below in Section 3.4.3.1.

#### *3.2.1.8 Major Hydrologic Control Structures*

Major control structures important for comparison of modeled flow, stage and nutrient concentrations were determined during previous WAM applications (including the 2009 study) in the study area. These control structures were identified in the AHED dataset and incorporated, and the structures are shown in Figure 12. Further information and listings of the control structures are given in Section 3.3.2.

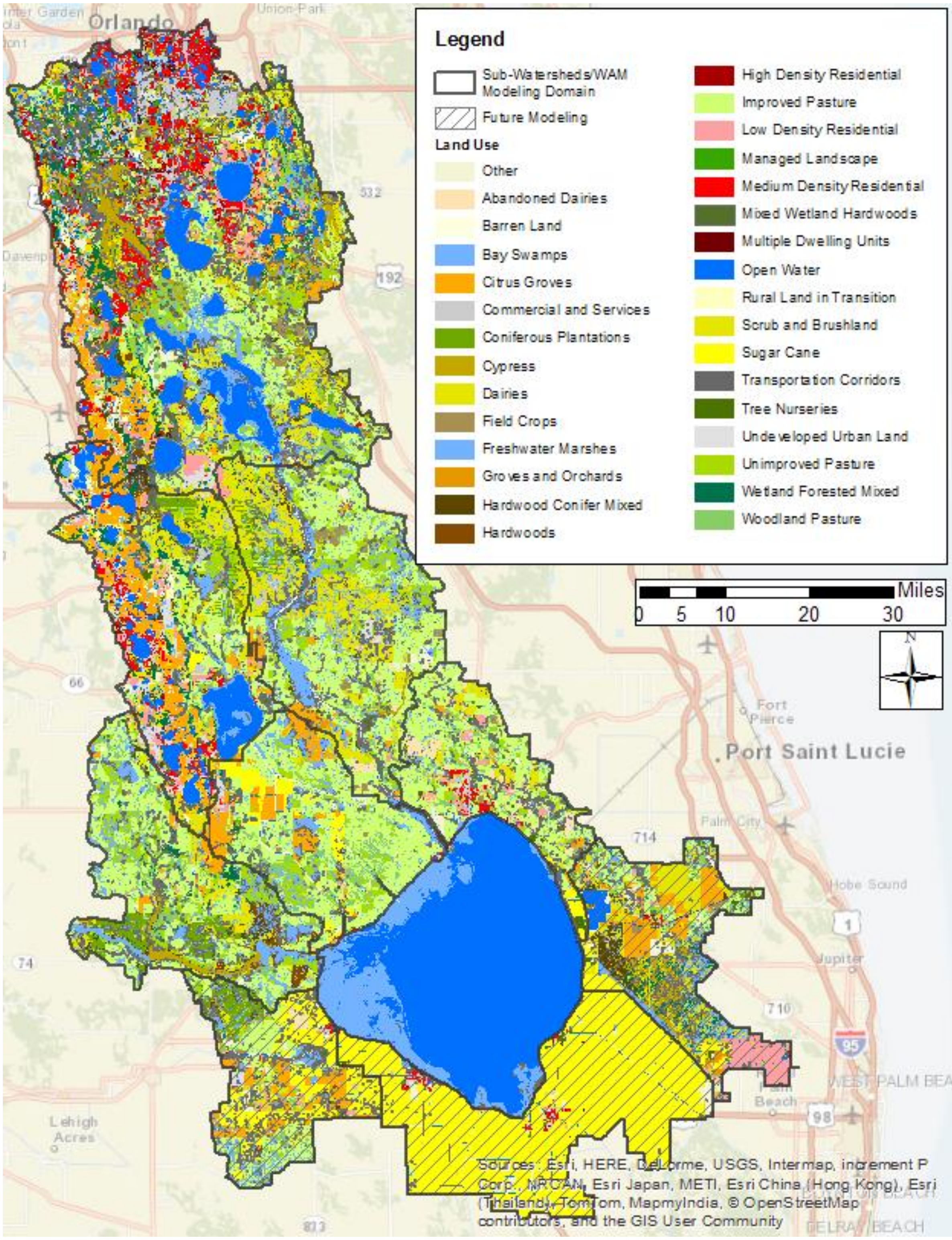


**Figure 9. Land use feature class for the LOW currently incorporated into WAM.**

**Table 2. The top 30 land use acreages in the northern six Lake Okeechobee sub-watersheds.**

| Land Use | Upper Kissimmee | Taylor Creek/ Nubbin Slough | Lower Kissimmee | Lake Istokpoga | Indian Prairie | Fisheating Creek | Total Acres |
|---|---|---|---|---|---|---|---|
| Improved Pasture | 128,004 | 91,432 | 130,041 | 39,743 | 120,985 | 102,612 | 612,817 |
| Scrub and Brushland | 100,243 | 4,424 | 91,522 | 56,102 | 7,830 | 23,319 | 283,440 |
| Freshwater Marshes | 74,493 | 10,128 | 66,900 | 26,472 | 29,135 | 46,505 | 253,633 |
| Open Water | 141,861 | 2,421 | 3,480 | 58,126 | 2,887 | 848 | 209,622 |
| Unimproved Pasture | 38,535 | 10,044 | 44,506 | 13,546 | 24,191 | 36,922 | 167,744 |
| Citrus Groves | 47,327 | 3,481 | 10,511 | 51,537 | 30,233 | 7,877 | 150,966 |
| Woodland Pasture | 36,755 | 13,509 | 10,931 | 3,669 | 21,390 | 24,973 | 111,227 |
| Mixed Wetland Hardwoods | 49,774 | 6,288 | 17,881 | 9,746 | 5,140 | 12,637 | 101,465 |
| Medium Density Residential | 71,103 | 4,323 | 187 | 17,028 | 826 | 130 | 93,597 |
| Cypress | 71,514 | 408 | 2,248 | 5,203 | 258 | 9,259 | 88,890 |
| Low Density Residential | 43,178 | 8,376 | 4,157 | 19,374 | 1,973 | 2,291 | 79,348 |
| Wetland Forested Mixed | 37,344 | 510 | 1,259 | 18,827 | 1,005 | 6,166 | 65,111 |
| Commercial and Services | 44,956 | 2,341 | 1,852 | 7,965 | 332 | 321 | 57,766 |
| Hardwood Conifer Mixed | 26,078 | 2,238 | 6,056 | 7,272 | 1,556 | 10,666 | 53,867 |
| Coniferous Plantations | 6,416 | 55 | 7,785 | 10,848 | 404 | 20,071 | 45,580 |
| Undeveloped Urban Land | 18,564 | 1,594 | 2,206 | 16,140 | 1,764 | 575 | 40,843 |
| Sugar Cane | | 5,217 | | 2,382 | 19,207 | 20 | 26,827 |
| Dairies | 53 | 10,222 | 6,480 | 3,158 | 198 | 27 | 20,137 |
| Hardwoods | 6,049 | 905 | 2,037 | 2,749 | 851 | 7,288 | 19,880 |
| Field Crops | 8,023 | 1,372 | 8,234 | 411 | 393 | 793 | 19,225 |
| Transportation Corridors | 14,055 | 313 | 189 | 1,561 | 106 | 704 | 16,928 |
| Barren Land | 5,131 | 1,545 | 2,248 | 1,998 | 3,680 | 1,203 | 15,805 |
| Managed Landscape | 12,908 | 519 | 91 | 1,616 | | | 15,134 |
| Rural Land in Transition | 4,953 | | | 8,398 | | | 13,350 |
| High Density Residential | 8,552 | 368 | 105 | 2,870 | 123 | 21 | 12,040 |
| Abandoned Dairies | | 8,602 | 2,220 | | | | 10,823 |
| Multiple Dwelling Units | 10,367 | 41 | 25 | 104 | | | 10,537 |
| Bay Swamps | 5,492 | 308 | 434 | 1,960 | 185 | 1,119 | 9,498 |
| Row Crops | 1,120 | 315 | 4,613 | 555 | 1,168 | 19 | 7,790 |
| Sod Farms | 3,537 | 1,521 | | 180 | | 737 | 5,976 |
| Other | 12,041 | 4,973 | 992 | 4,666 | 760 | 939 | 24,371 |
| **Total Acres** | **1,028,425** | **197,796** | **429,190** | **394,205** | **276,578** | **318,044** | **2,644,238** |

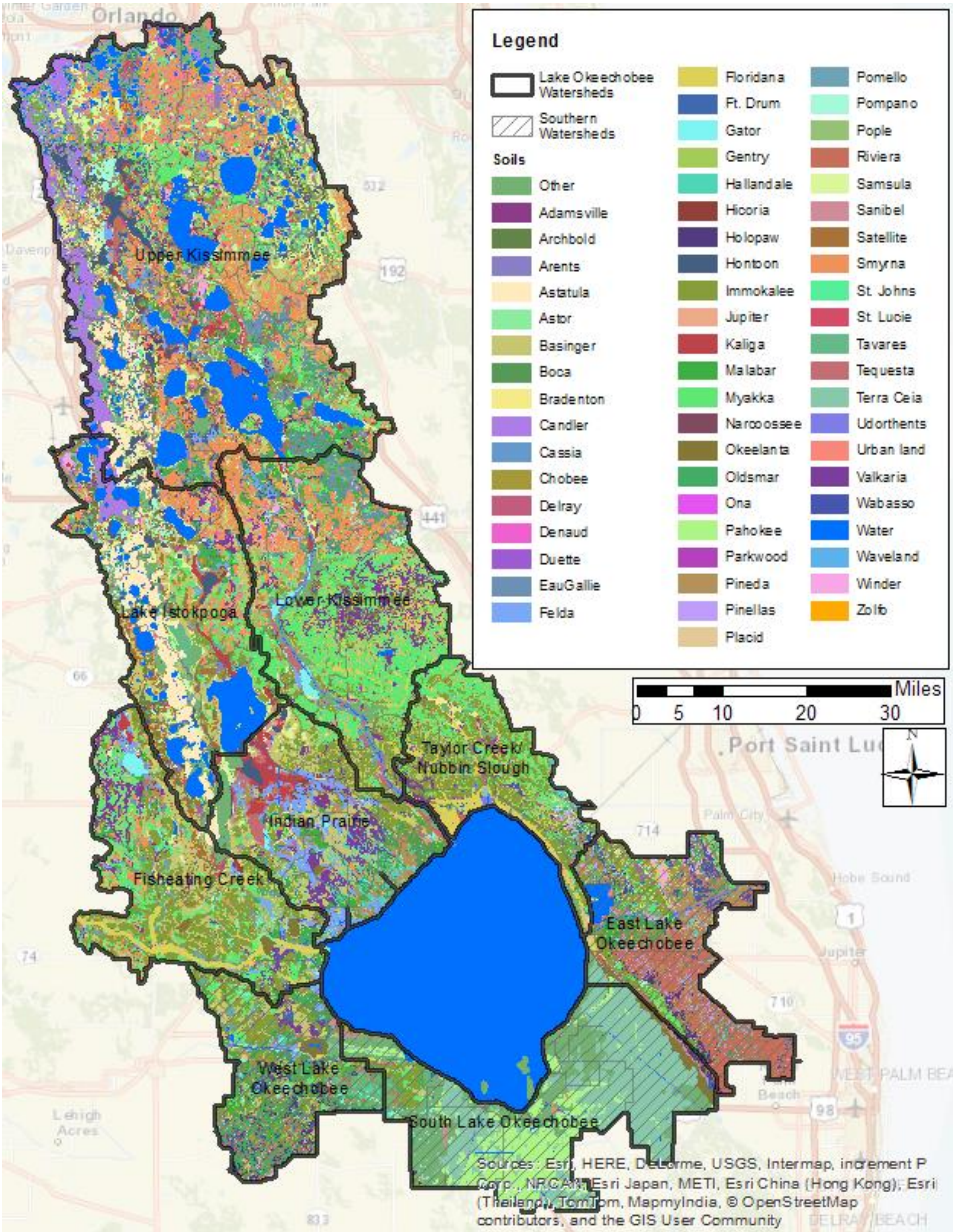


**Figure 10. Soil distribution in the LOW.**

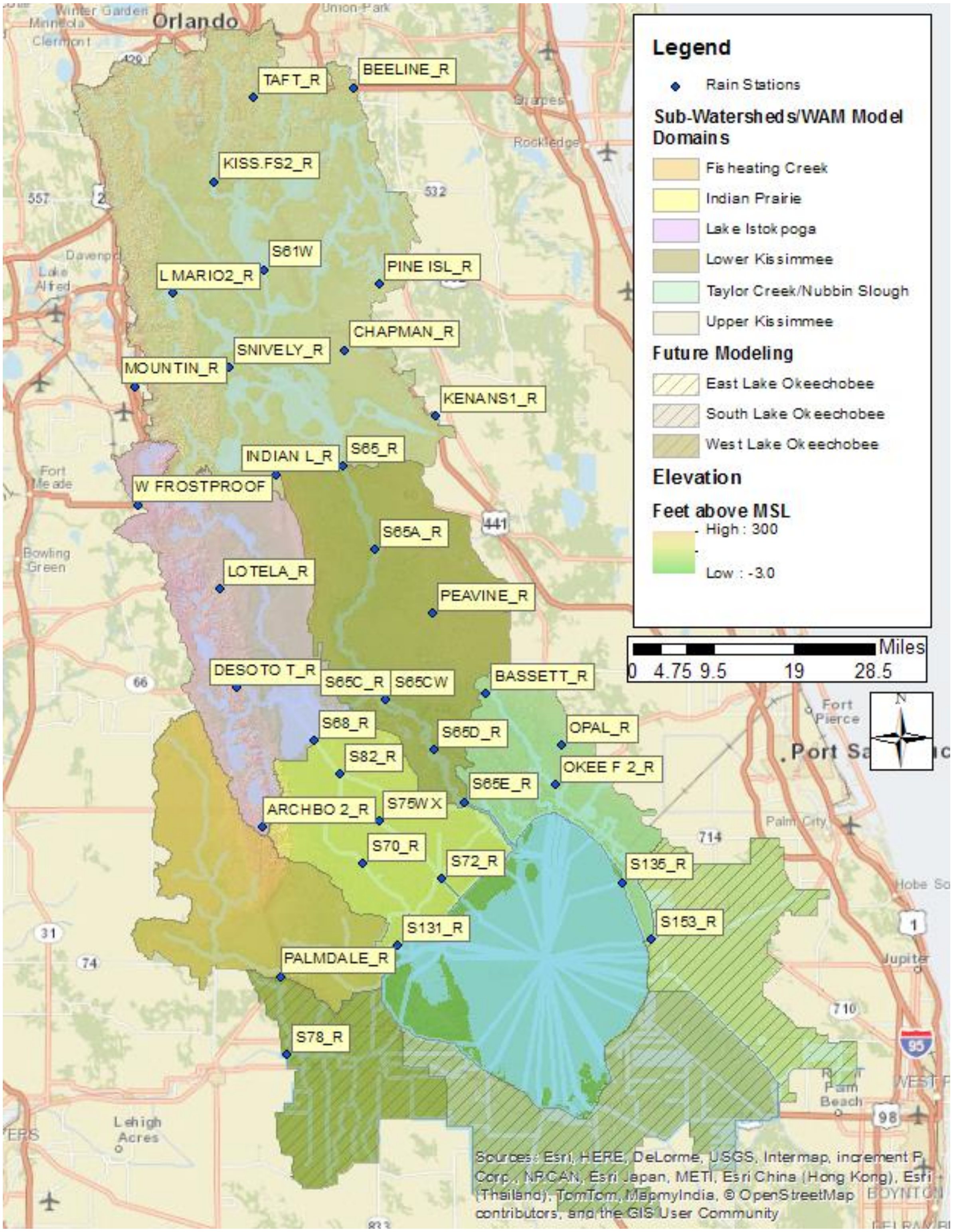


**Figure 11. Rainfall stations within the Lake Okeechobee watershed used in WAM simulations.**

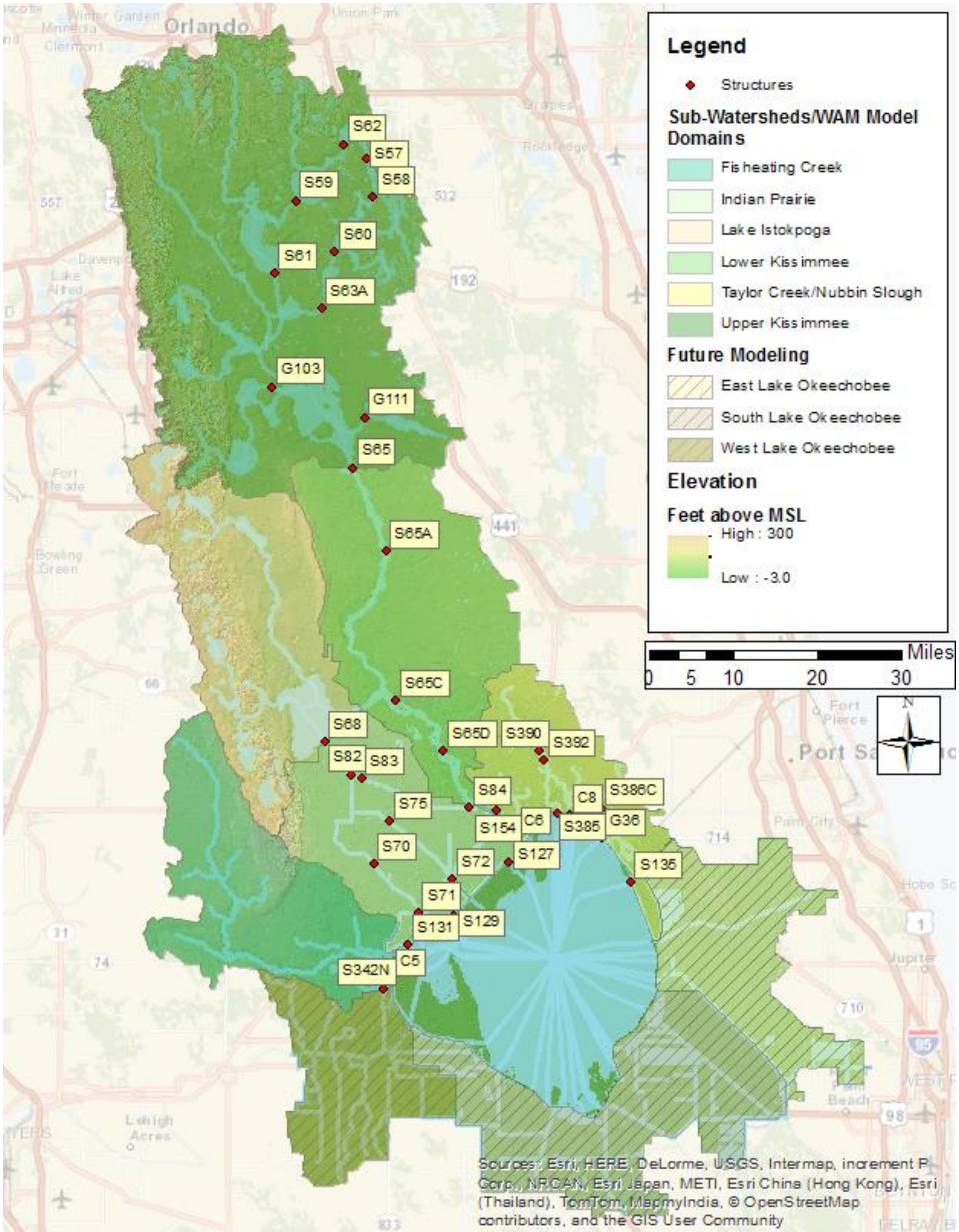


**Figure 12. SFWMD hydraulic control structures used in the WAM simulations.**

*3.2.1.9 Utility (wastewater) zones.*
This is a polygonal feature class that delineates areas that are served by a wastewater utility services. Within the feature class, areas that are served by a utility service are designated by a simple integer attribute of 1, otherwise the attribute is set to 0. For this project, wastewater utility zones were not incorporated into the model for the base scenario. Consequently, urban land uses that are typically served by treatment systems (such as high/medium residential or commercial and services) undergo treatment that is equivalent to that provided by a treatment plant (such as a sprayfield). The treated water is then assumed by the model to have been released on-site rather than routed to a treatment plant and released there. This is the typical approach unless detailed information about treatment plant locations and discharge is available. In this case, the utility zone feature class is simply a mirror of the watershed boundary with the attribute set to 0 everywhere.

*3.2.1.10 Location of water and nutrient point sources (or sinks)*
WAM has the ability to include point sources of water and/or nutrients, such as discharges from treatment plants, various types of industrial plants, or mining areas. Typically, if an area is served by a wastewater zone (as described above) and the treated water is reintroduced into the same sub-watershed, WAM simulates these point sources by adding the water and nutrient loads directly to reaches. Conversely, point sources can also be used to simulate withdrawals of water directly from reaches. For the base scenarios simulated, no point sources or sinks were incorporated into the model. However, point sources (or sinks) may be added during later stages of modeling if found to be important, these can be added quickly to the model if the appropriate time series are provided.

*3.2.1.11 Irrigation source specification*
This dataset is used to specify the origin of water used for irrigation purposes. There are three choices available:

1. Irrigation water is taken from deep groundwater (e.g., the Floridan aquifer).
2. Irrigation water is taken from the shallow, surficial aquifer.
3. Irrigation water is taken from surface water, i.e., the stream network.

In this project, irrigation water is assumed to be taken from the shallow surficial aquifer (option 2).

Of the spatial datasets discussed above, it is the soils, land use, rainfall stations, and utility zones that are used to define the unique combinations of cells (see Figure 5) that are simulated by the land source model to produce daily contributions of runoff, percolation, and nutrient loads.

## 3.3 Databases

All measured flow, stage, rainfall, and water quality data described in the following sections were stored in a Microsoft Access database. For each type of data there are two tables; one table is a list of the stations and related information, and the other table houses the measured data. Flow and stage information were kept in the same table, however rainfall and water quality data are in separate tables. For example, there is one table listing all the flow and stage stations with data in the database. Another table contains the actual values for average daily flow and stage for every structure.

#### *3.3.1.1 Flow and Stage Data*

Time series of flow data, recording the mean daily flow in cubic feet per second (CFS) – was collected at the stations listed in Table 3 and shown in Figure 13. Generally, the time series data covers the period of record (POR) from the beginning of calendar year 1972 through the end of 2013. Where available, the time series in DBHYDRO that were marked as "PREF" were downloaded. This annotation indicates that the recorded value is the preferred value. If these data were not available, time series marked as "MOD1" were used. These are baseline hydrologic datasets developed for regional modeling. For some stations, data for the entire period was not available – whether marked as modeling or preferred time series. Since the flow data was primarily used to calibrate the model developed with WAM, it was not critical to have data of the entire POR at every flow station.

**Table 3. Stations used for flow and water quality data listed by sub-watershed. Note that the second station (02273198) in the Lake Istokpoga sub-watershed (at S-68) has water quality data from 2005 onward.**

| Sub-Watershed | Station | DBKey |
|---|---|---|
| **Fisheating Creek** | FISHP (US-27) | 15627 |
| | FISHCR (US-78) | WH036 |
| **Indian Prairie** | S-129 | 15642 |
| | S-127 | 15641 |
| **Lake Istokpoga** | S68 | 15632 |
| | 02273198 | |
| **Lower K** | S-65A | J9202 |
| | S-65C | 04458 |
| | S-65D | 04470 |
| | S-65E | 15631 |
| **TCNS** | S-133 | 15637 |
| | S-135 | 15638 |
| | S-191 | 15639 |
| **Upper K** | S-65 | H0289 |

#### *3.3.1.2 Rainfall*

There were 35 rainfall stations where rainfall data was collected and input to the WAM models of the sub-watersheds (Figure 11). Time series rainfall data for most of the 35 stations were collected from the SFWMD's DBHYDRO database. Note that there are considerably more than 35 stations located within (or near to) the six sub-watersheds with data contained in DBHydro. However, many of these stations have short PORs, and many stations may have a longer POR but still not cover the entire simulation POR. In a number of cases, the rainfall station was relocated or re-instrumented, necessitating a new station key (DBKey) in DBHydro. To account for this, all rainfall data in the study area was downloaded into a Microsoft Access database. Data from each rainfall station that was used for the 2009 study and the 2012 update was extracted from the database. Where data was missing (due to the station being moved or decommissioned) data from the nearest rain station was used to fill in those missing values. In addition, data for Frostproof Tower,

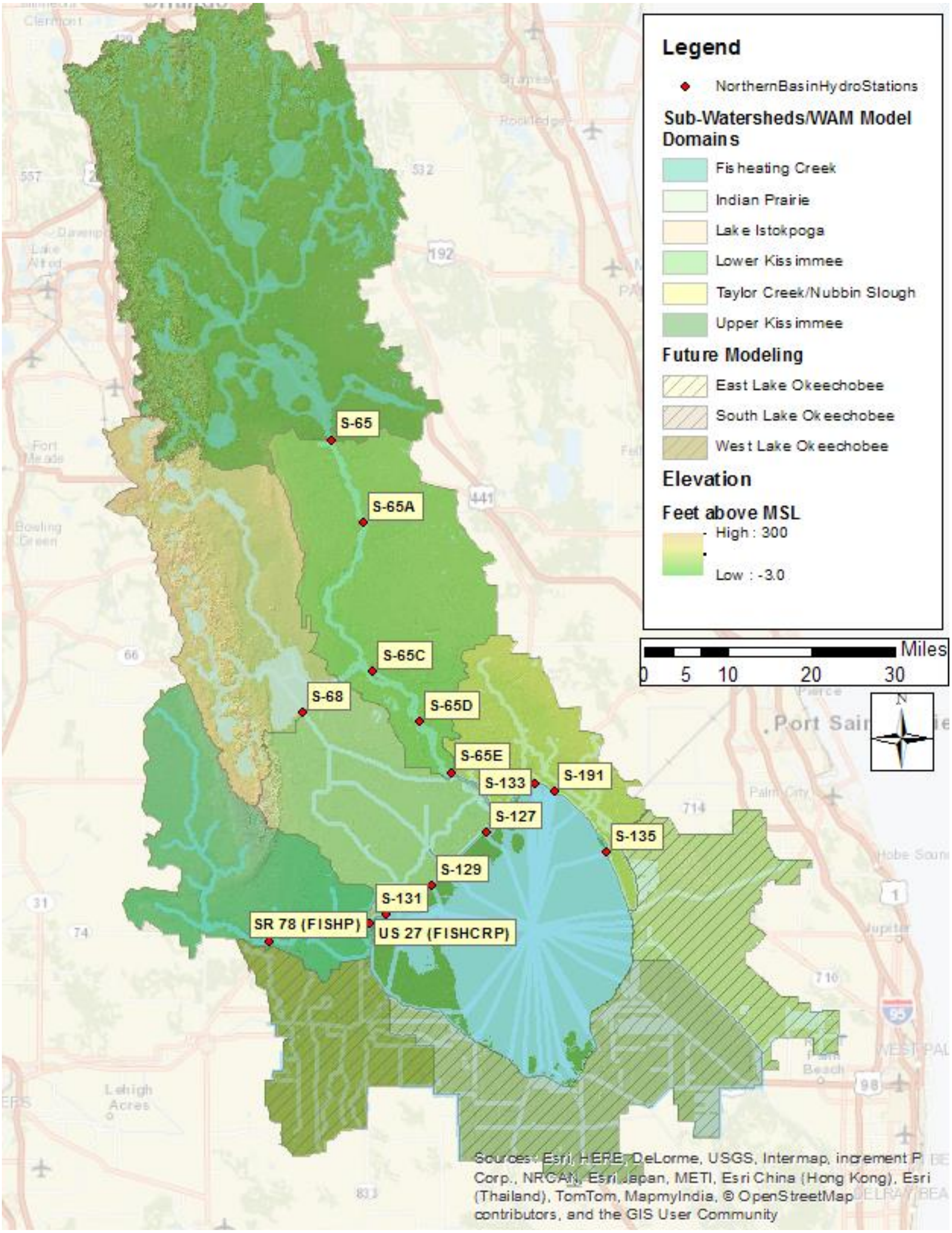


Figure 13. Location of flow and water quality measurement stations.

the rainfall station with no rainfall data in DBHYDRO, was collected from the SWFWMD website. When the input files for WAM are generated, a Theissen polygonalization of the rain gage network is generated. Each Thiessen polygon defines an area around a rain gage so that any location inside the polygon is closer to that gage than any of the other rain gages. Each source cell is then assigned the rainfall time series associated with that polygon.

##### *3.3.1.3 Evapotranspiration*

To calculate potential evapotranspiration (PET), WAM uses average monthly high and low temperatures, solar radiation, wind, and dewpoint values. The data from the 2009 study were used for these values.

##### *3.3.1.4 Temperature*

One of the land source models (EAAMod) requires air temperature data for use in determining the phosphorus soil mineralization rate. While the output from EAAMod is not particularly sensitive to these values, they must be provided. These data were obtained from the SFWMD at the S-65CW and S-65DWX stations, and was supplemented with values obtained from NOAA at the Kissimmee and Avon Park weather stations.

##### *3.3.1.5 Water Quality*

Water quality data of surface water phosphorus and nitrogen concentrations were collected from DBHYDRO for the major water control structures (where recorded) listed in Table 3 and shown in Figure 13. These stations are the same locations used for the previous 2009 study. Both data from grab samples and autosamplers were downloaded. Most of the data downloaded was, however, collected from grab samples. Concentrations of total P were directly recorded, while concentrations of total N were rarely present and were calculated from summing nitrate (or nitrate+nitrite) and TKN.

### 3.3.2 System Operations

Descriptions of major control structures from the 2009 study and the 2012 update were used for parameterizing the structures in this work. The data were originally obtained from the Structure Information Site available on the internal SFWMD website. For structures added for this project (e.g., STA pumps and spillways in Taylor Creek/Nubbin Slough) these details need to be determined via conversation with the SFWMD. The hydraulic structures used are shown in Table 4.

The two structures that are denoted as being a “Farm Weir” are structures that are not part of the SFWMD control network, but have been located by field work done by SWET.

## 3.4 Data preparation

### 3.4.1 Reach Delineation

The current version of WAM (compiled to run on ArcMap 10.2.2) was able to use the current version of the SFWMD-wide AHED. WAM includes tools that are integrated with ArcMap (the “WAM Toolbar”) that allow users to import and modify hydrography, and then create a reach network, index the reaches, and assign reach types (stream, canal, etc.) In order to do this, each segment in the network must be connected, and looping within the network must be accounted for.

**Table 4. Structures used in the WAM simulations.**

| Structure Name | Structure Type | WAM Type | Sub-watershed | Stream/Canal |
|---|---|---|---|---|
| **C-5** | Culvert | Gate | Fisheating Creek | Nicodemus Slough |
| **C-6** | Spillway? | Gate | Taylor Creek/Nubbin Slough | |
| **C-8** | Spillway? | Gate | Taylor Creek/Nubbin Slough | |
| **Farm Weir** | Spillway-Unknown | Weir | Fisheating Creek | Fisheating Creek |
| **Farm Weir** | Spillway? | Weir | Taylor Creek/Nubbin Slough | |
| **G-103** | Spillway/Weir-Sheetpile | Weir | Upper Kissimmee | Zipperer Canal |
| **G-111** | Culvert | Weir | Upper Kissimmee | Jackson Canal |
| **G-113** | Culvert | Weir | Upper Kissimmee | Outlet of Lake Marian |
| **G-36** | Spillway? | Gate | Taylor Creek/ Nubbin Slough | |
| **S-127** | Spillway | Gate | Indian Prairie | L-48 |
| **S-127** | Pump | Pump | Indian Prairie | L-48 |
| **S-129** | Spillway | Gate | Indian Prairie | L-49 |
| **S-129** | Pump | Pump | Indian Prairie | L-49 |
| **S-131** | Gate | Gate | Indian Prairie | L-50 |
| **S-131** | Pump | Pump | Indian Prairie | L-50 |
| **S-133** | Pump | Pump | Taylor Creek/ Nubbin Slough | L-47 |
| **S-135** | Pump | Pump | Taylor Creek/ Nubbin Slough | L-47 |
| **S-135** | Spillway | Gate | Taylor Creek/ Nubbin Slough | L-47 |
| **S-154** | Culvert-Box | Gate | Taylor Creek/ Nubbin Slough | LD-4 |
| **S-154C** | Culvert-Box | Gate | Taylor Creek/ Nubbin Slough | LD-4 |
| **S-191** | Spillway-Concrete | Gate | Taylor Creek/ Nubbin Slough | Nubbin Slough |
| **S-342** | Culvert | Gate | Fisheating Creek | Nicodemus Slough |
| **S-385** | Pump | Pump | Taylor Creek/ Nubbin Slough | |
| **S-386A-B** | Spillway? | Weir | Taylor Creek/ Nubbin Slough | |
| **S-387A-C** | Spillway? | Weir | Taylor Creek/ Nubbin Slough | |
| **S-390** | Pump | Pump | Taylor Creek/ Nubbin Slough | |
| **S-392** | Spillway? | Weir | Taylor Creek/ Nubbin Slough | |
| **S-57** | Culvert | Weir | Upper Kissimmee | C-30 |
| **S-58** | Culvert | Weir | Upper Kissimmee | C-32 |
| **S-59** | Culvert | Gate | Upper Kissimmee | C-31 |
| **S-60** | Spillway-Concrete | Gate | Upper Kissimmee | C-33 |
| **S-61** | Spillway-Concrete | Gate | Upper Kissimmee | C-35 |
| **S-62** | Spillway-Concrete | Gate | Upper Kissimmee | C-29 |
| **S-63A** | Spillway-Concrete | Gate | Upper Kissimmee | C-34 |
| **S-63A** | Spillway-Concrete | Gate | Upper Kissimmee | C-34 |
| **S-65** | Spillway - Concrete | Weir and Gate | Upper Kissimmee | C-38 |
| **S-65A** | Spillway-Concrete | Gate | Lower Kissimmee | C-38 |

| | | | | |
|---|---|---|---|---|
| **S-65C** | Spillway-Concrete | Gate | Lower Kissimmee | C-38 |
| **S-65D** | Spillway-Concrete | Gate | Lower Kissimmee | C-38 |
| **S-65E** | Spillway-Concrete | Gate | Lower Kissimmee | C-38 |
| **S-68** | Spillway-Concrete | Gate | Lake Istokpoga | To C-41 from Lake Istokpoga |
| **S-70** | Spillway-Concrete | Gate | Indian Prairie | C-41 |
| **S-71** | Spillway-Concrete | Gate | Indian Prairie | C-41 |
| **S-72** | Spillway-Concrete | Gate | Indian Prairie | C-40 |
| **S-75** | Spillway-Concrete | Gate | Indian Prairie | C-40 |
| **S-82** | Spillway-Concrete | Gate | Indian Prairie | C-41A to C-41 |
| **S-83** | Spillway-Concrete | Gate | Indian Prairie | C-41A |
| **S-84** | Spillway-Concrete | Gate | Indian Prairie | C-41A |

Small or disconnected reaches must be deleted or modified to attach correctly to the rest of the network. In addition, tools are available for the user to create and modify the cross-sectional profiles of each reach and modify bottom elevations. The connectivity of the network is then generated, meaning the relation between reaches – i.e., which reach flows into which other reach – must be determined.

As was discussed briefly in Section 3.2.1.4, the "hydroedge" feature class contained in AHED served as the basis for developing the hydrologic network, together with the WAM reach dataset from 2009. Extensive processing of the hydroedge feature class was required to get it into a form usable by WAM. This included merging many of the smaller segments in the hydroedge feature class, ensuring that small features (e.g., segments on the order of a few meters) had been accounted for, and that any segments that had been detached during the modification had been re-attached. Also, features in the hydroedge class that were originally disconnected from the network (e.g., isolated wetlands or lakes) had to either be deleted or attached to an appropriate reach.

After that work was finished, classification of the reaches needed to begin. Most reaches in the study area fall into one of three main types:

1) Streams
2) Canals
3) Sloughs

These classifications are used by WAM to assign specific nutrient attenuation coefficients to each type of reach. In addition to the three main types listed above, new subcategories of reach types may be created during the modeling processes if indicated by the recalibration phase, or if reach-specific information is obtained from an agency. Because there was rarely an indication in the AHED as to which category a particular reach fell into, this was a somewhat laborious process that necessitated examination of the reach in aerial imagery. Some assignments were straightforward (many canals are obvious), but distinguishing between streams and sloughs is not always clear.

Another effort was requested in the statement of work (SOW) to assign what are termed "shoreline" reaches to the boundaries of the larger lakes that are found in the Upper Kissimmee and Lake Istokpoga Sub-watersheds. These reaches primarily serve to intercept water and nutrients flowing into a lake via overland flow and then allow the water and nutrients to flow into the lake.

As such, they act as an accounting mechanism so that the amount of water and nutrients flowing into a lake via overland flow can be easily determined.

After the reach network was set up, model runs were required to ensure that simulation run times were sufficiently short. One of the primary methods for optimization of a reach network is to ensure that the bottom elevations, cross-sectional profiles, and structure information are appropriate. During the model setup process, the first two sets of parameters (bottom elevations and cross-sectional profiles) are estimated using algorithms incorporated into WAM. The reach cross-sectional profiles are estimated by determining the upstream contributing area for each reach while the bottom elevations are estimated from averaging the near-reach elevations (i.e., elevations obtained from the topography dataset that are within 100 meters of the reach) combined with the estimated cross sections. For the major reaches, particularly canals, the cross-sections were adjusted by hand by using aerial imagery and/or measured data if available. . For all of the simulated sub-watersheds this was an extended process that could only use limited information from the 2009 study due to changes in the configuration of the boundary and changes to the hydrography. In particular, the changes in the Kissimmee River in the Lower Kissimmee Sub-watershed due to restoration efforts has required a significant time investment. It is anticipated that modifications to the reach network will continue as feedback is obtained from the Coordinating Agencies.

### 3.4.2 GIS Dataset Reconciliation

*3.4.2.1 Land Use*

The current version of WAM uses the same land use database as in previous versions. All of the land use codes present in the feature class provided by the SFWMD are listed in the WAM land use database. A correspondence between the land use FLUCCS code and the WAM land use IDs (LUID) assigned to those areas is shown in Table 30 in the Appendix (Section 5.1).

**Since the 2009 study and the 2012 update, the input files for EAAMod (one of the land source models (see Section 2.2.2)) have been updated to include data for urban and natural area land use types. With these modifications the land uses listed in**

Table 5 will be run using EAAMod when Bucshell is run if the soil type is appropriate (i.e., high water table soils). This change necessitated adding a significant amount of data to the WAM scenario database and also increases simulation run times since EAAMod simulations take longer for equivalent simulation periods. This change alters simulation outputs significantly and as a result will necessitate recalibration.

The land use dataset will continue to receive updates from the Coordinating Agencies as areas that were incorrectly mapped are noted. The new land use dataset will be incorporated into WAM.

*3.4.2.2 Soils*

As discussed in Section 3.2.1.6, soils data was obtained from the NRCS. Each dataset covers at most a single county (some counties have multiple associated datasets) and consequently 12 datasets needed to be downloaded for the 11 counties (

Table 6). Some counties (Charlotte, Desoto) only covered small portions of the study area. The datasets were downloaded from the USDA NRCS web site at https://gdg.sc.egov.usda.gov/GDGOrder.aspx. After downloading, the feature classes were extracted, re-projected, and imported into a geodatabase feature set with the appropriate spatial projection. At this point, the features from each dataset were merged into a single dataset that covered all of the counties for which data was obtained. The data was then clipped to the LOW

**Table 5. Land uses that may be run using EAAMOD (if the soil type allows).**

| Land Use Name | LUID | Is New |
|---|---|---|
| **Low Density Residential** | 2 | Yes |
| **Commercial and Services** | 3 | Yes |
| **Pastureland and Rural Land in Transition** | 4 | Yes |
| **Scrub and Brushland** | 5 | Yes |
| **Hardwoods** | 6 | Yes |
| **Hardwood Conifer Mixed** | 7 | Yes |
| **Coniferous Plantations** | 8 | Yes |
| **Transportation Corridors** | 18 | Yes |
| **Medium Density Residential** | 19 | Yes |
| **High Density Residential** | 20 | Yes |
| **Multiple Dwelling Units** | 21 | Yes |
| **Industrial** | 22 | Yes |
| **Managed Landscape** | 23 | Yes |
| **Row Crops** | 25 | No |
| **Improved Pasture** | 26 | No |
| **Unimproved Pasture** | 27 | No |
| **Woodland Pasture** | 28 | No |
| **Tree Nurseries** | 35 | No |
| **Sod Farms** | 36 | No |
| **Ornamental Nurseries** | 37 | No |
| **Horse Farms** | 38 | Yes |
| **Dairies** | 39 | Yes |
| **Field Crops** | 62 | No |
| **Sugar cane** | 68 | No |
| **Citrus** | 84 | No |
| **Intensive Dairy Pasture** | 85 | No |
| **Field Crops - Dairy Sprayfield** | 86 | No |
| **Abandoned Dairies** | 89 | No |
| **Dairy Outer Pasture** | 90 | No |

**Table 6. Listing of soils datasets obtained from NRCS by county.**

| County | Associated Datasets |
|---|---|
| **Charlotte** | FL015 |
| **Desoto** | FL027 |
| **Glades** | FL043 |
| **Highlands** | FL055 |
| **Lake** | FL607, FL609 |
| **Martin** | FL085 |
| **Okeechobee** | FL093 |
| **Orange** | FL095 |
| **Osceola** | FL097 |
| **Polk** | FL105 |
| **St. Lucie** | FL111 |

boundary (see Figure 10). To import the data for use in WAM, the "compname" field was used to associate the soil features and the WAM LUID for each soil type. This was done using a lookup table for soils similar to that used for land use discussed in the previous section. Note that since the join between the feature class table and the lookup table is done on a text field, many small, but significant differences had to be accounted for. For example, extra blanks or missing periods ("Ft" vs. "Ft." for "Fort") will cause joins to fail.

To obtain the "compname" for each map unit, the soil map unit feature class (typically named "soilmu_a_flXXX" where "XXX" is the numeric designation for each county) is joined with the "mapunit" data table obtained with the feature class. This is then joined with the "component" table, which contains the "compname" field. Since each map unit may contain several components, the component with "majcompflag" equal to "Yes" is used to select the primary component. If multiple components have "majcompflag" set to "Yes", the component with the highest percentage is used and the map unit is assigned the chosen value of "compname". Using this methodology, each map unit in the study area was able to be assigned a soil type corresponding to a soil contained in the WAM database.

### 3.4.3 Time Series Dataset Preparation

Time series datasets for flow, stage, and water quality was used for comparison with WAM output. No processing of the collected datasets for flow, stage, and water quality was performed. Rainfall and ET time series were input to WAM and had the ability to be applied to sub-regions of the model domain or uniformly over the entire model domain.

#### *3.4.3.1 Rainfall*

Rainfall is a primary input to WAM and as such, missing portions of the time series must be patched with the best available rainfall data. A detailed review of the rainfall data collected initially from DBHYDRO was conducted for this report as described below. It was apparent from the initial effort to collect rainfall data that at some rainfall monitoring stations separate time series were available which, when combined, covered the entire POR.

Each collected time series was summarized on a yearly basis and inspected to determine if the data was a viable input to WAM. This quality check was important because WAM generates a time series of flow and concentration for unique combinations of soils, land use, and rainfall values in the model domain on a one hectare scale. The routing module of WAM will simulate zero flow in a reach if there is insufficient rainfall to generate runoff. This may be a valid occurrence, or, because a rainfall gage only represents rainfall measured at a discrete point, applying that rainfall over a large area may not be accurate. In cases where observed flow is different from simulated flow by roughly 10%, the accuracy of the contributing rain stations may be re-examined. Missing portions of the time series were filled with the data of the closest station that contained original data during that time. The time series, identified by DBHYDRO code, that were used for each rain station in WAM are listed in Table 7.

**Table 7. Rain station used in the WAM model setup. Some stations have multiple records, indicated by more than one DB key.**

| Rain Station | DBKey | Rain Station | DBKey |
|---|---|---|---|
| **ARCHBO 2_R** | 16604 | **S135_R** | 05849 |
| **BASSETT_R** | 06047 | | 16580 |
| | 15577 | **S153_R** | 16582 |
| **BEELINE_R** | 05963 | **S61_R** | 05868 |
| | TY244 | **S65_R** | 05940 |
| **CHAPMAN_R** | 05902 | **S65A_R** | 05981 |
| **DESOTO T_R** | 06096 | **S65C_R** | 06024 |
| **INDIAN L_R** | 05946 | **S65D_R** | 06068 |
| | P6922 | | 16658 |
| **KENANS1_R** | 06867 | **S65E_R** | 06071 |
| | T0958 | | F9542 |
| **KISS.FS2_R** | 05859 | **S68_R** | 06066 |
| | 16617 | **S70_R** | F9543 |
| **L MARIO2_R** | 05884 | **S72_R** | 16666 |
| **LOTELA_R** | 05853 | | K8691 |
| | TA345 | **S75_R** | 16663 |
| **MOUNTIN_R** | 06134 | | 16663 |
| **OKEE F 2_R** | 06070 | | K8692 |
| | 16697 | **S75WX** | RQ467 |
| | 16285 | **S78_R** | 06243 |
| **OPAL_R** | 06052 | | 16625 |
| | 15580 | **S82_R** | 16655 |
| **PALMDALE_R** | 06093 | | K8694 |
| | 15786 | **SNIVELY_R** | 05912 |
| **PEAVINE_R** | 05858 | | T0933 |
| | T0919 | **TAFT_R** | 06042 |

| | | | | |
|---|---|---|---|---|
| **PINE ISL_R** | 05876 | | | T0964 |
| | T0929 | | **W FROSTPROOF** | N/A |
| **S131_R** | 06120 | | | |
| | 16286 | | | |

## 3.5 Conclusions

The information collected and formatted in this task was sufficient to use in WAM to simulate water and nutrient runoff in the basins. As with any study, however, there is always room for improvement in terms of the input information. In particular, as land uses and the actual practices become better known the model will improve significantly. Furthermore, any additional information about stream and canal elevations, depths, and cross-sectional profiles that can be incorporated into the model can improve model results.

# 4 Model Results

Comparisons of model results with measured data are presented below for each of the six sub-watersheds. The model simulation period was 1975-2013; however, there was a three-year skip period where the first three years of output from BUCShell was not used in Blasroute. Consequently, results from Blasroute starts in 1978 and runs through the end of 2013.

As described in the SOW, even though the model was run from 1975-2013, the validation period was limited to the time period 2003-2013 (11 years) since the land use conditions are most representative for this period. The charts shown are over this time frame. Charts that show accumulated water volume represent the cumulative water volume since January 1, 2003. This is the case with all following charts that show water volume. The presented goodness-of-fit (GOF) statistics are calculated over the 2003-2013 time frame.

As was discussed in the previous sections, there have been significant updates to the basin areas, land use, soils, and hydrography datasets, while the model was run "as-is" and no values were recalibrated. The input land use and soils parameters for GLEAMS, EAAMOD, and special case land uses were identical to those used for the 2009 study. However, the feature classes associated with both land use and soils have been updated so not all areas simulated fall under the same categories as in the previous study. Additionally, changes to the model domains have resulted in some domains that were simulated as independent areas in 2009 now being incorporated into a larger sub-watershed. This makes direct comparisons between the two studies difficult without extensive recalibration. Lastly, due to the use of hydrography from AHED rather than the datasets used in 2009, many reaches have to be re-parameterized with respect to cross-sections, bottom elevations, and water quality attenuation coefficients.

Consequently, many of the results do not match measured values well. **Recalibration of the model is required before any water volume or nutrient loading predictions are to be made. Recalibration will first require the verification of input parameters' accuracy, particularly for structure controls and hydrography connectivity. These initial setup runs also used the default assimilation/attenuation coefficients without calibration, therefore the results presented below should be considered as preliminary test runs. These results will be used during the upcoming recalibration process to identify input data errors and then used as the**

**starting point for recalibration focusing on those parameters identified during the upcoming sensitivity analysis as important.**

The general approach to recalibration is to calibrate the simulated flow values to measured values of flow first. Only after a satisfactory fit has been obtained will the model be calibrated for nutrient data. The reasoning for this is that while concentrations can be affected by a large extent by flow, it is rare that a change in calibration for water quality has an influence on flow. That will typically only happen when, for example, changes in fertilization practices affect crop growth, which in turn can affect runoff and percolation to some extent. Such effects are typically not large.

The technique for calibration when there are external flows entering a model domain (generally referred to as "pass through" water) is to use either the measured flow and concentration data for the inlet structure or the simulated flow and concentration data from the upstream model domain as inflow boundary conditions. Pass through water only exists for the Indian Prairie and Lower Kissimmee sub-watersheds where S-68 flows from the Istokpoka sub-watershed enter the Indiana Prairie sub-watershed and S-65 from the Upper Kissimmee sub-watershed and S84 from the Indiana Prairie sub-watershed flow into the Lower Kissimmee sub-watershed. Generally measured data boundary conditions will be used when available and the upstream simulated data used when measured data are not available.

## 4.1 Fisheating Creek

### 4.1.1 Flows and Water Quality Data at SR-78

Accumulated flow at SR-78 (SFWMD Station FISHCR) over the 2003-2013 period is shown in Figure 14, while tabulated annual volumes are shown over the same period in Table 8. Note that measured data was not collected prior to 1997. As can be seen, the simulation results underestimate the true values over the validation period by 14%, with the largest underestimates in 2003 and 2005 and a pronounced overestimate in 2010. Relevant statistics for daily values from 2003-2013 are shown in Table 9. The statistics show a large underestimation of the measured flow data at SR-78, and the Nash-Sutcliffe efficiency statistic is barely greater than zero, indicating a poor fit on the daily statistics.

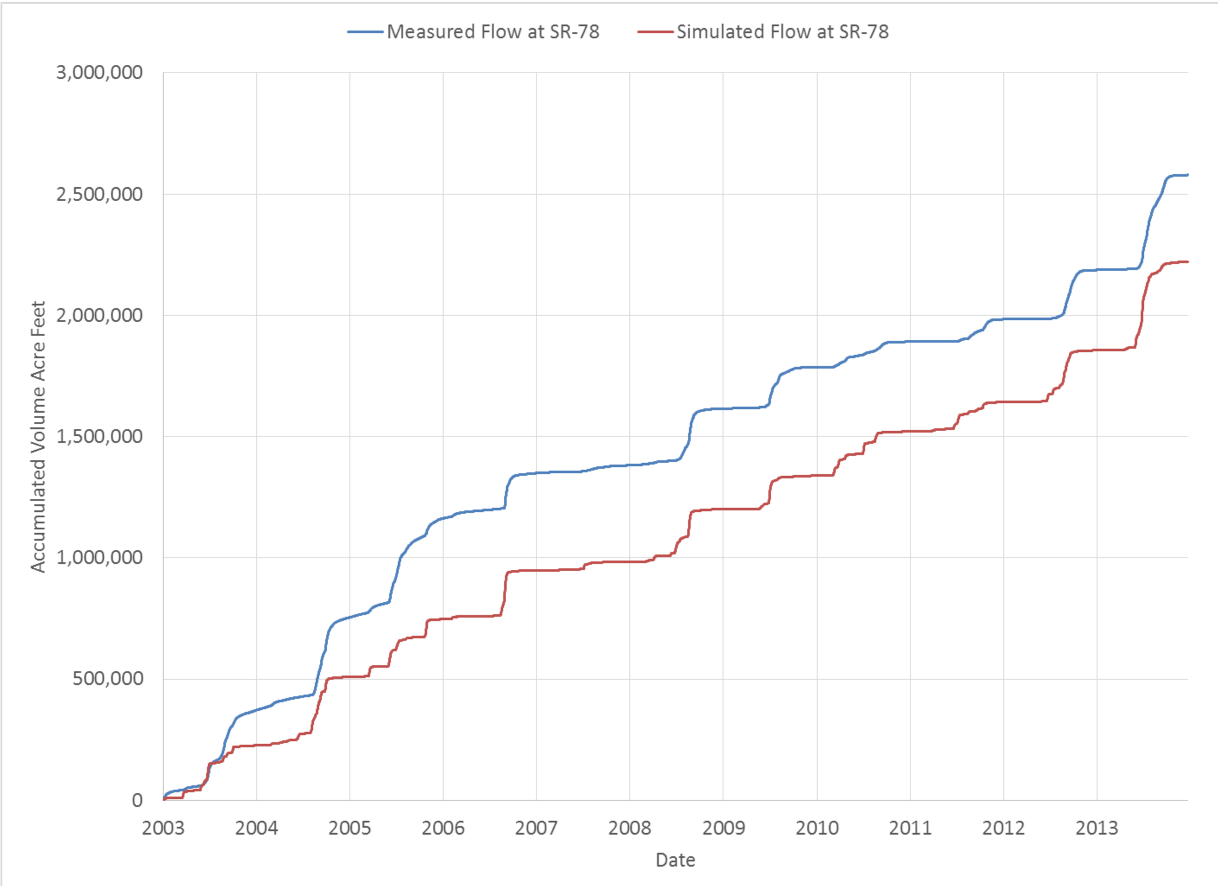


**Figure 14. Measured and simulated accumulated water volumes at SR-78.**

**Table 8. Comparison of measured and simulated water volumes at SR-78.**

| Year | Measured Volume (Acre/Feet) | Simulated Volume (Acre/Feet) | Ratio of Simulated to Measured |
|---|---|---|---|
| **2003** | 373,353 | 227,209 | 61% |
| **2004** | 382,493 | 281,921 | 74% |
| **2005** | 408,393 | 238,028 | 58% |
| **2006** | 186,635 | 201,429 | 108% |
| **2007** | 32,533 | 35,237 | 108% |
| **2008** | 233,656 | 216,563 | 93% |
| **2009** | 171,137 | 140,972 | 82% |
| **2010** | 104,877 | 179,257 | 171% |
| **2011** | 92,379 | 121,352 | 131% |
| **2012** | 203,101 | 213,885 | 105% |
| **2013** | 392,484 | 364,456 | 93% |
| Total | **2,581,041** | **2,220,308** | **86%** |

**Table 9. Statistics of daily flow values at SR-78.**

| Statistic | Value | Unit |
|---|---|---|
| **Bias** | -1.28 | m^3/s |
| **Nash–Sutcliffe** | 0.02 | - |
| **RMSE** | 17.24 | m^3/s |
| **RMSE/Sigma** | 0.99 | - |

Comparisons between measured and simulated total N concentrations are shown in Figure 15. The simulated total N concentrations show considerably more variability than the measured values, with the lowest simulated values in the 0.5 mg/l range, with a number of spikes peaking above 3 mg/l.

The overall pattern indicates that the background concentration parameter in WAM is too low for this sub-watershed (at least for the areas above the measurement point), while the spikes in concentration result from too little attenuation of nitrogen in runoff during rainfall events. The recalibration effort will focus on adjusting the background concentration values (the WAM *Cb* parameter) close to the lowest observed values of 1 mg/l, and concurrently increasing the WAM attenuation coefficient *a*.

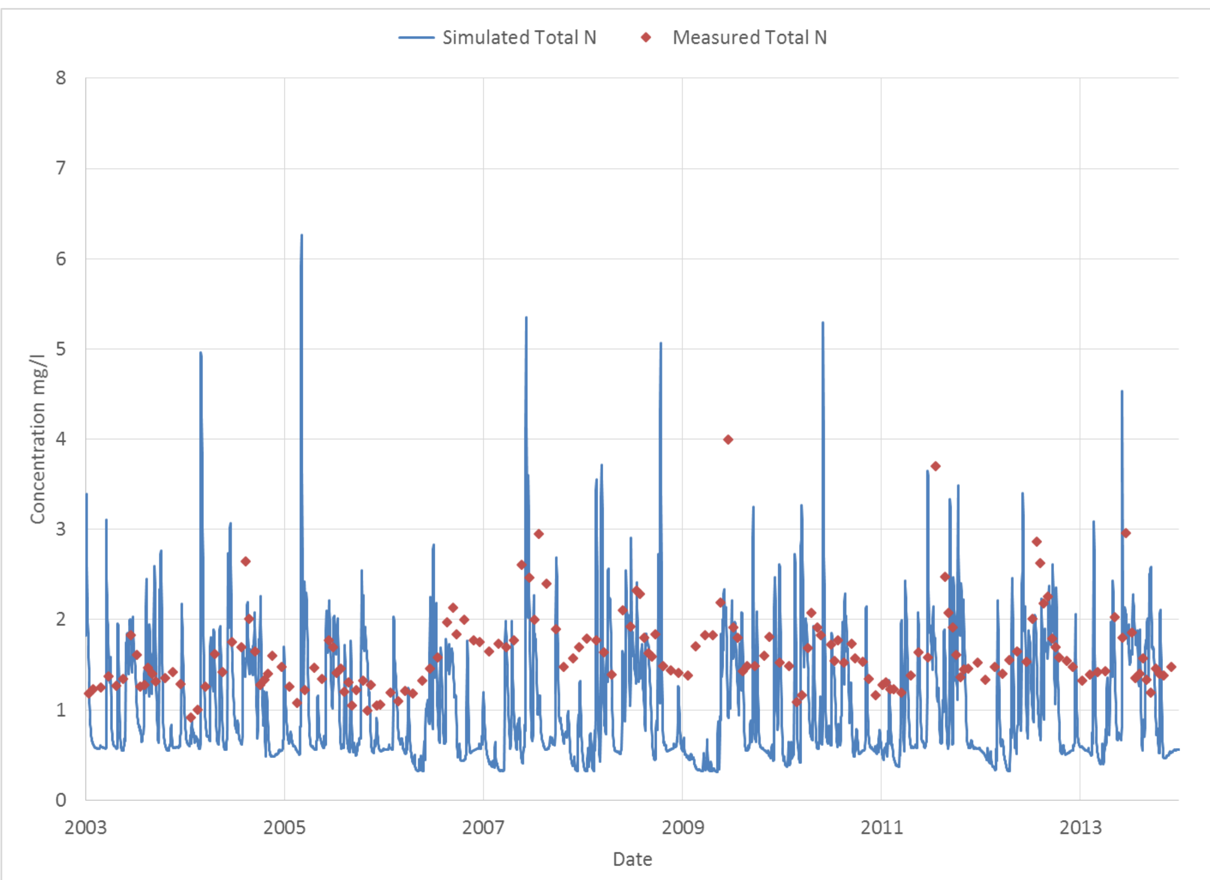


**Figure 15. Comparison of measured and simulated total N concentrations at SR-78**

Comparisons between measured and simulated total P concentrations at SR-78 are shown in Figure 16. The lower range of simulated values is quite close to the lower range of the measured values, but the simulated values do not display as much variability as the measured values, with peak values falling below the peak measurements.

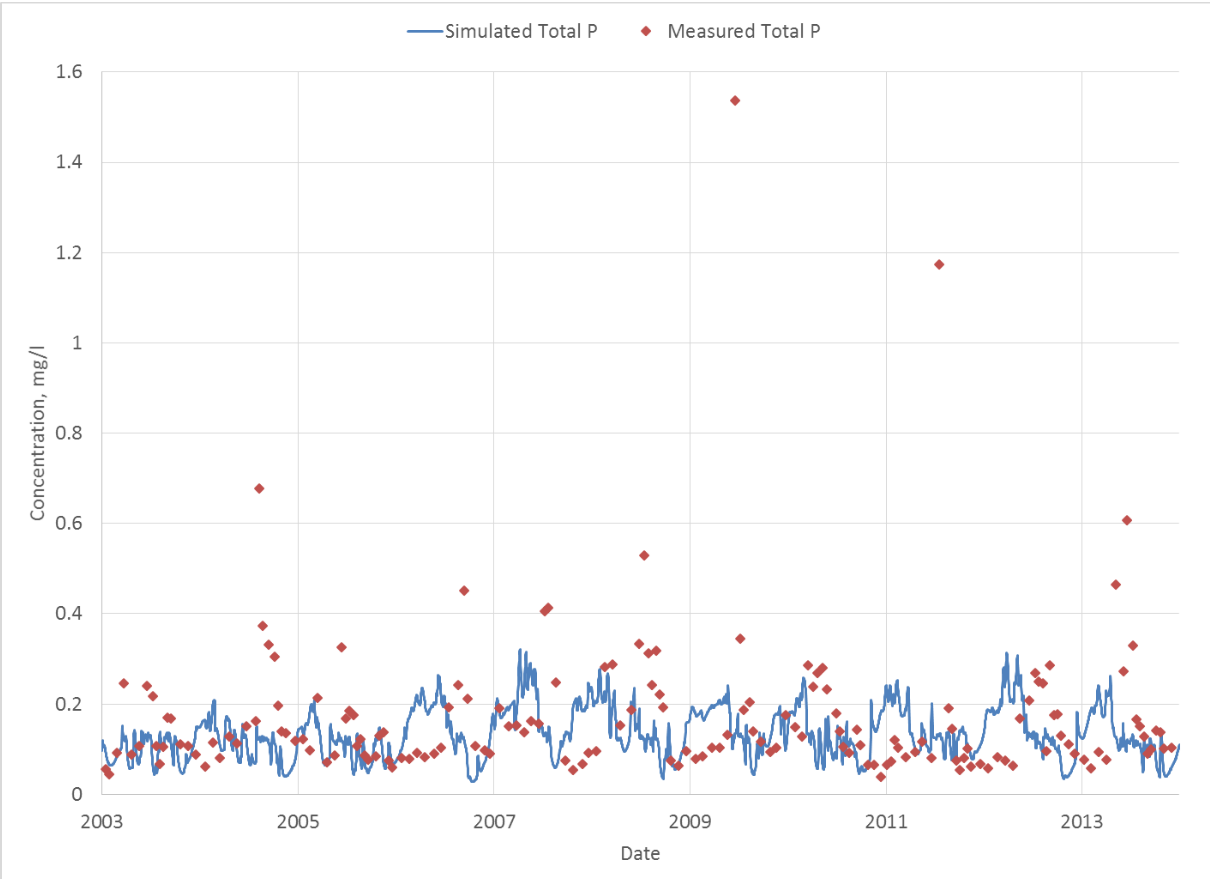


**Figure 16. Comparison of measured and simulated total P concentrations at SR-78.**

### 4.1.2 Flow Data at US-27

The accumulated flow at US-27 (SFWMD Station FISHP) is shown in Figure 17 with tabulated annual volumes shown in Table 10. As with the data at SR-78, simulated volumes in 2003, 2005, and 2009 considerably underestimate the measured values, while the simulated volume in 2006 and 2010 overestimates the measured volume for that year. Overall, for the 11 year comparison period, the model underestimates the measured volume by 13%. Relevant statistics for daily values from 2003-2013 are shown in Table 11. The statistics show a large underestimation (bias) of the measured flow data at US-27, and the Nash-Sutcliffe efficiency statistic is slightly less than zero, indicating a poor fit (worse than simply using the average measured value) on the daily statistics.

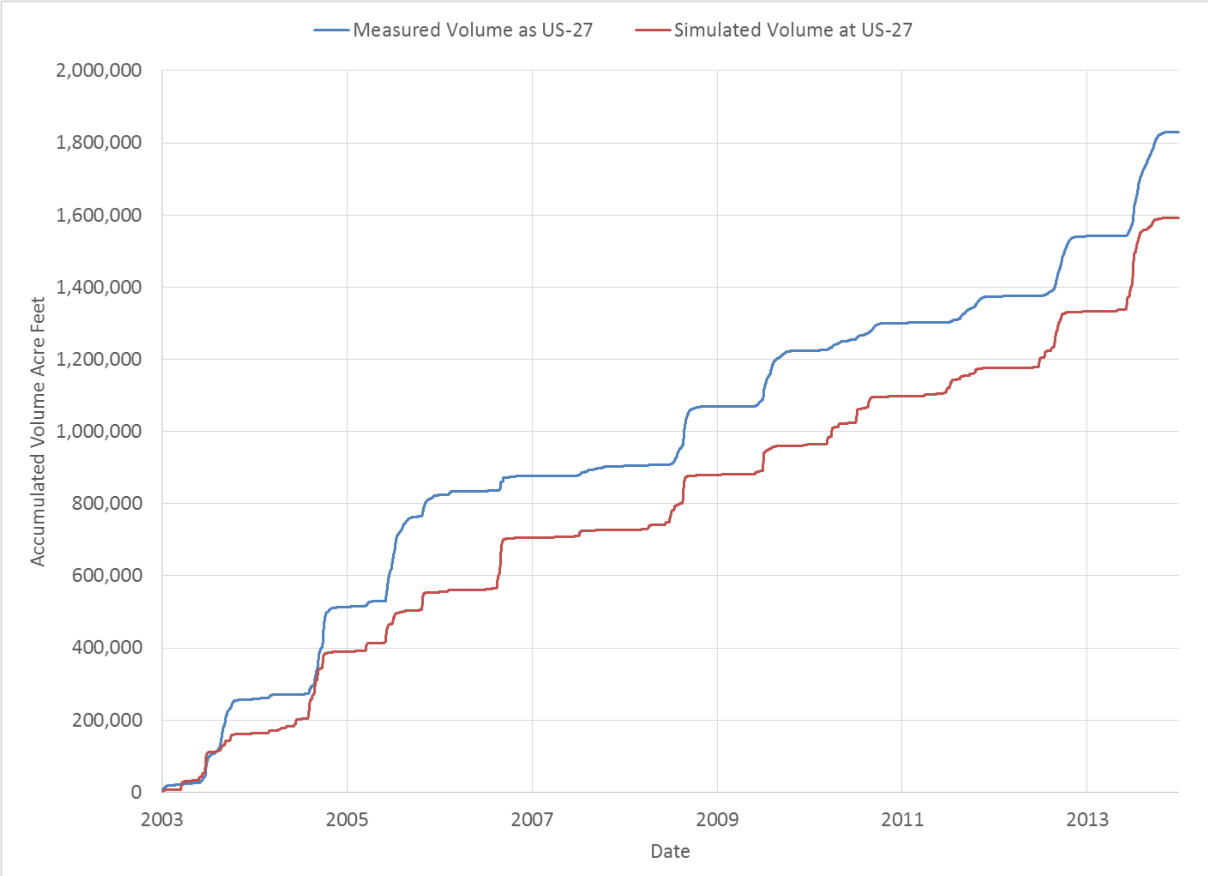


**Figure 17. Measured and simulated accumulated water volumes at US-27.**

**Table 10. Comparison of measured and simulated water volumes at US-27.**

| Year | Measured Volume (Acre/Feet) | Simulated Volume (Acre/Feet) | Ratio of Simulated to Measured |
|---|---|---|---|
| **2003** | 258,514 | 163,525 | 63% |
| **2004** | 254,841 | 226,450 | 89% |
| **2005** | 309,987 | 164,601 | 53% |
| **2006** | 52,515 | 150,957 | 287% |
| **2007** | 28,172 | 21,550 | 76% |
| **2008** | 165,864 | 153,063 | 92% |
| **2009** | 153,898 | 83,655 | 54% |
| **2010** | 76,785 | 133,357 | 174% |
| **2011** | 73,702 | 78,418 | 106% |
| **2012** | 166,899 | 156,913 | 94% |
| **2013** | 288,786 | 260,288 | 90% |
| **Total** | **1,829,963** | **1,592,776** | **87%** |

**Table 11. Statistics of daily flow values at US-27.**

| Statistic | Value | Unit |
|---|---|---|
| **Bias** | -0.84 | m^3/s |
| **Nash–Sutcliffe** | -0.03 | - |
| **RMSE** | 15.44 | m^3/s |
| **RMSE/Sigma** | 1.02 | - |

Water quality data have not been collected at US-27 since a small amount of samples were collected in the mid-1980s. Those data are not shown.

## 4.2 Indian Prairie

As discussed in the proceeding sections, the Indian Prairie sub-watershed includes several areas that were studied as separate basins in the 2009 WAM study. In that study, the L-48 and L-49 basins were simulated independently of the rest of the lower C-38 basin. The changes to the model domain have in turn significantly altered the WAM setup for the hydrography which has then caused some difficulty in obtaining satisfactory results. This will be remedied during the recalibration phase, as reach elevations and cross-sectional profiles will be adjusted to obtain better performance of the model in this basin.

### 4.2.1 Flow and Water Quality Data at S-127

Measured and simulated accumulated water volumes at the S-127 pump station are shown in Figure **18**. This drains the area of the sub-watershed that was modeled as the independent L-48 basin in the 2009 study. It is obvious that the model is not performing well, as the simulated volume is far below the measured values. One parameter that needs to be adjusted during the recalibration process is the seepage rate across the Lake Okeechobee levee. Seepage is simulated in WAM using reaches that incorporate small weirs between the lake and each canal reach outside the levee, with the weir sizing dependent on the length of the canal reach. That is done to allow larger reaches to accumulate more seepage using wider weirs. Since the hydrography setup changed between this study and the 2009 work these seepage reaches and weirs need to be resized via recalibration. The 2009 study determined seepage values across the levee between approximately 0.7 – 2.2 CFS per mile of levee. In addition, the collection areas for each reach must be examined in detail to ensure that no water is being routed incorrectly to other areas of Indian Prairie. This latter step was not required in the 2009 study since this was simulated as an independent basin, and all water within the basin was routed out the S-127 pump station.

Tabulated annual volumes at S-127 for the 2003-2013 time frame are shown are shown in Table 12 while statistics for flow values over the same period are shown in Table 13. The results show that the model is underestimating the total volume leaving the basin by over 70%. This is further indicated by the large negative bias.

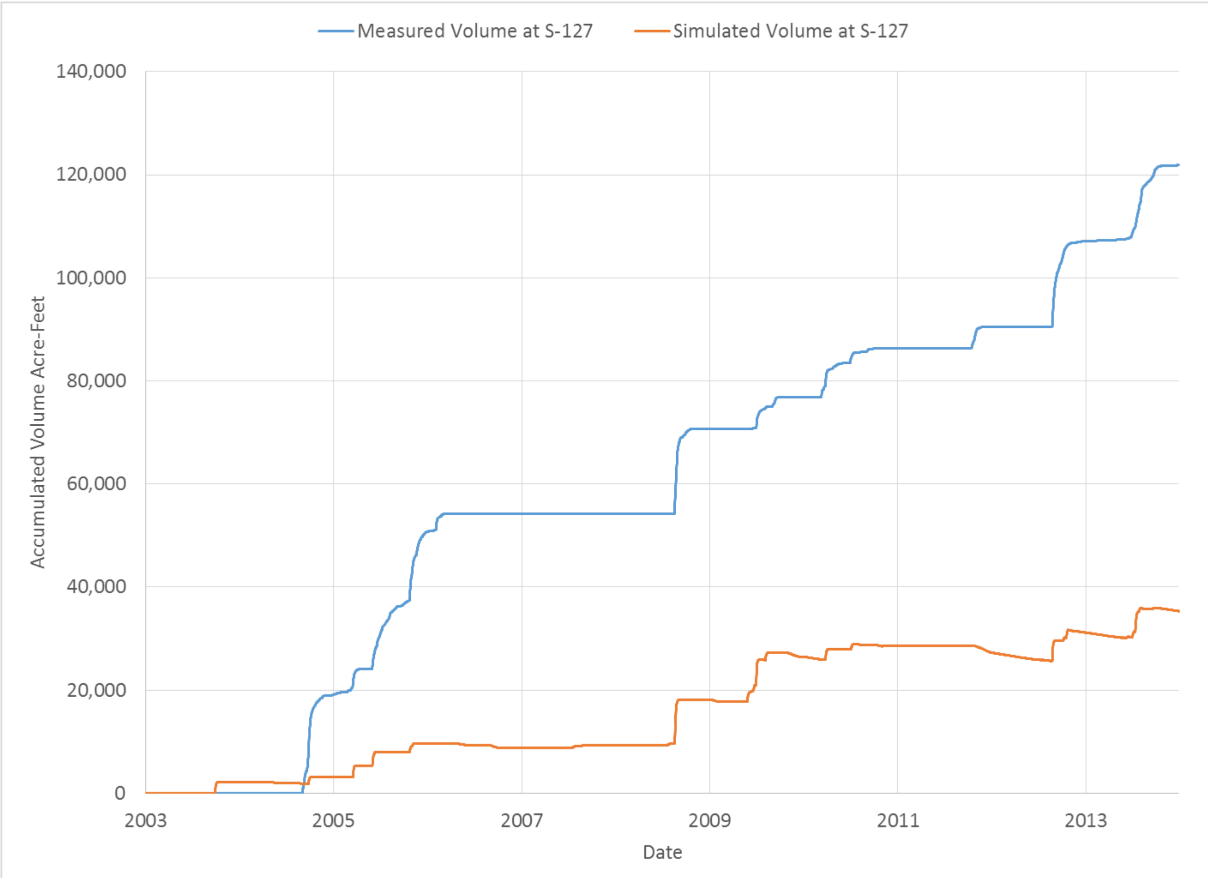


**Figure** 18. **Comparison of measured and simulated flow at S-127.**

**Table 12. Comparison of measured and simulated water volumes at S-127. In 2003 and 2007, there was no measured flow, so the ratio could not be determined, indicated by "N/A".**

| Year | Measured Volume (Acre/Feet) | Simulated Volume (Acre/Feet) | Ratio of Simulated to Measured |
|---|---|---|---|
| **2003** | 0 | 2,135 | N/A |
| **2004** | 19,057 | 1,046 | 5% |
| **2005** | 31,712 | 6,502 | 21% |
| **2006** | 3,382 | -943 | -28% |
| **2007** | 0 | 465 | N/A |
| **2008** | 16,553 | 8,838 | 53% |
| **2009** | 6,096 | 8,339 | 137% |
| **2010** | 9,523 | 2,170 | 23% |
| **2011** | 4,093 | -1,243 | -30% |
| **2012** | 16,681 | 3,871 | 23% |
| **2013** | 14,820 | 4,137 | 28% |
| **Total** | **121,917** | **35,317** | **29%** |

**Table 13. Statistics of daily flow values at S-127**

| Statistic | Value | Unit |
|---|---|---|
| **Bias** | -21.55 | m^3/s |
| **Nash–Sutcliffe** | 0.30 | - |
| **RMSE** | 92.22 | m^3/s |
| **RMSE/Sigma** | 0.84 | - |

Comparison of measured and simulated total N at S-127 is shown in Figure 19. Because the simulated flow data are incorrect not much weight should be given to these results, as they may change considerably once the flow simulations are corrected. However, it is clear that the simulated values of total N are under predicting the measured values. The simulated TN values average just under 1 mg/l, while the measured values average approximately 2 mg/l. Additionally, the simulated total N values show a greater degree of variability than the corresponding measured values.

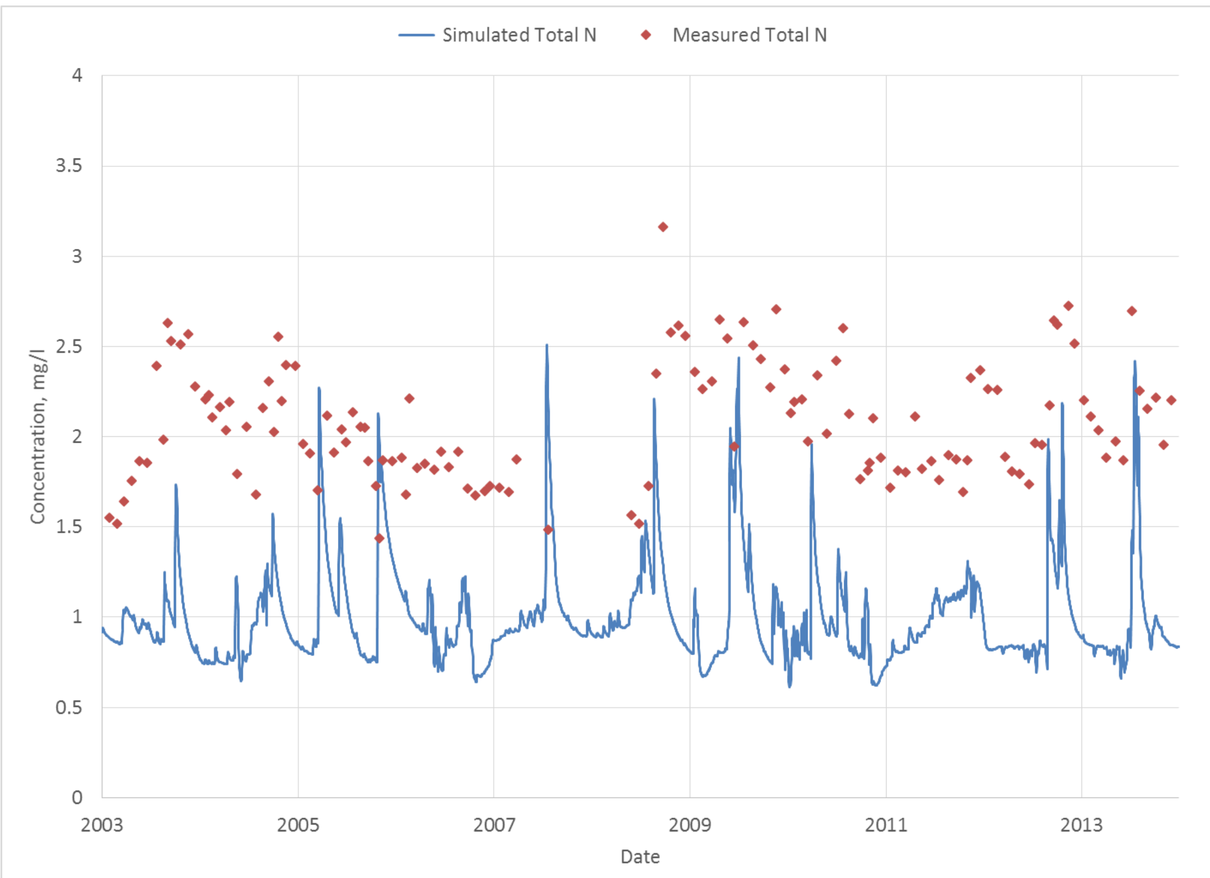


**Figure 19. Comparison of measured and simulated total N concentrations at S-127.**

Comparison of measured and simulated total P at S-127 is shown in Figure 20. As with the total N values, since the simulated flow data are incorrect little weight should be given to these results. Here, the simulated total P values clearly overestimate the measured value, with the simulated P values averaging approximately 0.3 mg/l and the measured P values averaging about 0.15 mg/l.

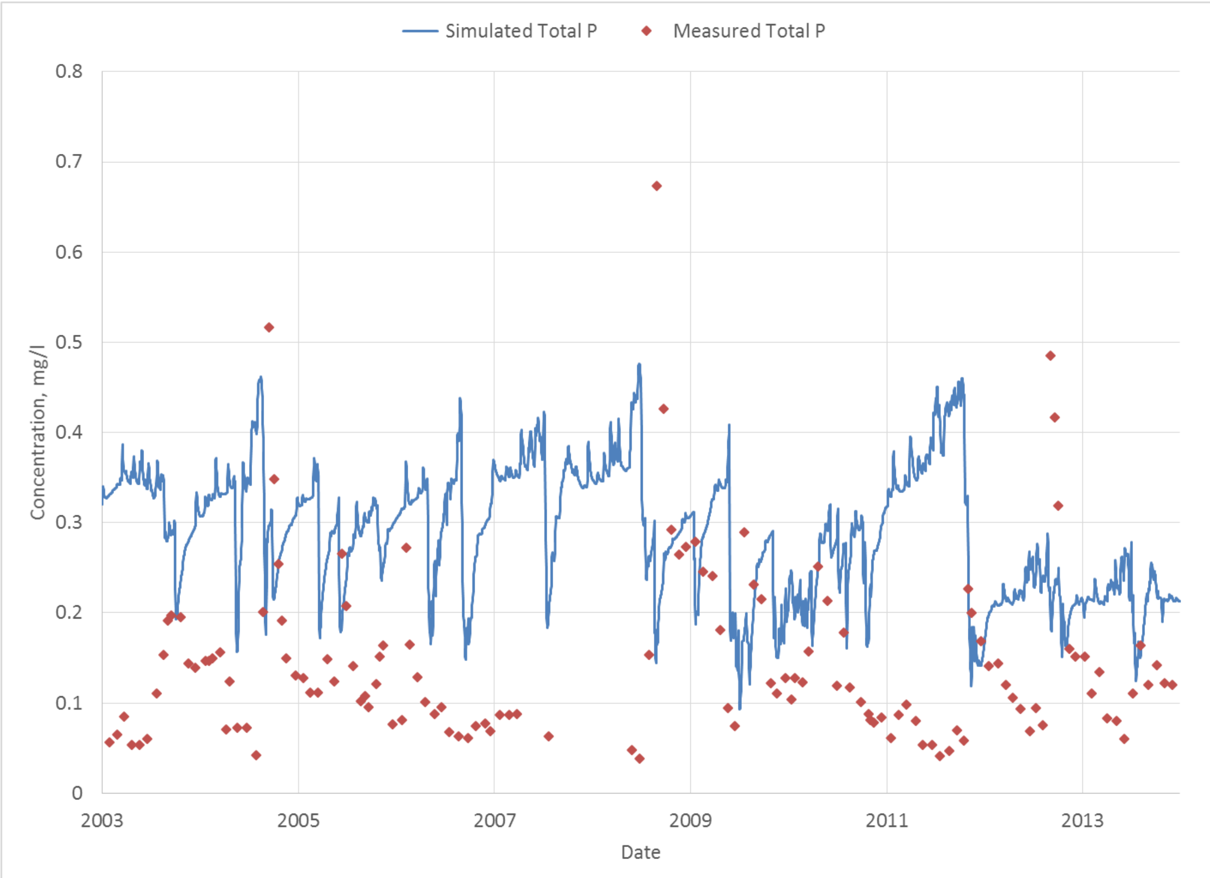


**Figure 20. Comparison of measured and simulated total P concentrations at S-127.**

### 4.2.2 Flow and Water Quality Data at S-129

Measured and simulated accumulated water volumes at the S-129 pump station are shown in Figure 21. This drains the area of the sub-watershed that was modeled as the independent L-49 basin in the 2009 study. As with the flow data at S-129, it is obvious that the model is not performing well, with the simulated volume again far below the measured values. Tabulated values of water volume leaving S-129 are shown in Table 14 while Table 15 shows the relevant statistics for daily values from the 2003-2013 period. The tabulated values and the statistics reflect the same large underestimate of the flow and volume.

Recalibration will again focus on the same potential issues that are occurring with the L-48 basin. Comparison of measured and simulated total N at S-129 is shown in Figure 21. As with the results for nutrients at the S-127 structure, not much weight should be given to these results, as they may change once the flow simulations are corrected. It is clear that the simulated values of total N are under predicting the measured values. The simulated total N values average approximately 0.75 mg/l, while the measured values average approximately 1.6 mg/l. Additionally, the simulated total N values show a greater degree of variability than the corresponding measured values.

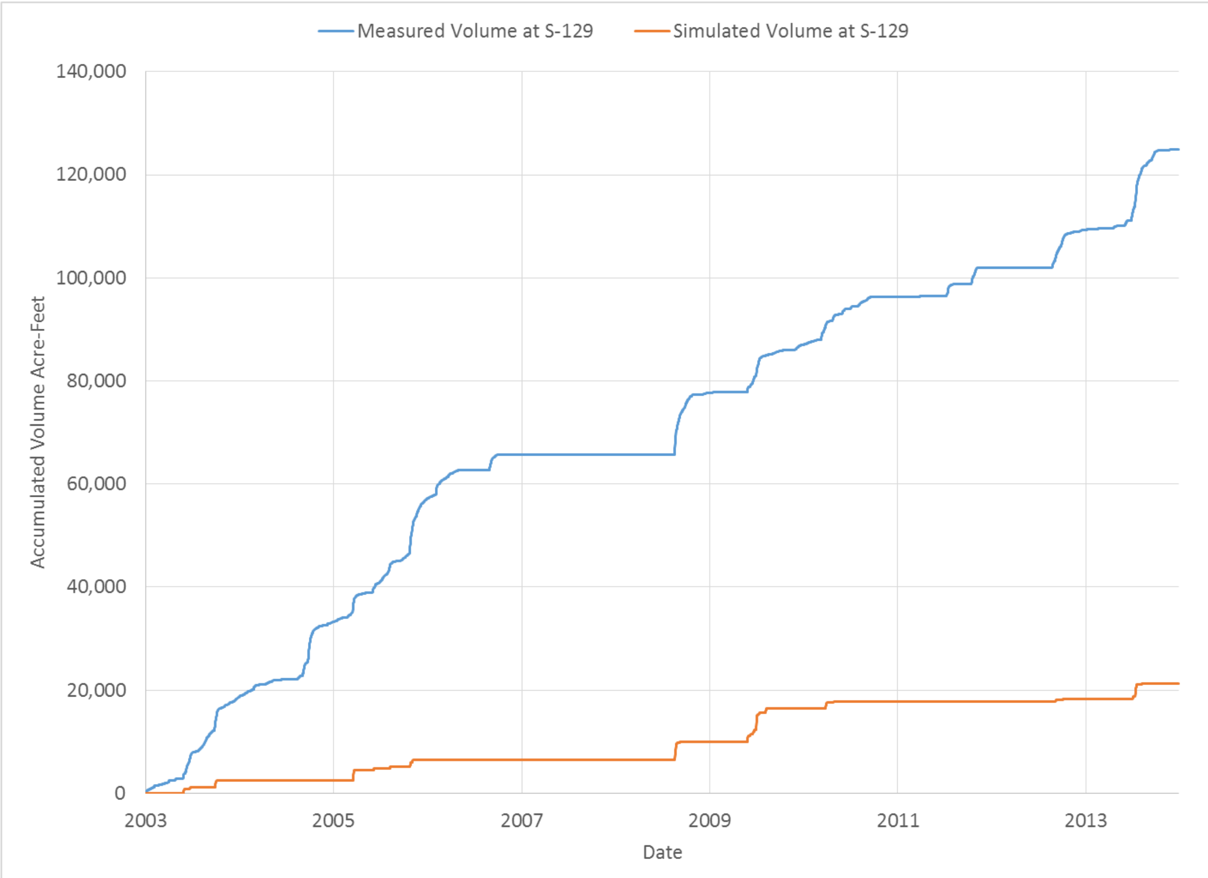


**Figure 21. Comparison of measured and simulated flow at S-129.**

**Table 14. Comparison of measured and simulated water volumes at S-129. In 2007 there was no measured flow, so the ratio could not be determined, indicated by "N/A".**

| Year | Measured Volume (Acre/Feet) | Simulated Volume (Acre/Feet) | Ratio of Simulated to Measured |
|---|---|---|---|
| **2003** | 18,825 | 2,531 | 13% |
| **2004** | 14,385 | 0 | 0% |
| **2005** | 23,945 | 3,904 | 16% |
| **2006** | 8,479 | -1 | 0% |
| **2007** | 0 | 89 | N/A |
| **2008** | 12,051 | 3,490 | 29% |
| **2009** | 9,367 | 6,407 | 68% |
| **2010** | 9,277 | 1,380 | 15% |
| **2011** | 5,706 | 0 | 0% |
| **2012** | 7,244 | 484 | 7% |
| **2013** | 15,632 | 2,995 | 19% |
| **Total** | **124,911** | **21,279** | **17%** |

**Table 15. Statistics of daily flow values at S-129.**

| Statistic | Value | Unit |
|---|---|---|
| **Bias** | -25.79 | m^3/s |
| **Nash–Sutcliffe** | 0.12 | - |
| **RMSE** | 76.25 | m^3/s |
| **RMSE/Sigma** | 0.94 | - |

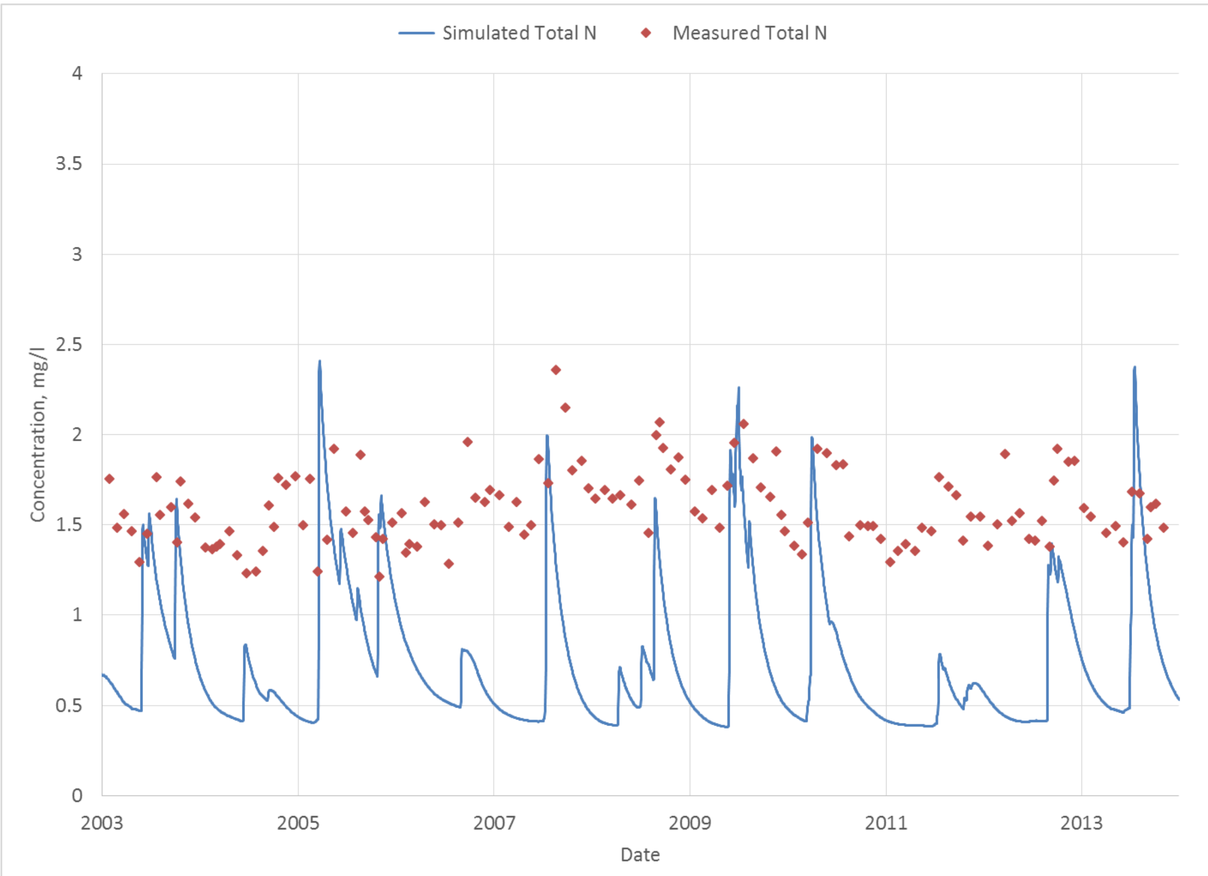


**Figure 22. Comparison of measured and simulated total N concentrations at S-129.**

Comparison of measured and simulated total P at S-129 is shown in Figure 23. As with the total N values, since the simulated flow data are incorrect little weight should be given to these results. Here, the simulated total P values clearly overestimate the measured value, with the simulated P values averaging just below 0.2 mg/l and the measured P values averaging about 0.07 mg/l.

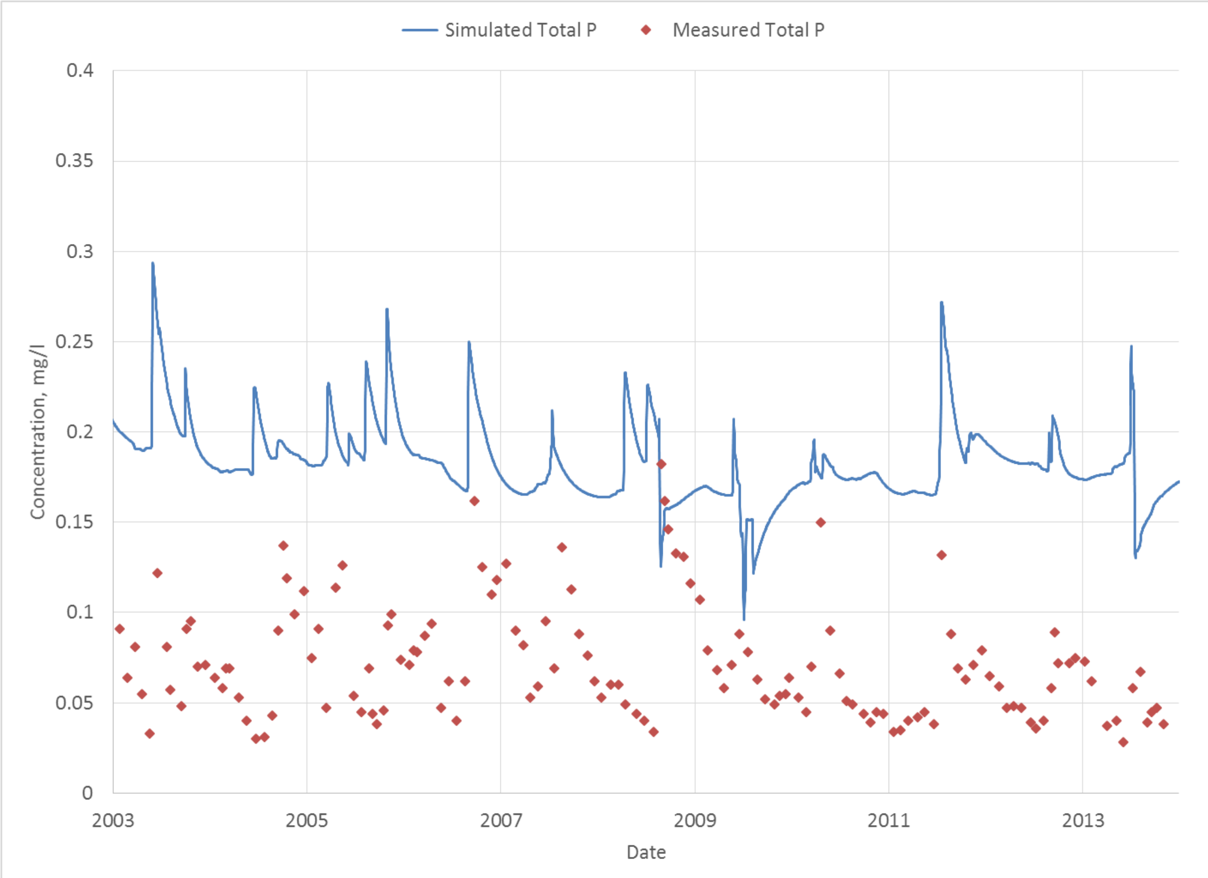


**Figure 23. Comparison of measured and simulated total P concentrations at S-129.**

## 4.3 Lake Istokpoga

The Lake Istokpoga sub-watershed has its main outflow at S-68, on the southeastern site of Lake Istokpoga. This discharge point is an inflow boundary to Indian Prairie.

### 4.3.1 Flow and Water Quality Data at S-68

Figure 24 shows the comparison between measured and simulated flow volumes at S-68. Corresponding tabulated data is shown in Table 16. Although the total volumes over the entire period are within 3%, a very good match, the model under predicts the volume in 2005, 2006, and 2008, while over predicting in 2010 and 2011. The separation shown in Figure 24 starting in 2005 reflects this, with the gap closing after 2011. The average measured flow over the period shown is 10.4 $m^3/s$, while the average simulated flow is nearly 10.7 $m^3/s$.

Relevant statistics for daily values from 2003-2013 are shown in Table 17. The statistics show a slight overestimation of the measured flow data at S-68 over the period, but the Nash-Sutcliffe efficiency statistic, at -0.33, is considerably less than zero, indicating a poor fit on the daily statistics. Improving the estimation during the 2005-2008 and 2010-2011 periods will help improve this fit.

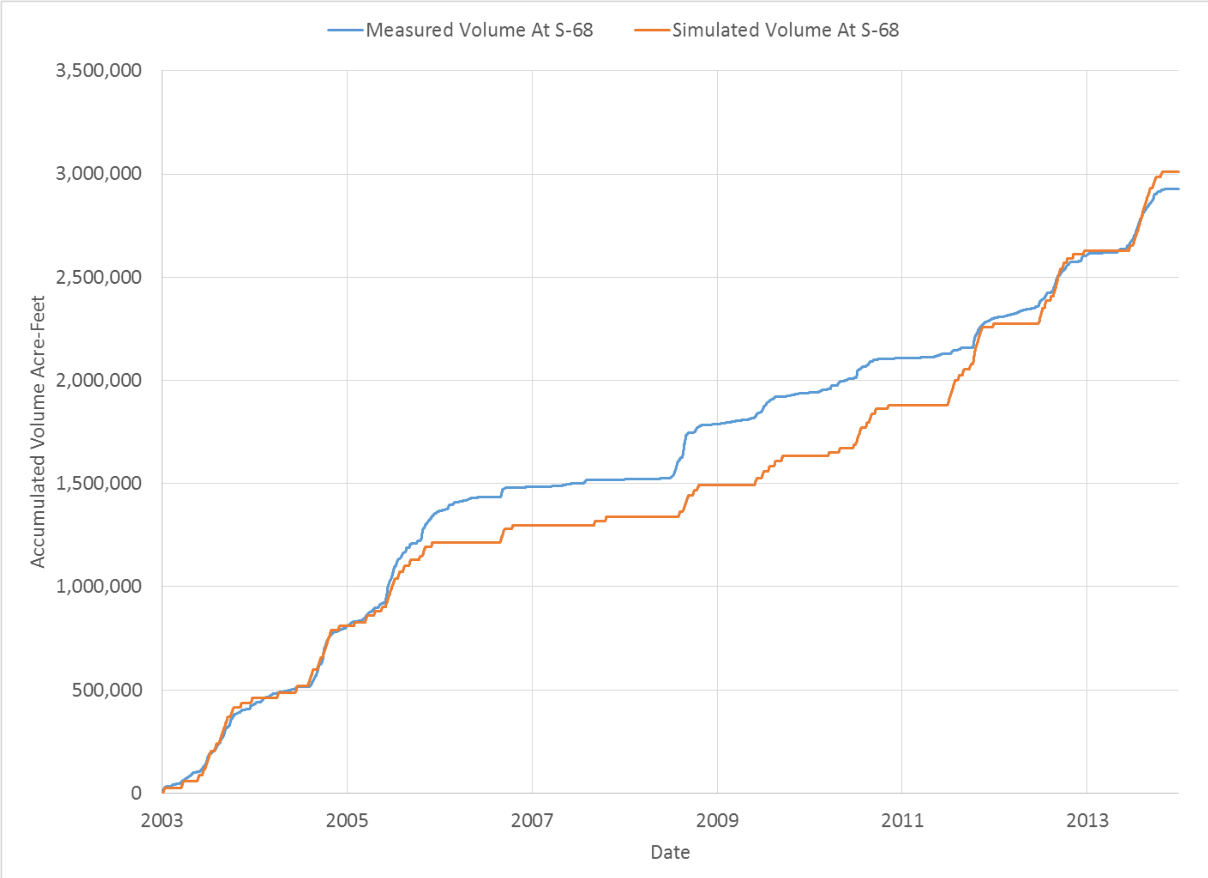


**Figure 24. Comparison of measured and simulated accumulative flow at S-68.**

**Table 16. Measured and simulated accumulative water volumes at S-68.**

| Year | Measured Volume (Acre/Feet) | Simulated Volume (Acre/Feet) | Ratio of Simulated to Measured |
|---|---|---|---|
| **2003** | 430,589 | 459,316 | 107% |
| **2004** | 377,520 | 349,548 | 93% |
| **2005** | 557,840 | 406,594 | 73% |
| **2006** | 117,052 | 82,726 | 71% |
| **2007** | 35,581 | 39,789 | 112% |
| **2008** | 268,961 | 154,365 | 57% |
| **2009** | 152,237 | 140,080 | 92% |
| **2010** | 168,026 | 248,701 | 148% |
| **2011** | 192,845 | 395,026 | 205% |
| **2012** | 304,932 | 353,369 | 116% |
| **2013** | 323,488 | 381,434 | 118% |
| **Total** | 2,929,071 | 3,010,949 | 103% |

**Table 17. Statistics of daily flows at S-68**

| Statistic | Value | Unit |
|---|---|---|
| **Bias** | 0.29 | m^3/s |
| **Nash–Sutcliffe** | -0.33 | - |
| **RMSE** | 20.50 | m^3/s |
| **RMSE/Sigma** | 1.15 | - |

Figure 25 shows comparison between measured total N and the simulated total N values at S-68. The simulated values show less variability than the measured values over the simulation period and appear on average to underestimate the measured values.

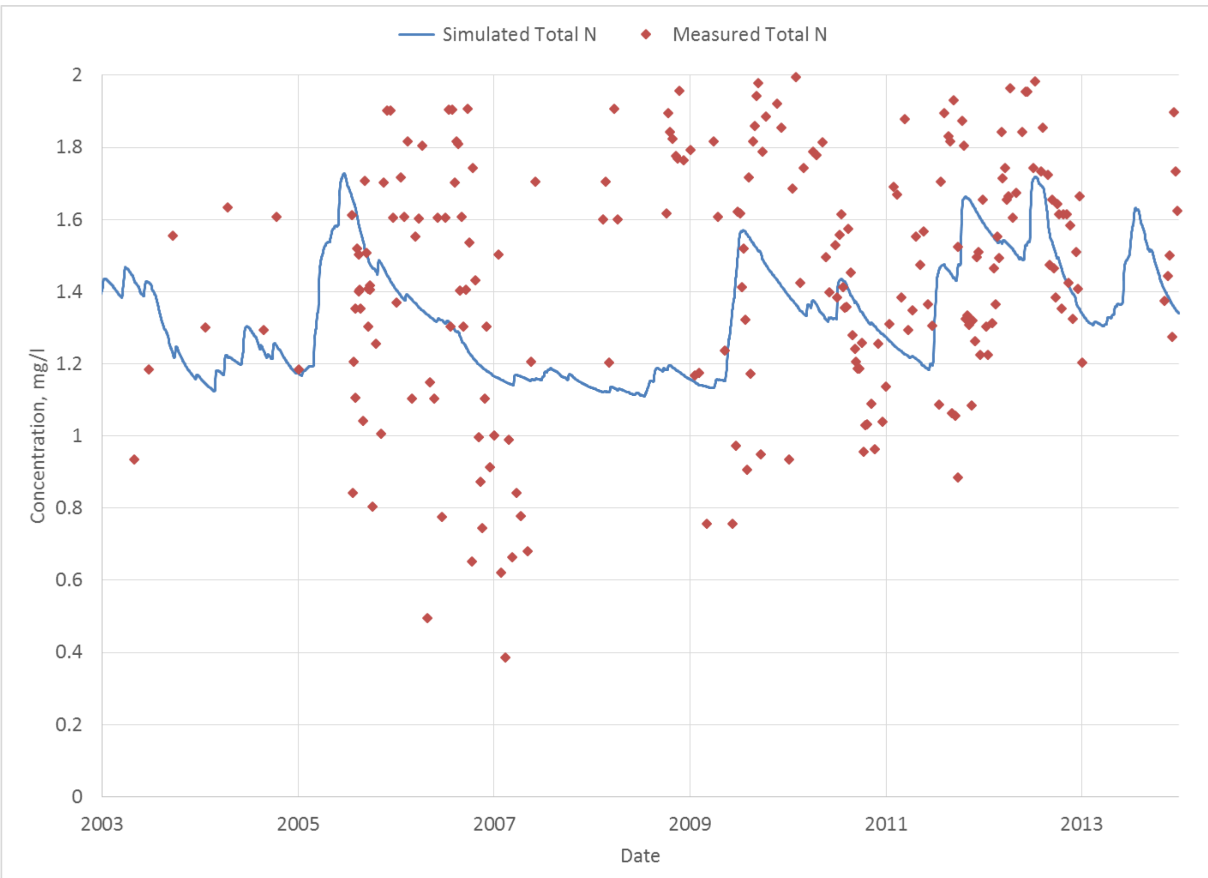


**Figure 25. Comparison of measured and simulated total N concentrations at S-68**

Figure 26 shows the comparison between measured total P data and the simulated total P values. It is clear that the model is underestimating the total P at S-68 by a large margin. This most likely indicates a need to pay particular attention to the attenuation parameters in Lake Istokpoga, since it acts as a significant buffer to nutrient concentrations at S-68, which is at the exit point from the lake.

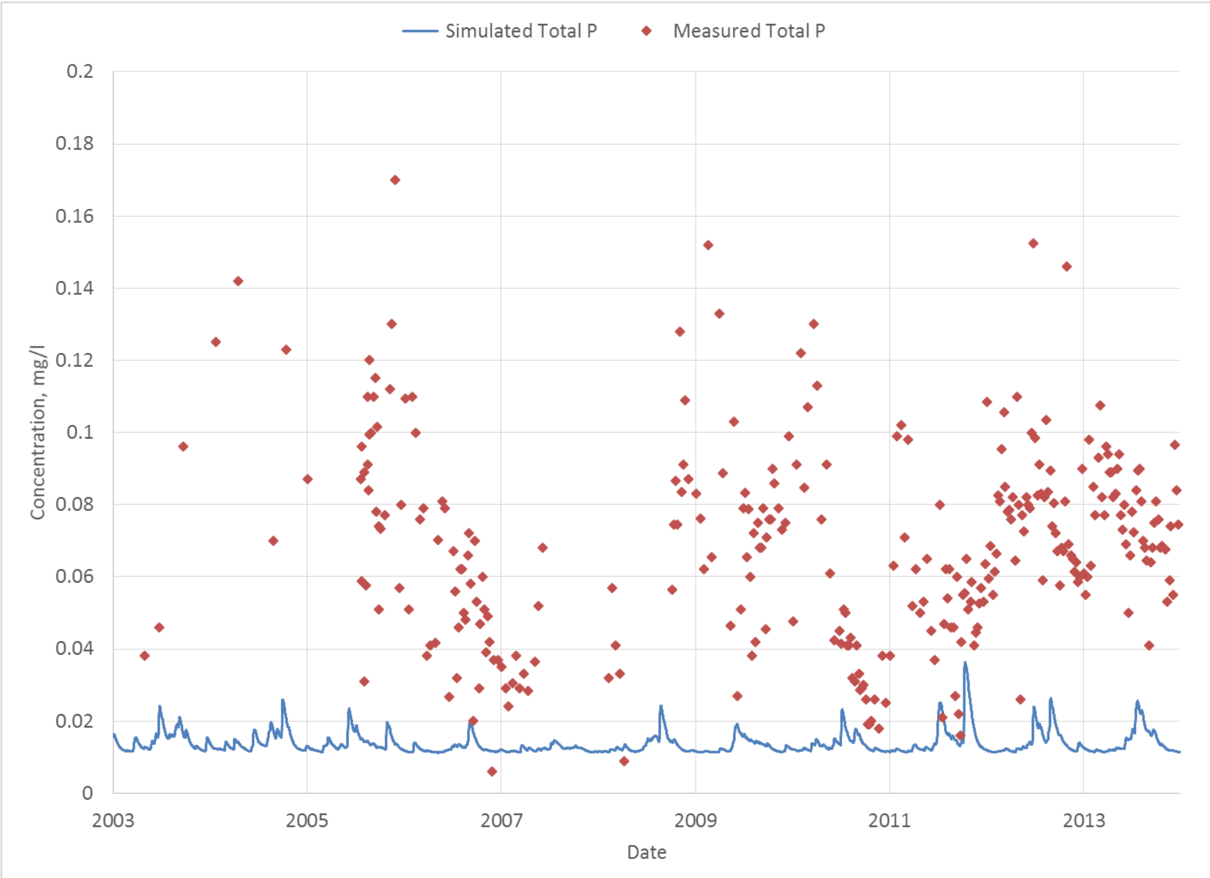


**Figure 26. Comparison of measured and simulated total P concentrations at S-68**

## 4.4 Lower Kissimmee

During the initial set up of WAM for the Lower Kissimmee sub-watershed, the decision was made to use the measured outflow at S-65 for the inflow at the upper boundary of the model. We want to emphasize that for the calibration of the model, once the Upper Kissimmee sub-watershed is satisfactorily calibrated the **modeled outflow**, not the measured outflow, at S-65 will be used as the upper boundary inflow for the Lower Kissimmee model domain. The rationale for using the measured flow data for model input was to avoid making decisions about the hydrographic network as well as any initial calibration decisions based on the use of un-calibrated inflow data.

To show an appropriate comparison for this report, the flow data presented for S-65A, S-65C, S-65D, and S-65E all represent the differences in flow by subtracting the daily inflows from both the measured and simulated values. The “flow differences” (both measured and simulated) are then compared at each structure. While not providing an exact comparison between measured and simulated values, it does give a good indication of how well the model is simulating the contributing area to the structure, without the identical flow values contributed at the inflow dominating the comparisons.

Note that the same issue exists for the nutrient concentration data, however there is no meaningful way to subtract concentration values to arrive at a useful comparison, since the in-stream attenuation processes dominate the simulated concentration values. The comparisons between total N and total P are simply of the “raw” measured and simulated values.

### 4.4.1 Flow and Water Quality Data at S-65A

Figure 27 shows a comparison between measured and simulated accumulated water volumes differences at S-65A compared to S-65. As was discussed above, the chart data were calculated by subtracting the boundary inflow data at the S-65 structure from both the simulated and measured values, so the chart data reflects the contribution from the sub-watershed between the S-65 and S-65A structures. The total accumulated volume over the 2003-2013 period matches quite closely (within 1%), but over the first half of the time period the simulated values over predict flow, while in 2008, 2012, and 2013 the simulated values under predict the measured values, see Table 13.

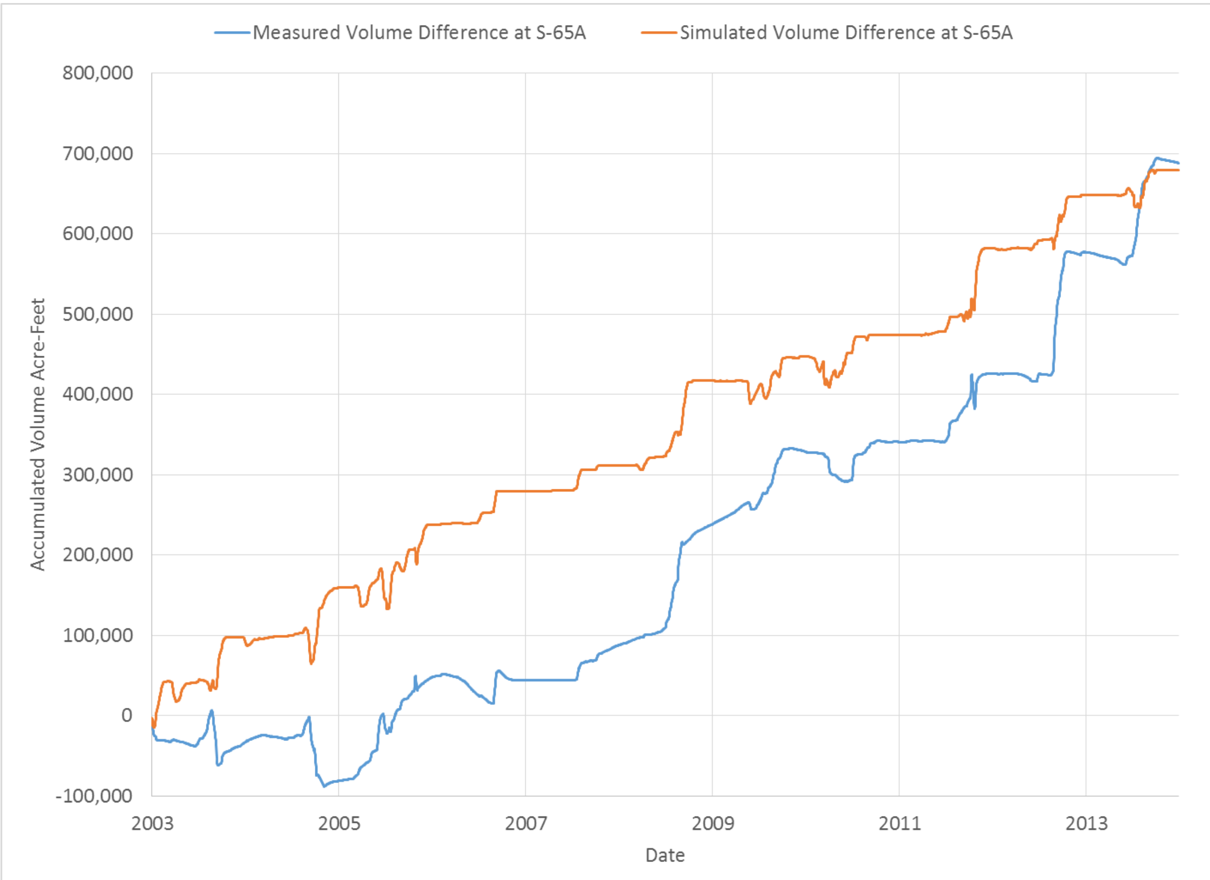


**Figure 27. Comparison of measured and simulated accumulative flow differences between S-65 and S-65A.**

**Table 18. Measured and simulated accumulative water volumes between S-65 and S-65A.**

| Year | Measured Volume (Acre/Feet) | Simulated Volume (Acre/Feet) | Ratio of Simulated to Measured |
|---|---|---|---|
| **2003** | -33,064 | 92,687 | -280% |
| **2004** | -47,831 | 66,791 | -140% |
| **2005** | 128,797 | 78,308 | 61% |
| **2006** | -3,192 | 42,204 | -1322% |
| **2007** | 42,917 | 31,740 | 74% |
| **2008** | 150,870 | 105,293 | 70% |

| | | | |
|---|---|---|---|
| **2009** | 90,224 | 30,204 | 33% |
| **2010** | 11,997 | 27,232 | 227% |
| **2011** | 85,479 | 107,432 | 126% |
| **2012** | 151,150 | 66,535 | 44% |
| **2013** | 110,773 | 30,606 | 28% |
| **Total** | 688,120 | 679,031 | 99% |

Figure 28 shows comparisons of measured and simulated total N concentrations at S-65A. The measured values mostly lie in a fairly narrow range between 1 and 1.5 mg/l. The simulated values are far more variable, with most of the “baseline” levels far too low at 0.1 mg/l and periodic spikes over 2.5 mg/l.

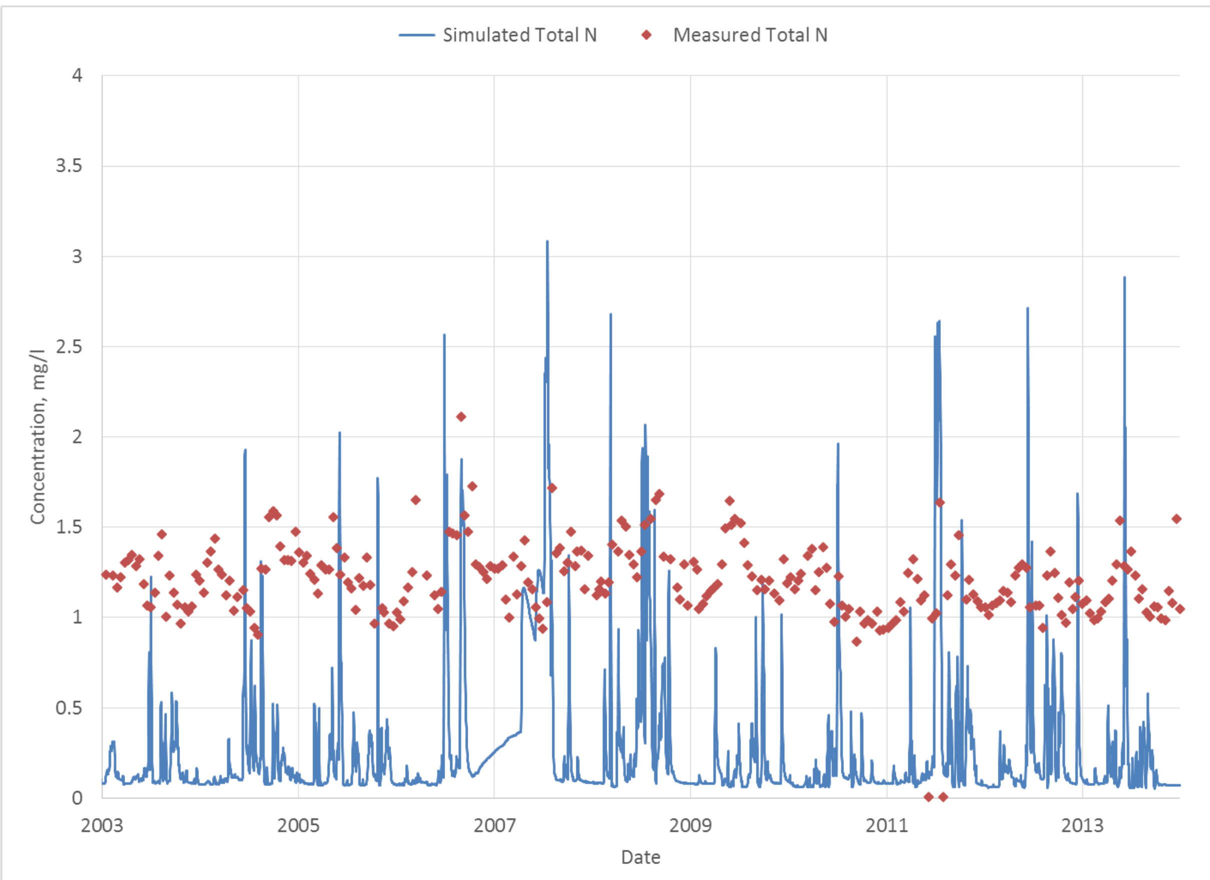


**Figure 28. Comparison of measured and simulated total N concentrations at S-65A.**

Figure 29 shows comparisons of measured and simulated total P concentrations at S-65A. In contrast with total N values, the measured P values are much more variable, with many values at the lower end clustered around 0.035 mg/l, but spiking up over 0.15 mg/l, with some values topping 0.3. The simulated total P values track the measured values moderately well, but the “baseline” levels somewhat too low at 0.02 mg/l

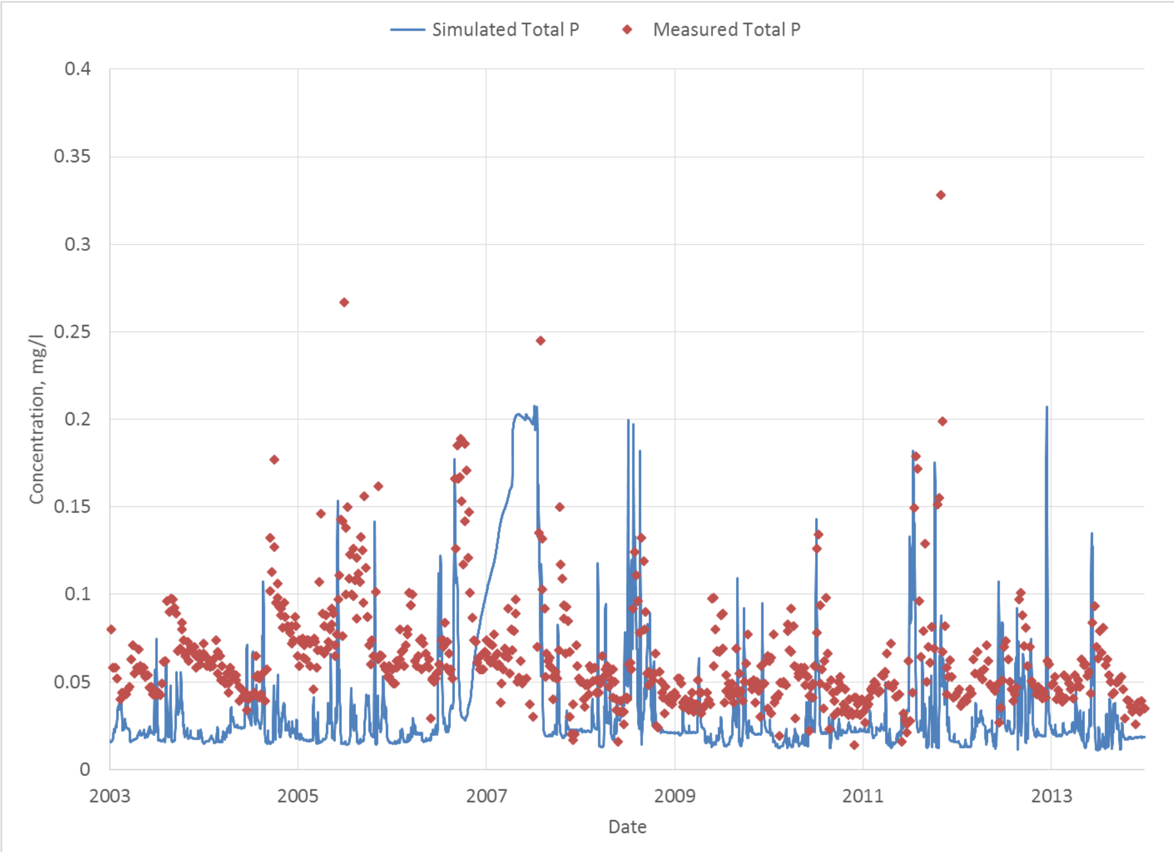


**Figure 29. Comparison of measured and simulated total P concentrations at S-65A.**

### 4.4.2 Flow and Water Quality Data at S-65C

Figure 30 shows a comparison between measured and simulated accumulated water volumes at S-65C. As was discussed above, the chart data were calculated by subtracting the boundary inflow data at the S-65 structure from both the simulated and measured values, so the chart data reflects the contribution from the sub-watershed between the S-65 and S-65C structures. In contrast with the difference in accumulated volumes at S-65A shown in Figure 27 the simulated values under predict the measured values over the time period and end up considerably lower (by 43%) at the end. In only three years (2006, 2007, and 2008) do the simulated values over predict the measured values, while in all other years the simulation under predicts the observed values. This indicates that the contribution of water from the surrounding areas to the lower Kissimmee River between the S-65A and S-65C structures are much too low.

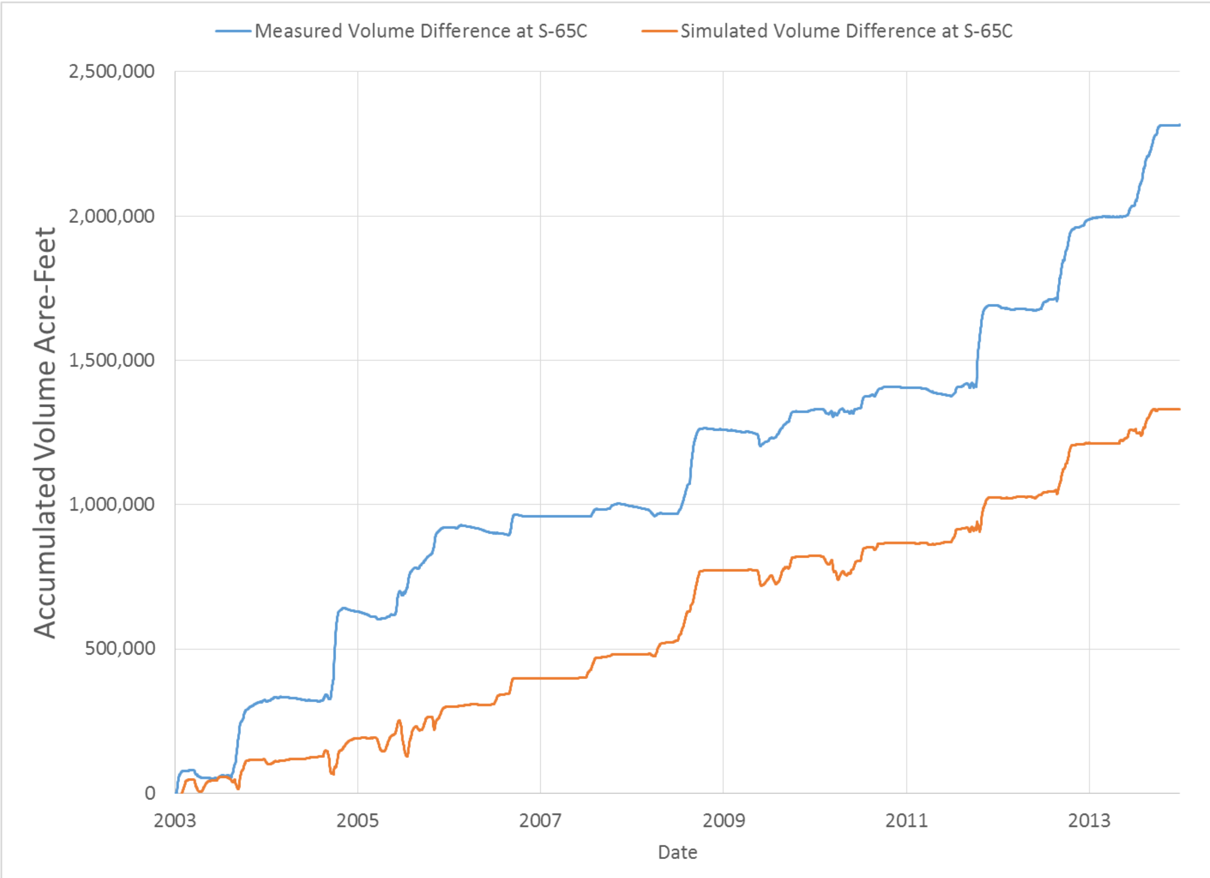


**Figure 30. Comparison of measured and simulated accumulative volume differences between S-65C and S-65.**

**Table 19. Measured and simulated accumulative volume differences between S-65C and S-65.**

| Year | Measured Volume (Acre/Feet) | Simulated Volume (Acre/Feet) | Ratio of Simulated to Measured |
|---|---|---|---|
| **2003** | 318,116 | 108,517 | 34% |
| **2004** | 310,661 | 81,586 | 26% |
| **2005** | 292,795 | 108,202 | 37% |
| **2006** | 36,768 | 99,672 | 271% |
| **2007** | 35,702 | 83,847 | 235% |
| **2008** | 264,306 | 290,904 | 110% |
| **2009** | 71,010 | 50,867 | 72% |
| **2010** | 76,001 | 42,467 | 56% |
| **2011** | 283,390 | 159,365 | 56% |
| **2012** | 298,446 | 187,747 | 63% |
| **2013** | 328,453 | 117,537 | 36% |
| **Total** | 2,315,647 | 1,330,710 | 57% |

Figure 31 shows comparisons of measured and simulated total N concentrations at S-65C. The measured values mostly lie in a fairly narrow range between 1 and 1.5 mg/l with a number of measured values above 1.5 mg/l. As was the case at S-65A, the simulated values are far more variable, with most of the "baseline" levels far too low at 0.1 mg/l and periodic spikes over 2.5 mg/l, with a single simulated spike reaching over 4 mg/l.

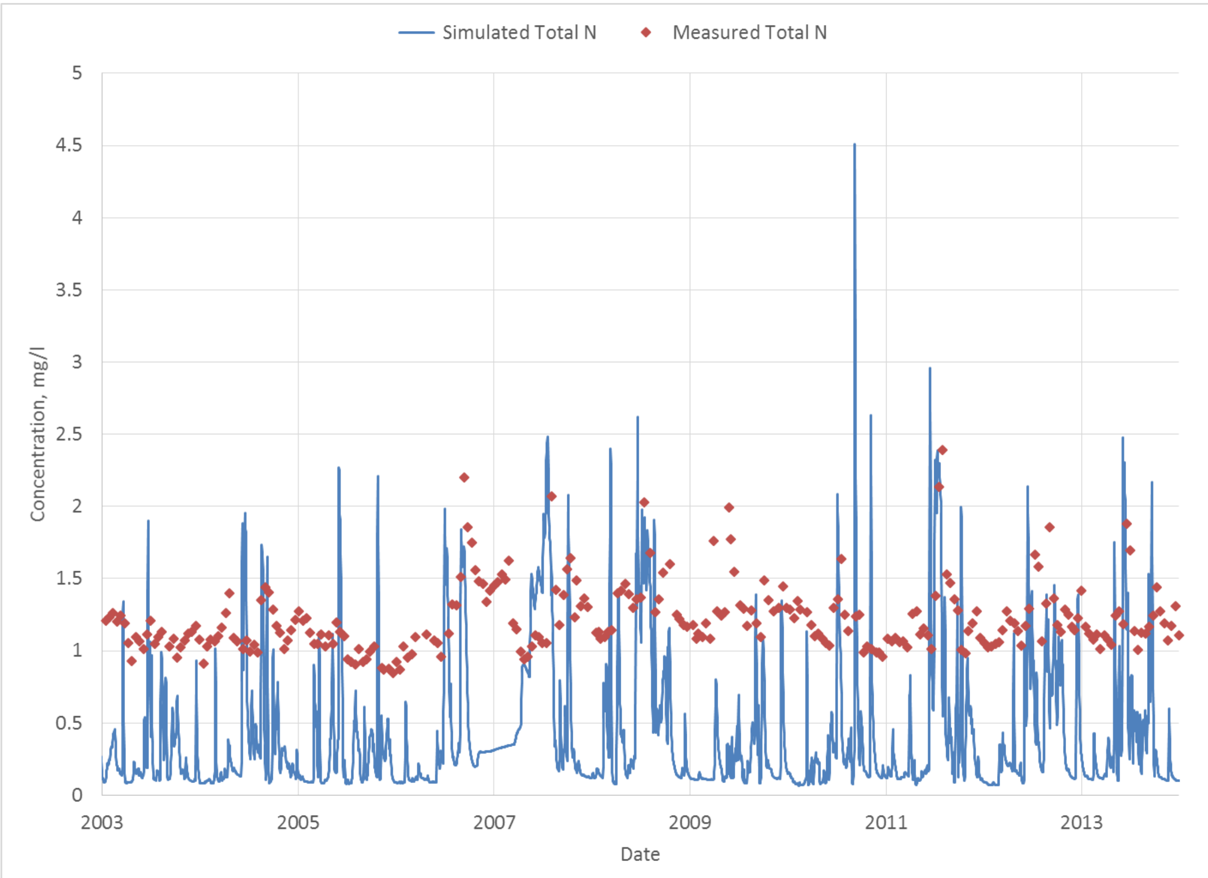


**Figure 31. Comparison of measured and simulated total N concentrations at S-65C.**

Figure 32 shows comparisons of measured and simulated total P concentrations at S-65C. As was the case at the S-65A station, the measured P values are much more variable than the measured total N values, with many values at the lower end clustered around 0.045-0.05 mg/l, but spiking up over 0.2 mg/l, with some values topping 0.35 mg/l. The simulated total P values track the measured values moderately well, but the "baseline" levels somewhat too low at about 0.025 mg/l.

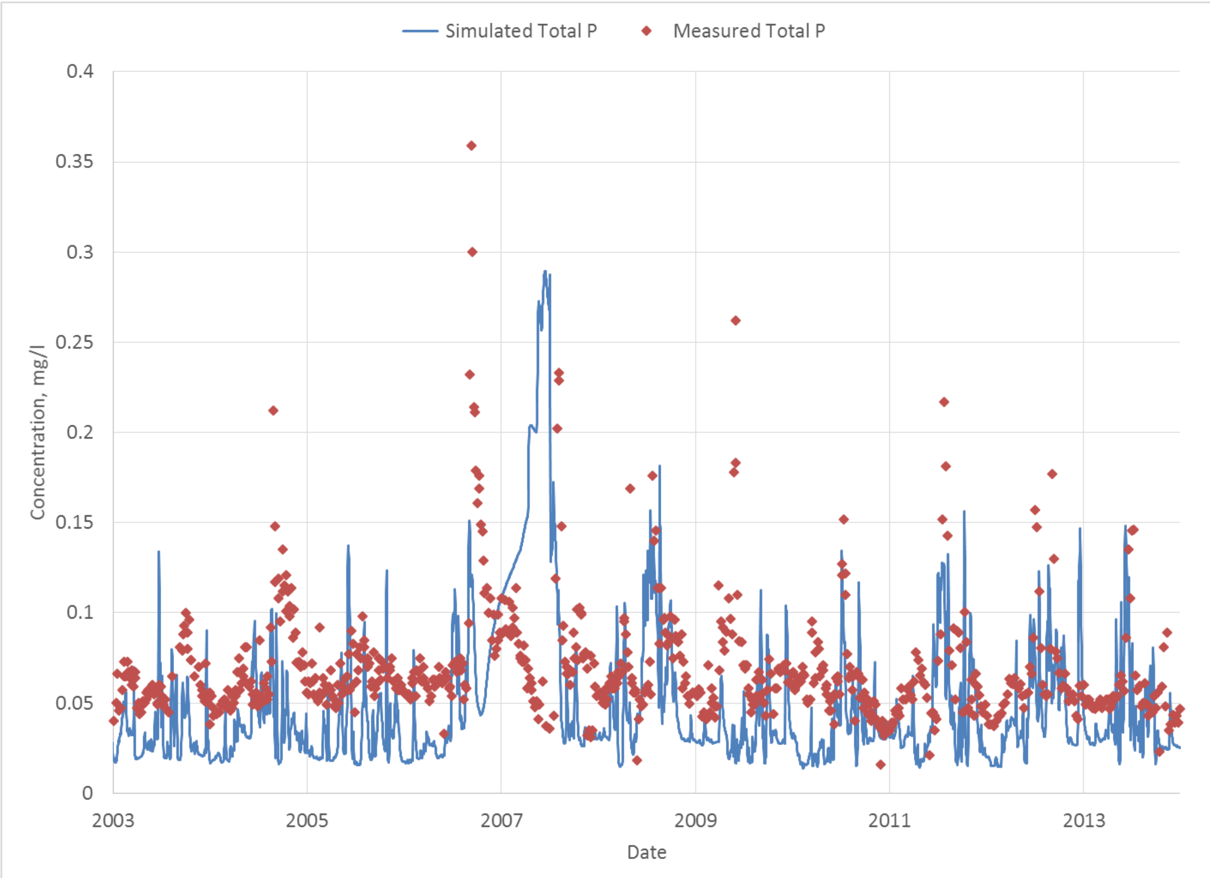


**Figure 32. Comparison of measured and simulated total P concentrations at S-65C.**

### 4.4.3 Flow and Water Quality Data at S-65D

Figure 33 shows a comparison between measured and simulated accumulated water volumes at S-65D. As was discussed above, the chart data were calculated by subtracting the boundary inflow data at the S-65 structure from both the simulated and measured values, so the chart data reflects the contribution from the sub-watershed between the S-65 and S-65D structures. Similar to the difference in accumulated volumes at S-65C shown in Figure 30, the simulated values under predict the measured values over the time period and end up much lower at the end, although the effect is even more pronounced that at S-65C with the predicted values being only 20% of the measured. This indicates that the simulated contribution of water from the surrounding areas to the lower Kissimmee River between the S-65C and S-65D structures are much too low.

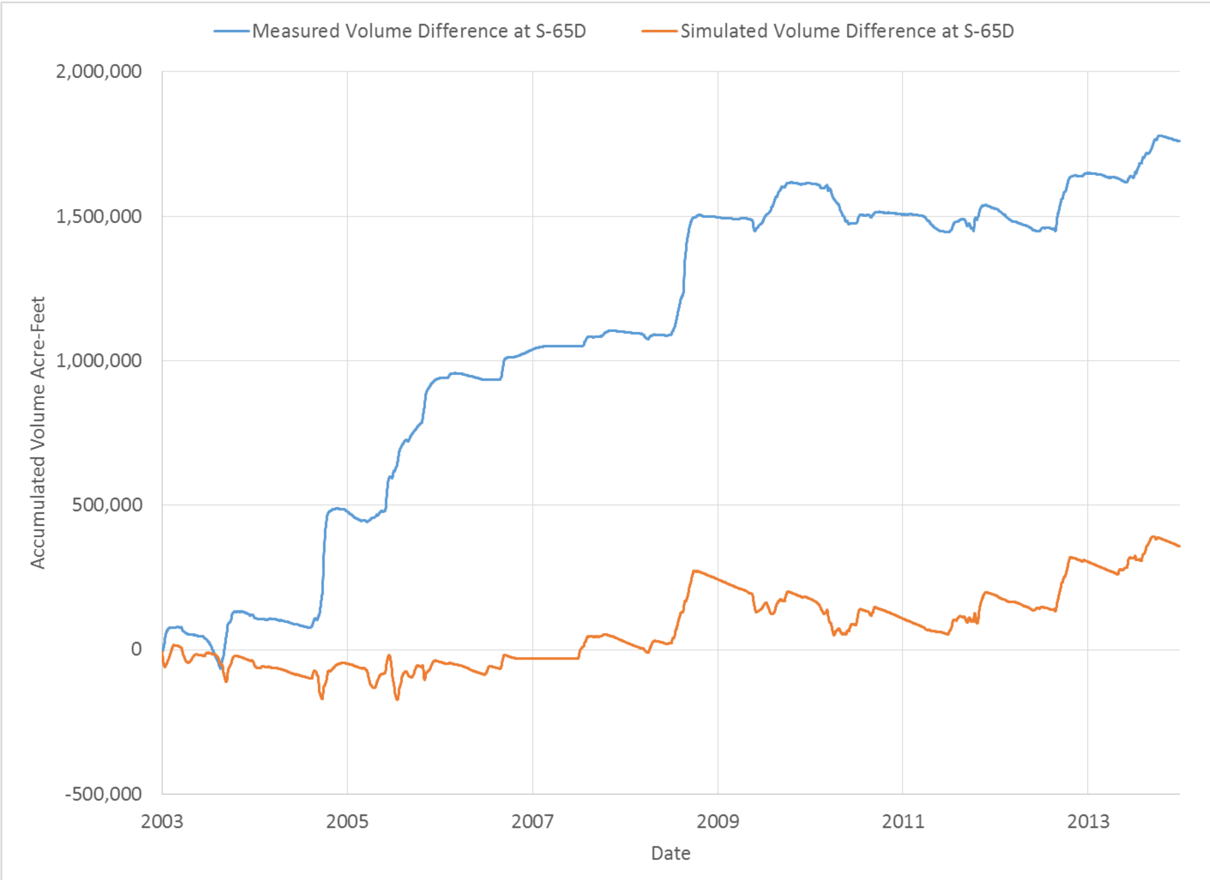


**Figure 33. Comparison of measured and simulated accumulative volume differences between S-65D and S-65.**

**Table 20. Measured and simulated volume differences between S-65D and S-65.**

| Year | Measured Volume (Acre/Feet) | Simulated Volume (Acre/Feet) | Ratio of Simulated to Measured |
|---|---|---|---|
| **2003** | 111,928 | -49,846 | -45% |
| **2004** | 366,890 | 1,594 | 0% |
| **2005** | 460,377 | 6,155 | 1% |
| **2006** | 98,498 | 10,761 | 11% |
| **2007** | 61,619 | 59,165 | 96% |
| **2008** | 397,384 | 216,318 | 54% |
| **2009** | 117,192 | -67,831 | -58% |
| **2010** | -107,528 | -67,763 | 63% |
| **2011** | 19,465 | 80,289 | 412% |
| **2012** | 123,188 | 115,928 | 94% |
| **2013** | 110,539 | 52,074 | 47% |
| **Total** | 1,759,552 | 356,846 | 20% |

Figure 34 shows comparisons of measured and simulated total N concentrations at S-65D. As with the measured values further upstream at S-65A and S-65C, the measured values mostly lie in a fairly narrow range between 1 and 1.5 mg/l. And as before, the simulated values are far more variable, with most of the "baseline" levels far too low at 0.1 mg/l and periodic spikes approaching 4 mg/l, and a large spike in 2007 approaching 12 mg/l.

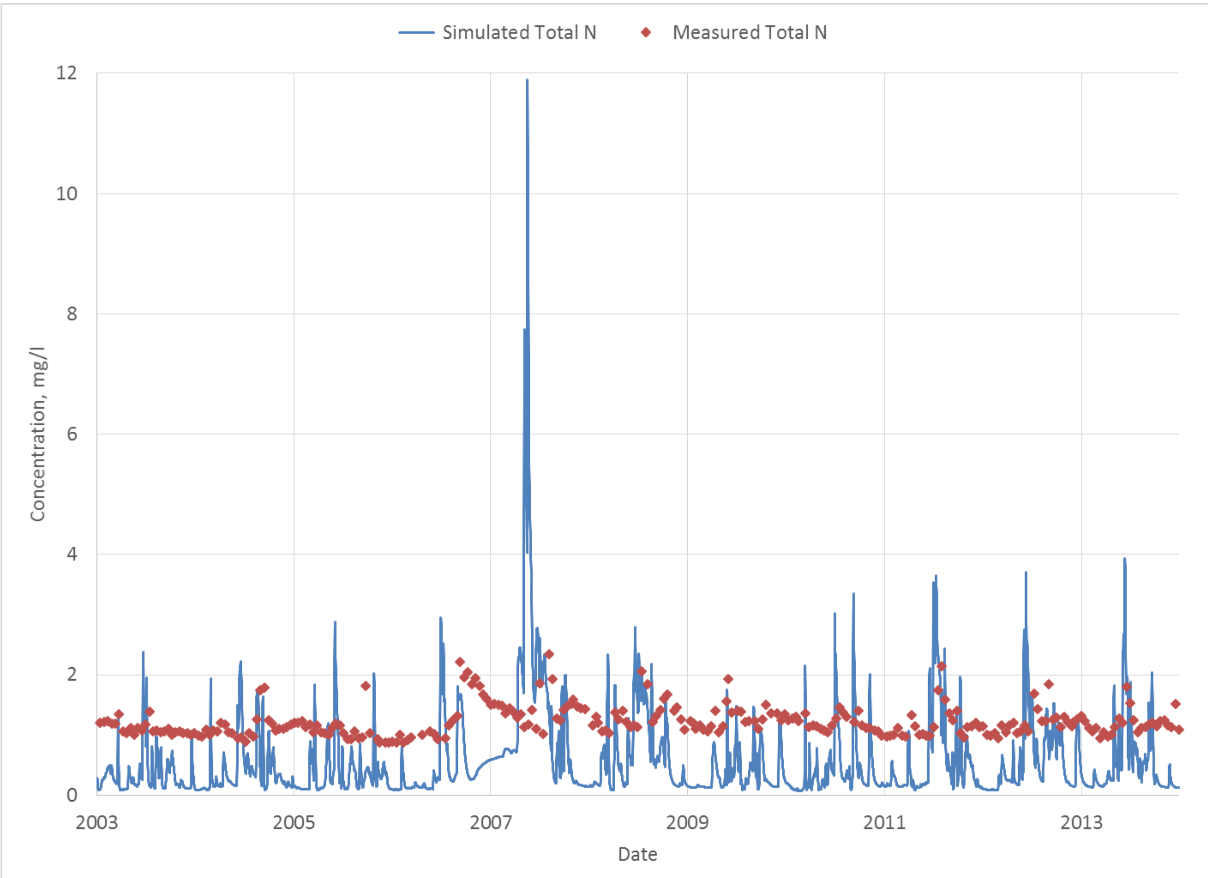


**Figure 34. Comparison of measured and simulated total N concentrations at S-65D.**

Figure 35 shows comparisons of measured and simulated total P concentrations at S-65D. As with the measurement stations at S-65A and S-65C, the measured P values are much more variable than the measured total N concentration. Many of the measured values at the lower end are clustered around 0.05 mg/l, but spiking up to nearly 0.3 mg/l, with at one value at 0.4 mg/l. The simulated total P values track the measured values moderately well, but as with the other stations the "baseline" levels are somewhat too low at about 0.02 mg/l.

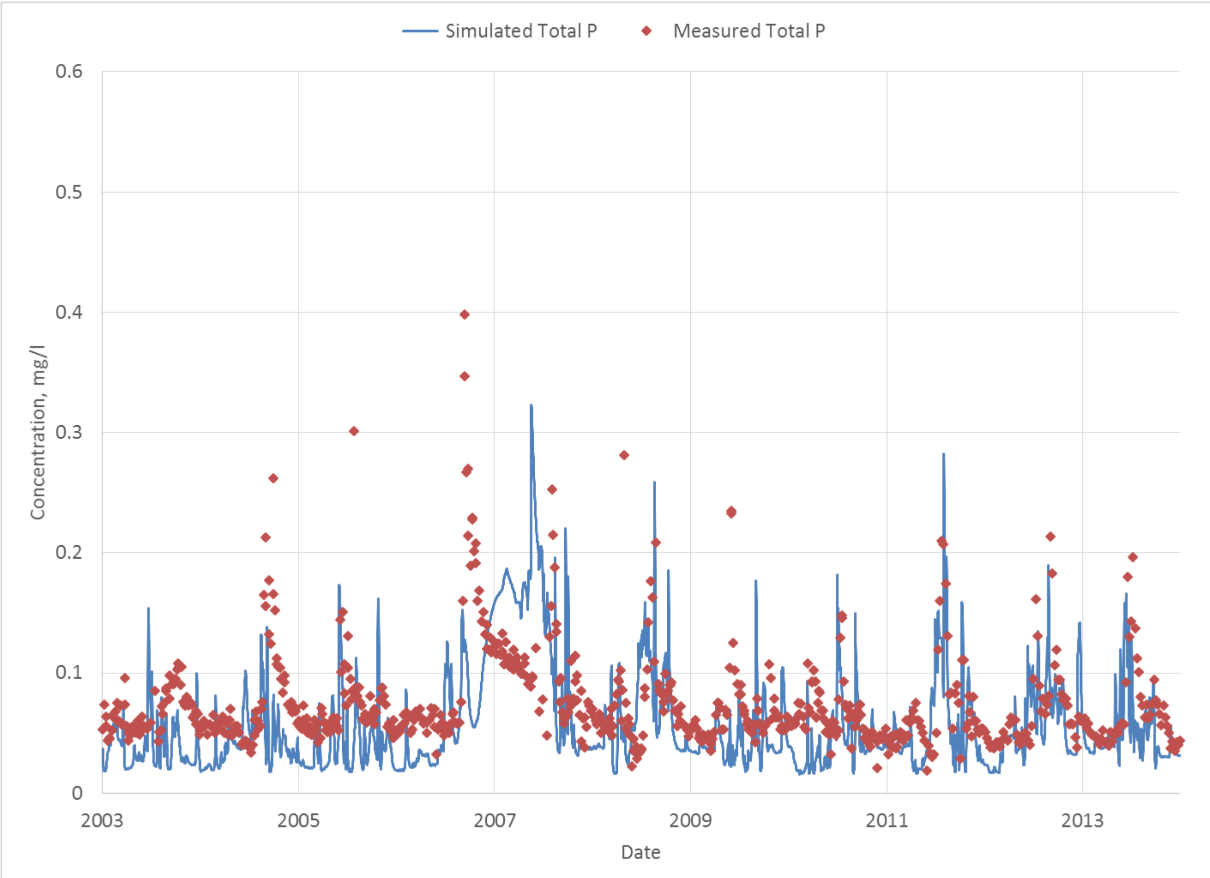


**Figure 35. Comparison of measured and simulated total P concentrations at S-65D.**

### 4.4.4 Flow and Water Quality Data at S-65E

Figure 36 shows a comparison between measured and simulated accumulated water volumes at S-65E while Table 21 shows total volumes on an annual basis. As was discussed above, the chart data were calculated by subtracting the boundary inflow data at the S-65 structure from both the simulated and measured values, so the chart data reflects the contribution from the sub-watershed over the entire sub-watershed. Similar to the difference in accumulated volumes at S-65C shown in Figure 30, the simulated values under predict the measured values over the time period and end up lower by 22% at the end, although the effect is much less pronounced than at S-65C or S-65D. Note that from 2006-2010 the model over predicted the total volumes while under predicting in all other years besides 2011. However, the difference is less than the observed difference at S-65D, indicating an increased amount of water contributing to the lower Kissimmee River between the S-65D and S-65E structures are. Overall, this suggests that the areas between the S-65A and S-65D structures needs to be giving particular care during the recalibration effort.

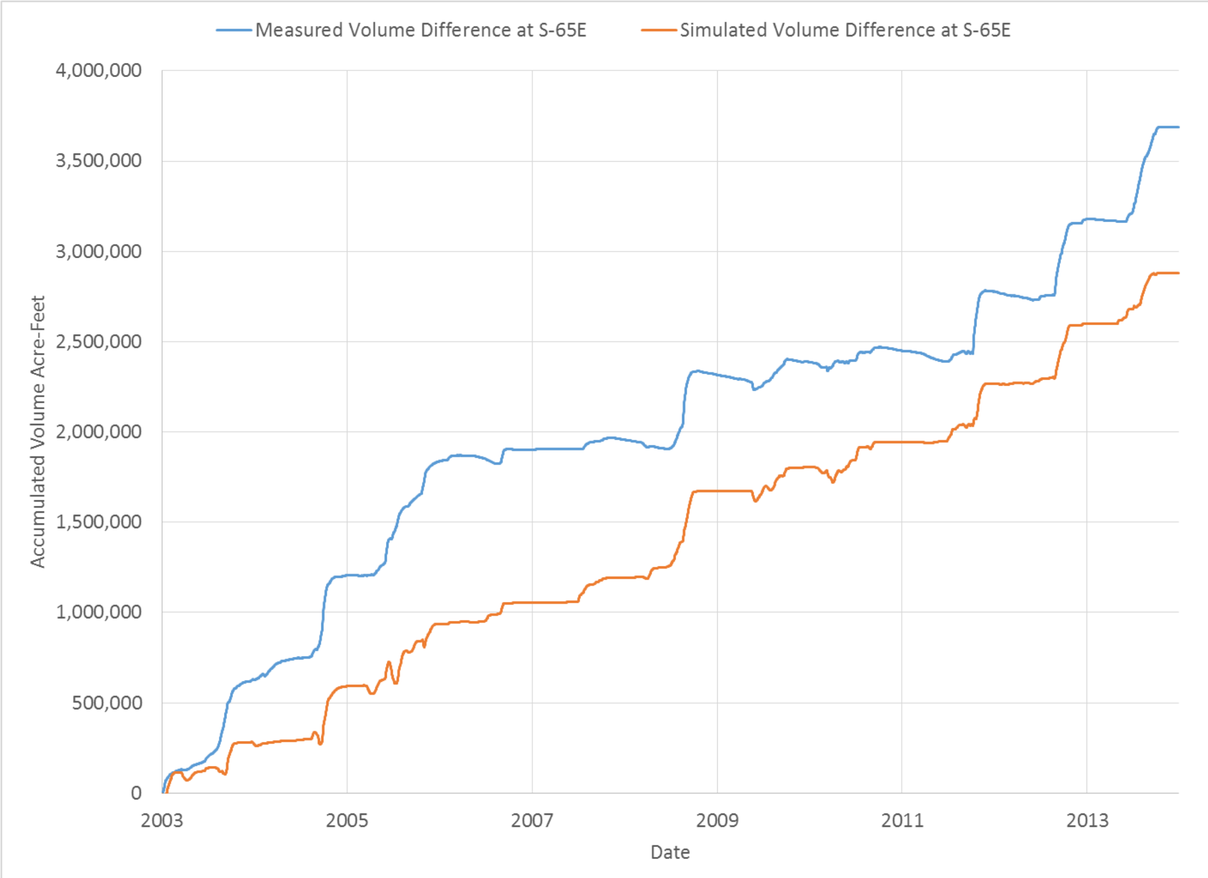


**Figure 36. Comparison of measured and simulated accumulative volume differences between S-65E and S-65.**

**Table 21. Measured and simulated accumulative volume differences between S-65E and S-65.**

| Year | Measured Volume (Acre/Feet) | Simulated Volume (Acre/Feet) | Ratio of Simulated to Measured |
|---|---|---|---|
| **2003** | 625,206 | 272,899 | 44% |
| **2004** | 579,946 | 318,264 | 55% |
| **2005** | 632,173 | 343,270 | 54% |
| **2006** | 65,384 | 119,462 | 183% |
| **2007** | 54,422 | 140,372 | 258% |
| **2008** | 359,488 | 478,591 | 133% |
| **2009** | 70,968 | 132,787 | 187% |
| **2010** | 62,784 | 137,460 | 219% |
| **2011** | 327,207 | 324,679 | 99% |
| **2012** | 399,857 | 330,901 | 83% |
| **2013** | 508,609 | 280,852 | 55% |
| **Total** | 3,686,046 | 2,879,536 | 78% |

Figure 37 shows comparisons of measured and simulated total N concentrations at S-65E. As with the measured values further upstream at S-65A, S-65C, and S-65D, the measured values mostly lie in a fairly narrow range between 1 and 1.5 mg/l, although there are a number of measurements at this station that are between 1.5 and 2 mg/l. And as before, the simulated values are far more variable, with most of the "baseline" levels far too low at 0.1 mg/l and periodic spikes approaching 4 mg/l, and the large spike in 2007 over 7 mg/l.

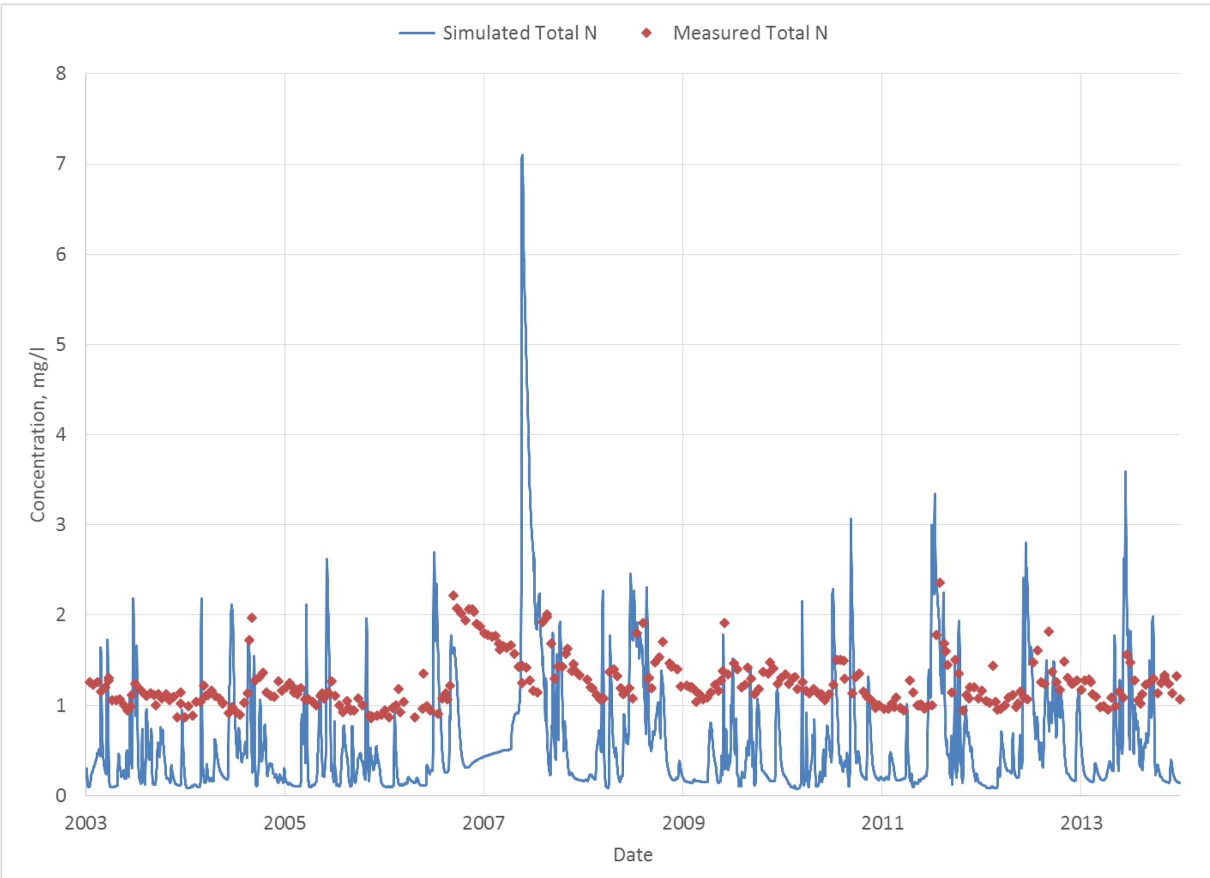


**Figure 37. Comparison of measured and simulated total N concentrations at S-65E.**

Figure 38 shows comparisons of measured and simulated total P concentrations at S-65E. As with the upstream stations, the measured P values are much more variable than the measured total N concentration. Many of the measured values at the lower end are clustered around 0.05 mg/l, but spiking up over 0.3 mg/l, at one value over 0.4 mg/l. The simulated total P values track the measured values moderately well, but the "baseline" levels somewhat too low at 0.02 mg/l.

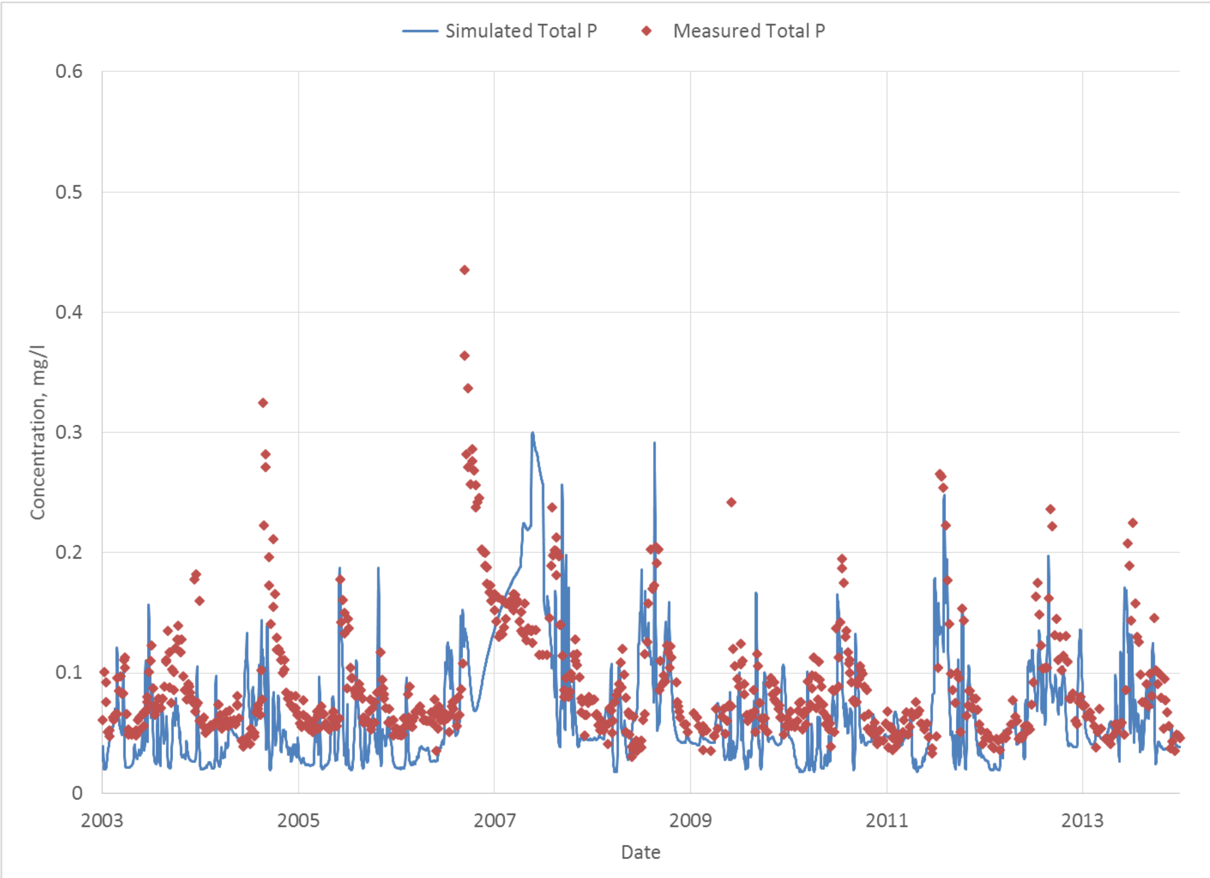


**Figure 38. Comparison of measured and simulated total P concentrations at S-65E.**

## 4.5 Taylor Creek/Nubbin Slough

### 4.5.1 Flow and Water Quality Data at S-191

Figure 39 shows the comparison between measured and simulated flow volumes at S-191. Corresponding tabulated data is shown in Table 22. The model under predicts the volume of the 2003-2013 period by about 27%. The only years that were over predicted by the model were 2004 and 2010. The model under predicted volumes in 2003, 2005, 2006, and 2013, accounting for much of the separation shown in Figure 39 . The average measured flow over the period shown is 3.4 $m^3/s$, while the average simulated flow is 2.5 $m^3/s$.

Relevant statistics for daily values from 2003-2013 are shown in Table 23. The statistics show an underestimation of the measured flow data at S-191 over the period, but the Nash-Sutcliffe efficiency statistic, at 0.7, indicates a fairly good fit given that the overall volume is too low. This value should improve slightly with calibration.

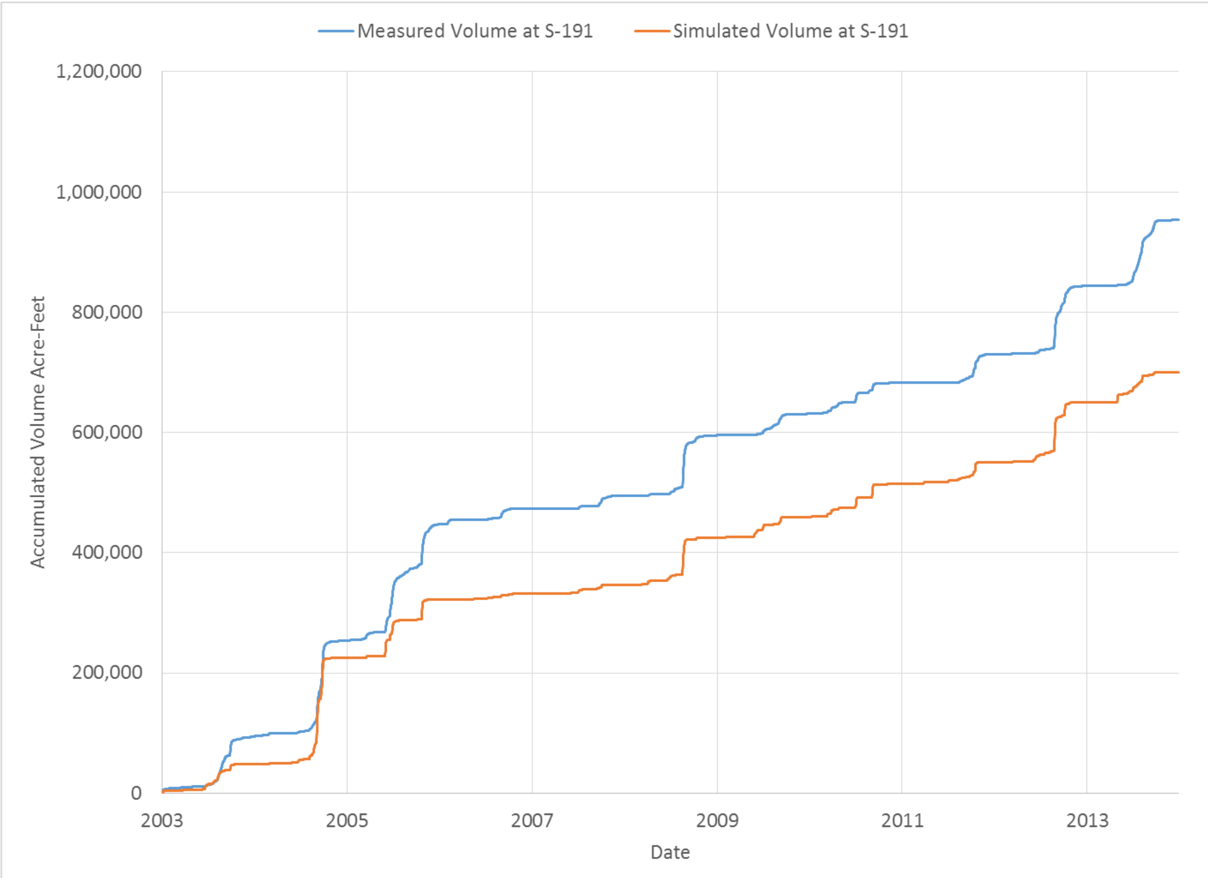


**Figure 39. Comparison of measured and simulated flow at S-191.**

**Table 22. Measured and simulated water volumes at S-191**

| Year | Measured Volume (Acre/Feet) | Simulated Volume (Acre/Feet) | Ratio of Simulated to Measured |
|---|---|---|---|
| **2003** | 94,437 | 48,048 | 51% |
| **2004** | 159,297 | 176,746 | 111% |
| **2005** | 193,412 | 97,535 | 50% |
| **2006** | 25,949 | 9,280 | 36% |
| **2007** | 21,339 | 15,305 | 72% |
| **2008** | 100,785 | 77,805 | 77% |
| **2009** | 35,901 | 34,633 | 96% |
| **2010** | 51,160 | 55,789 | 109% |
| **2011** | 47,917 | 34,444 | 72% |
| **2012** | 113,582 | 100,483 | 88% |
| **2013** | 109,349 | 50,055 | 46% |
| **Total** | 953,129 | 700,122 | 73% |

**Table 23. Daily statistics of flow at S-191.**

| Statistic | Value | Unit |
|---|---|---|
| **Bias** | -0.90 | m^3/s |
| **Nash–Sutcliffe** | 0.70 | - |
| **RMSE** | 6.17 | m^3/s |
| **RMSE/Sigma** | 0.55 | - |

Figure 40 shows comparisons of measured and simulated total N concentrations at S-191. The measured values show a moderate degree of variability, lying in a range between 1 and 3 mg/l. The simulated values are only slightly more variable and capture some of the measured trends quite well. The lowest values simulated tend to be about 0.3-0.5 mg/l too low, and a few simulated values spike above 4 mg/l, but overall the model performs well given that it has not been calibrated.

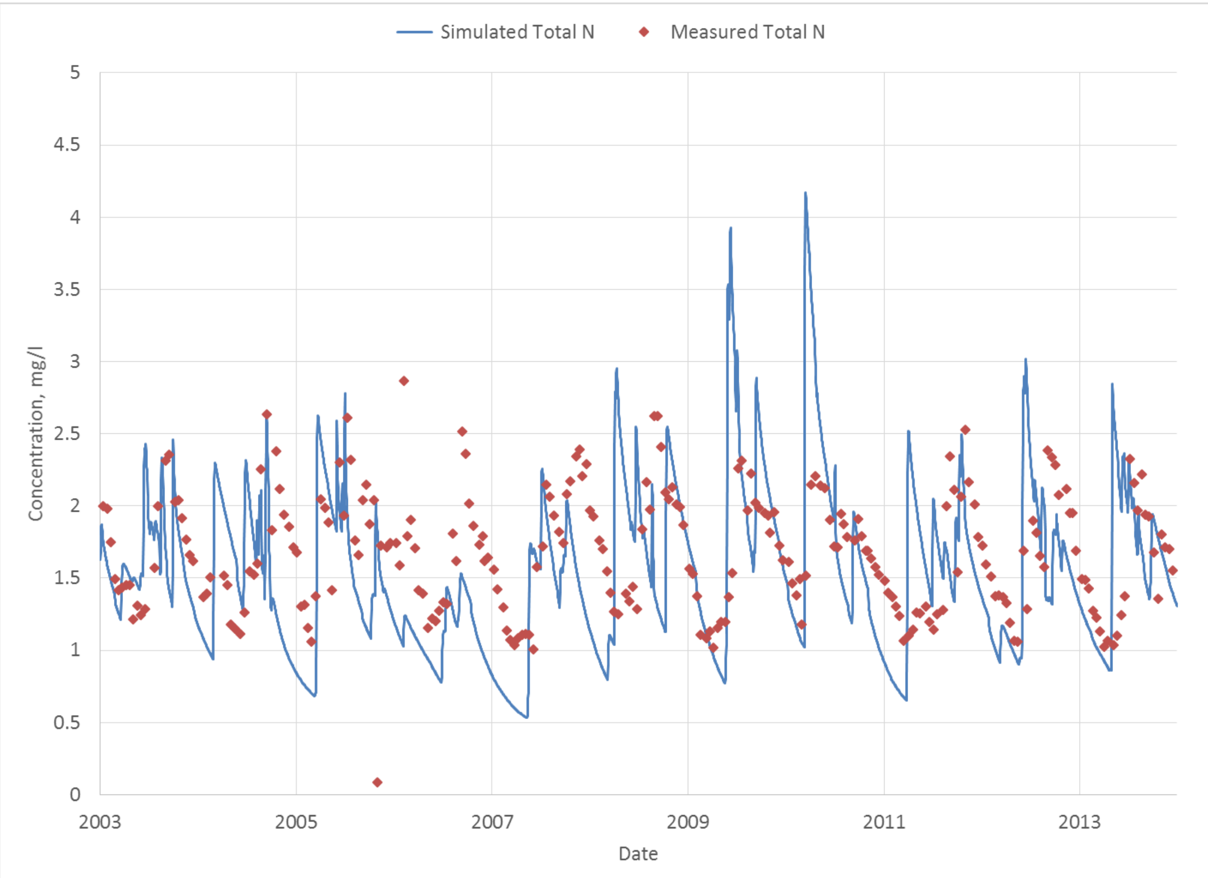


**Figure 40. Comparison of measured and simulated total N concentrations at S-191.**

Figure 41 shows the comparison between the measured total P data and the simulated total P values at S-191. It is clear that the model underestimates many of the measured total P values and does not capture the measured variability well. The observed values range from just over 0.1 to around 1 mg/l, while the simulated values line in a narrow range between 0.2 and 0.4 mg/l. It is apparent that the model does not reproduce the appropriate concentrations leaving the source cells, or is using inappropriate attenuation parameters, or both. The land use and attenuation parameters need to be checked and adjusted during calibration.

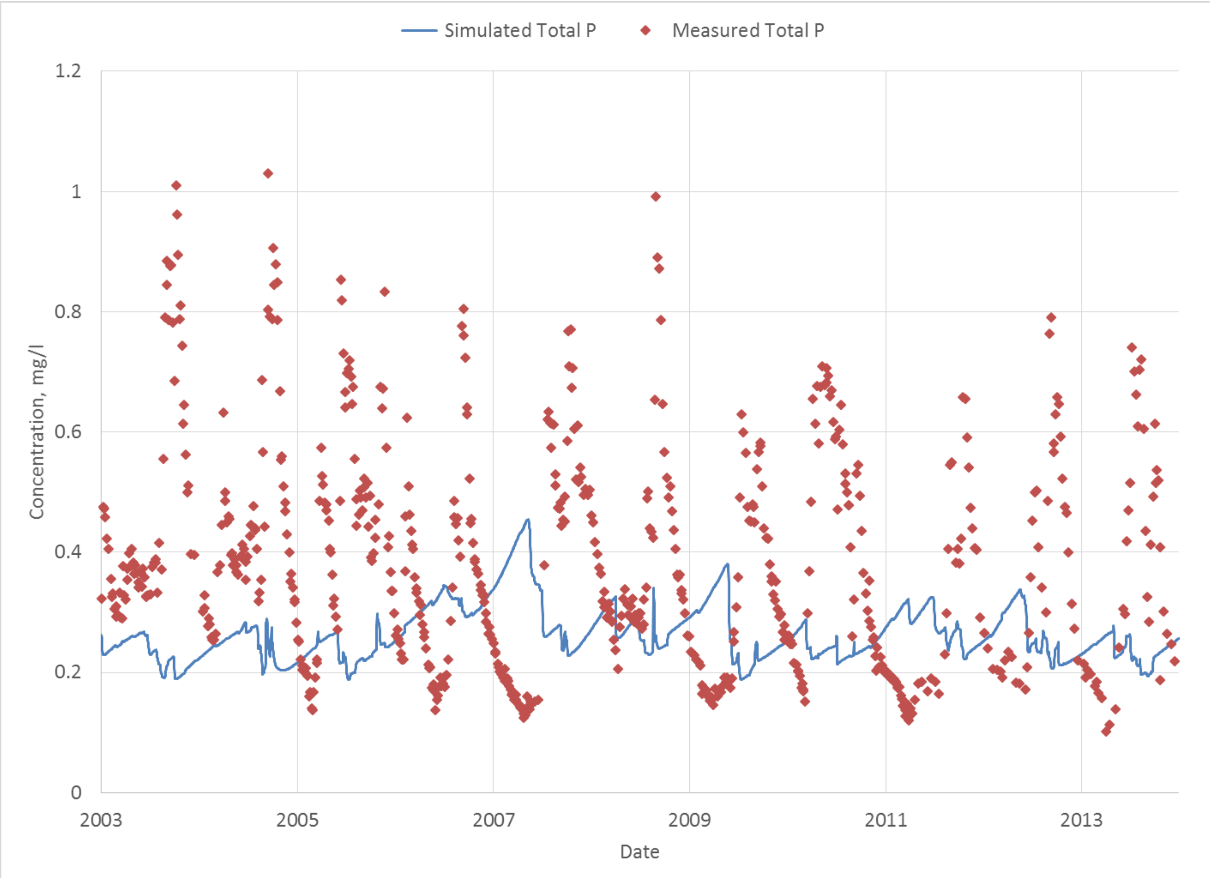


**Figure 41. Comparison of measured and simulated total P concentrations at S-191.**

### 4.5.2 Flow and Water Quality Data at S-133

Figure 42 shows the comparison between measured and simulated flow volumes at S-133. Corresponding tabulated data is shown in Table 24. The model over predicts the volume of the 2003-2013 period by about 15%. Note that in 2007, 2009, and 2011, little to no flow was observed. In particular, simulated flows during 2009 were much greater than the observed, accounting for much of the separation shown in Figure 42. The average measured flow over the period shown is 0.66 $m^3/s$, while the average simulated flow is 0.75 $m^3/s$.

Relevant statistics for daily values from 2003-2013 are shown in Table 25. The statistics show an overestimation of the measured flow data at S-133 over the period, but the Nash-Sutcliffe efficiency statistic, at 0.2, indicates a slightly better fit than simply using the average value. This value should improve with calibration.

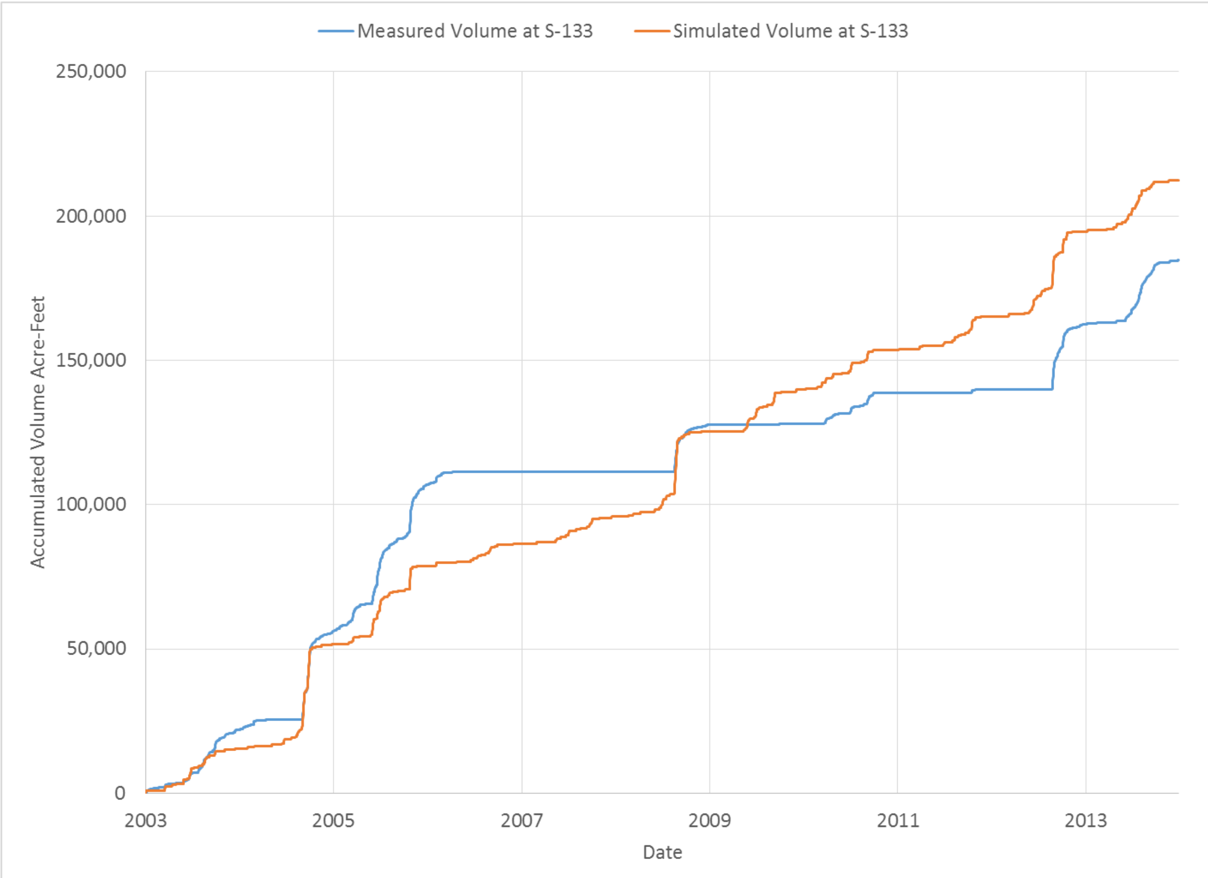


**Figure 42. Comparison of measured and simulated flow at S-133.**

**Table 24. Measured and simulated water volumes at S-133. In 2007, there was no measured flow, so the ratio could not be determined, indicated by "N/A".**

| Year | Measured Volume (Acre/Feet) | Simulated Volume (Acre/Feet) | Ratio of Simulated to Measured |
|---|---|---|---|
| **2003** | 22,078 | 15,458 | 70% |
| **2004** | 33,928 | 36,274 | 107% |
| **2005** | 50,821 | 27,059 | 53% |
| **2006** | 4,614 | 7,682 | 166% |
| **2007** | - | 9,394 | N/A |
| **2008** | 16,128 | 29,544 | 183% |
| **2009** | 394 | 14,344 | 3645% |
| **2010** | 10,845 | 13,782 | 127% |
| **2011** | 1,122 | 11,718 | 1045% |
| **2012** | 22,578 | 29,444 | 130% |
| **2013** | 22,122 | 17,561 | 79% |
| **Total** | 184,628 | 212,260 | 115% |

**Table 25. Daily statistics of flow at S-133.**

| Statistic | Value | Unit |
|---|---|---|
| **Bias** | 0.10 | m^3/s |
| **Nash–Sutcliffe** | 0.20 | - |
| **RMSE** | 1.99 | m^3/s |
| **RMSE/Sigma** | 0.89 | - |

Figure 43 shows comparisons of measured and simulated total N concentrations at S-133. The measured values mostly lie in a fairly narrow range between 1 and 2 mg/l, with a few peak values over 2. The simulated values are far more variable, with most of the “baseline” levels far too low at 0.8 mg/l and periodic spikes over 2.5 mg/l, with an outlier over 8 mg/l.

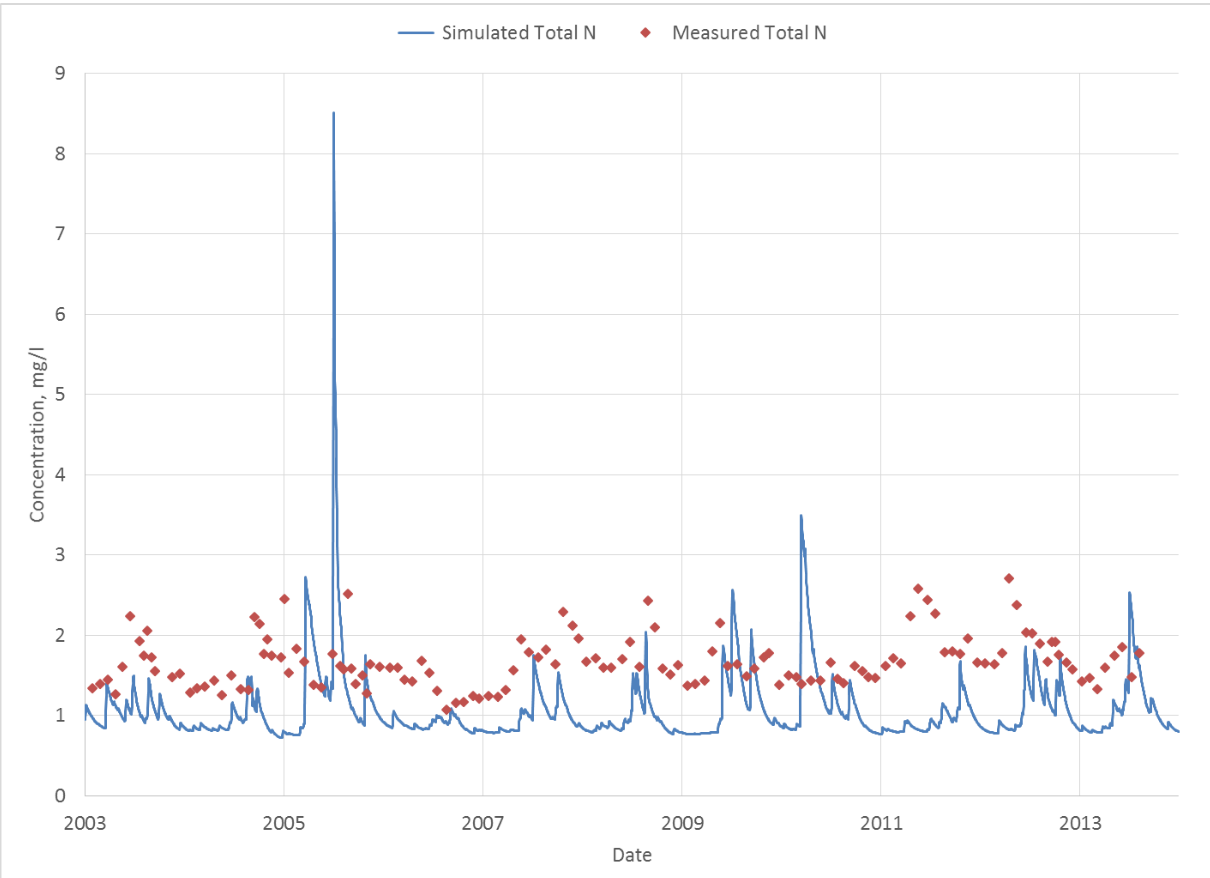


**Figure 43. Comparison of measured and simulated total N concentrations at S-133.**

Figure 44 shows comparisons of measured and simulated total P concentrations at S-133. In contrast with total N values, the measured P values are highly variable when compared with the measured values. The simulated values typically vary from 0.3 to 0.9 mg/l, with a few values outside that range. In contrast, measured values generally lie between 0.1 and 0.2 mg/l, although some measured values range up to 0.6 mg/l.

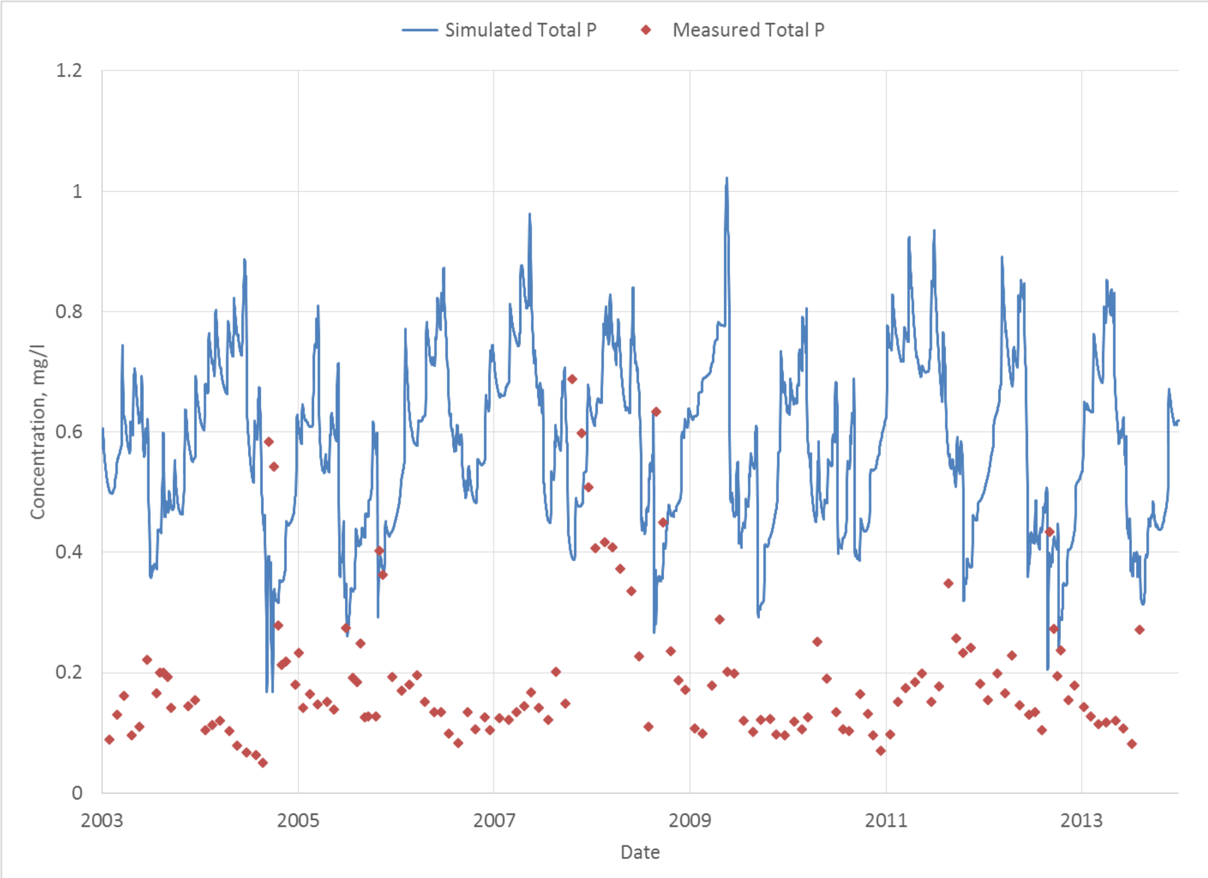


**Figure 44. Comparison of measured and simulated total P concentrations at S-133**

### 4.5.3 Flow and Water Quality Data at S-135

Figure 45 shows the comparison between measured and simulated flow volumes at S-135. Corresponding tabulated data is shown in Table 26. The model under predicts the volume of the 2003-2013 period by 20%. In particular, simulated flows under predict measured flows from 2003-2005, accounting for much of the separation shown in Figure 45. During some years, no flows were measured, although some simulated flows occurred, giving extreme mismatches in percentage, although the actual magnitudes of the values are low. The average measured flow over the period shown is 0.6 $m^3/s$, while the average simulated flow is 0.5 $m^3/s$.

Relevant statistics for daily values from 2003-2013 are shown in Table 29. The statistics show an underestimation of the measured flow data at S-135 over the period, but the Nash-Sutcliffe efficiency statistic, at 0.36, indicates a better fit than simply using the average value, but this value should improve with calibration.

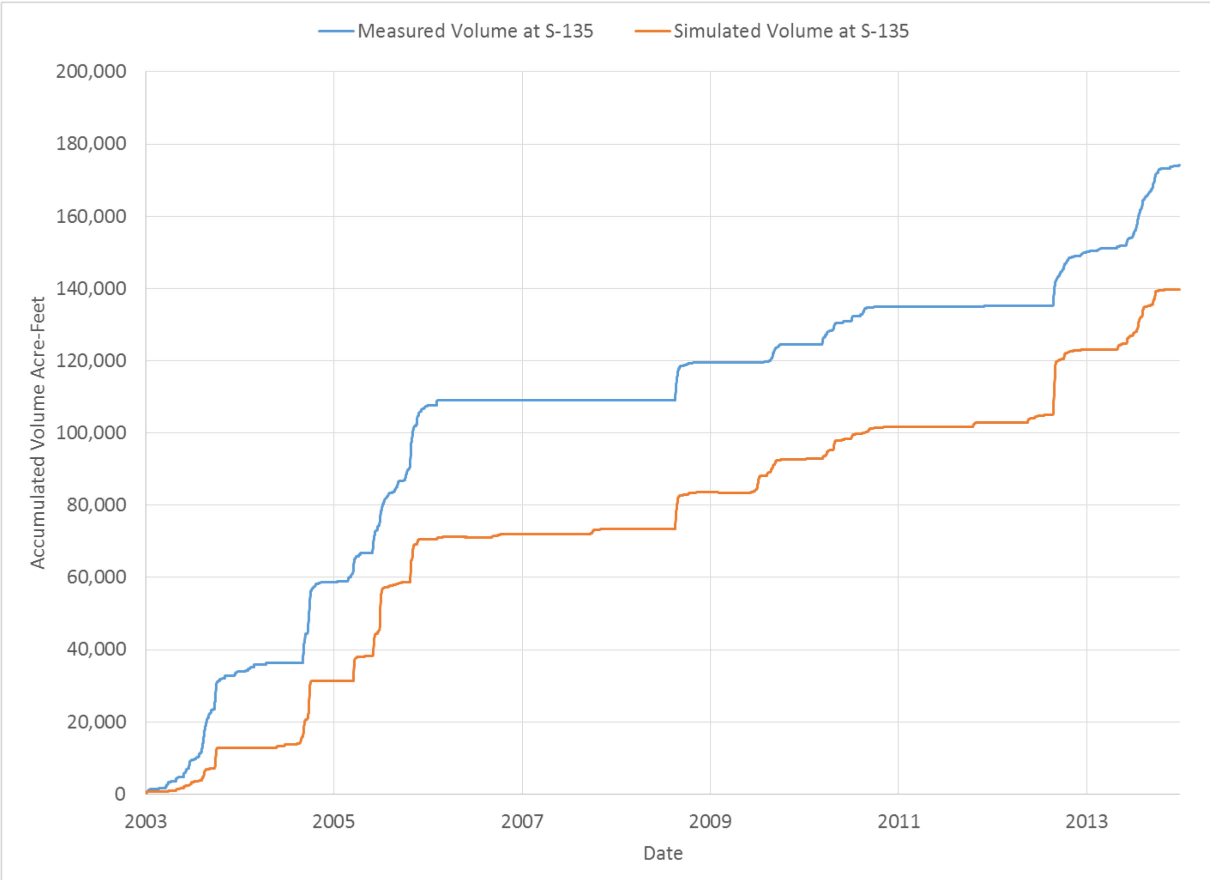


**Figure 45. Comparison of measured and simulated flow at S-135.**

**Table 26. Measured and simulated water volumes at S135. As with the results at S-133, in 2007 there was no measured flow, so the ratio could not be determined, indicated by "N/A".**

| Year | Measured Volume (Acre/Feet) | Simulated Volume (Acre/Feet) | Ratio of Simulated to Measured |
|---|---|---|---|
| **2003** | 33,923 | 12,901 | 38% |
| **2004** | 24,842 | 18,518 | 75% |
| **2005** | 48,780 | 39,208 | 80% |
| **2006** | 1,572 | 1,431 | 91% |
| **2007** | - | 1,305 | N/A |
| **2008** | 10,492 | 10,181 | 97% |
| **2009** | 4,838 | 9,208 | 190% |
| **2010** | 10,631 | 8,985 | 85% |
| **2011** | 22 | 1,185 | 5510% |
| **2012** | 14,924 | 20,105 | 135% |
| **2013** | 24,130 | 16,697 | 69% |
| **Total** | 174,155 | 139,723 | 80% |

**Table 27. Daily statistics of flow at S-135.**

| Statistic | Value | Unit |
|---|---|---|
| **Bias** | -0.12 | m^3/s |
| **Nash–Sutcliffe** | 0.36 | - |
| **RMSE** | 1.67 | m^3/s |
| **RMSE/Sigma** | 0.80 | - |

Figure 46 shows comparisons of measured and simulated total N concentrations at S-135. The measured values mostly lie in a fairly narrow range around 1.5 mg/l, with no values below 1.0 mg/l and only a few over 2.0 mg/l. The simulated values are far more variable than the measured values. This may indicate that significant attenuation is occurring in the canal adjacent to S-135 but is not accounted for in the model parameters.

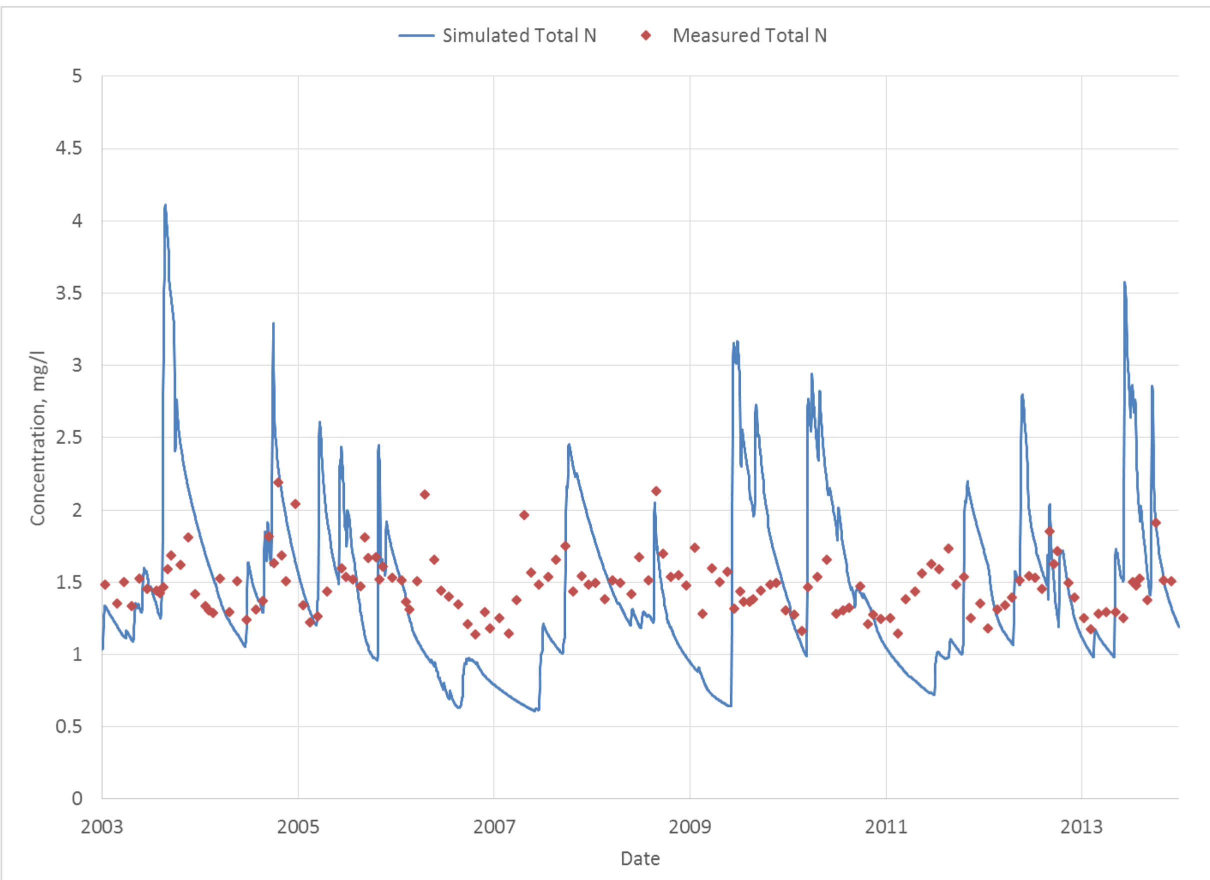


**Figure 46. Comparison of measured and simulated total N concentrations at S-135.**

Figure 47 shows the comparison between the measured total P data and the simulated total P values at S-135. It is clear that the model overestimates total P at S-135, with some peak values being unreasonably high. Many of the measured values cluster around 0.025 mg/l, with higher values over 0.2 mg/l. In contrast, simulated values peak at nearly 1.4 mg/l. In addition to attenuation parameters in the adjacent canals, the runoff values from nearby land uses need to be checked and some land use parameters possibly adjusted during calibration.

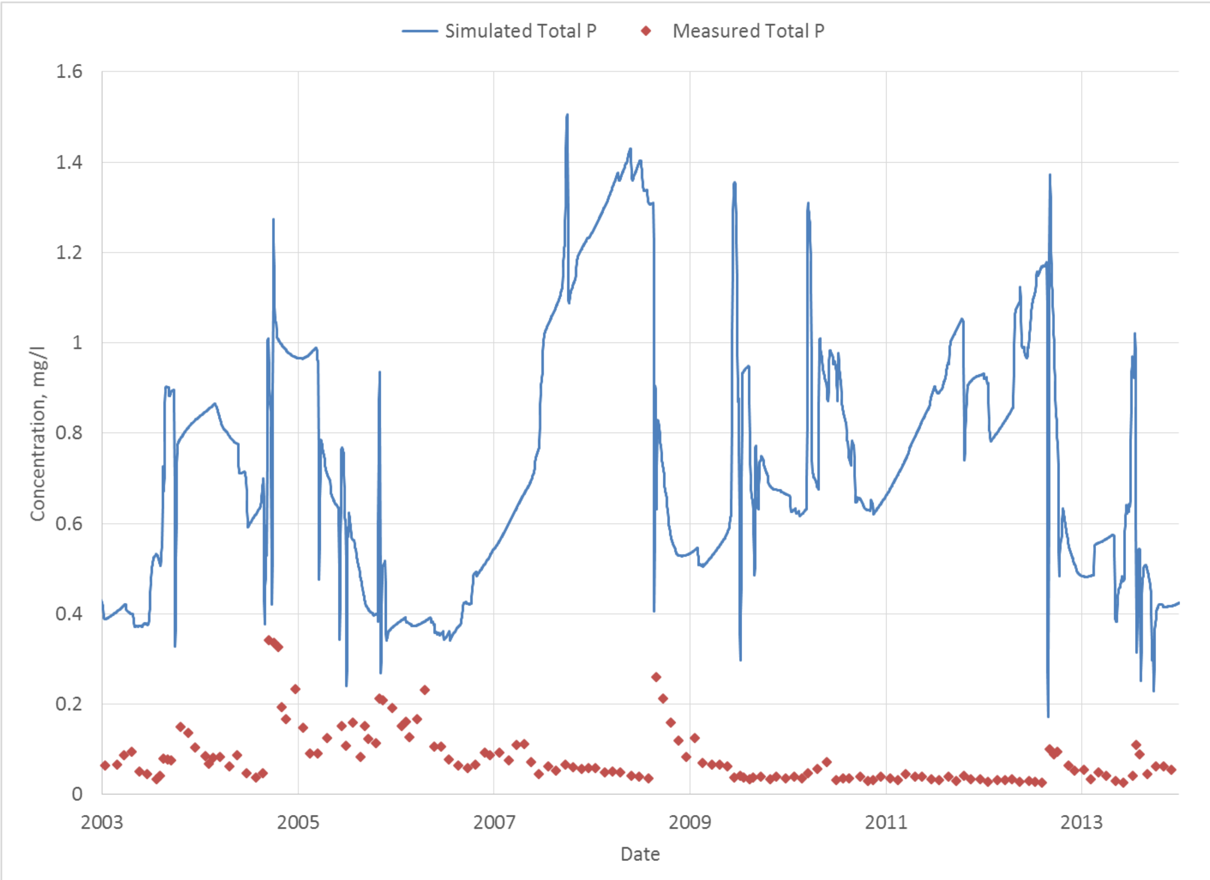


**Figure 47. Comparison of measured and simulated total P concentrations at S-135.**

## 4.6 Upper Kissimmee

### 4.6.1 Flow and Water Quality Data at S-65

Figure 48 shows the comparison between measured and simulated flow volumes at S-65. Corresponding tabulated data is shown in Table 28. Although the total volumes over the entire period are a good match within 9%, the model over predicts the volume in 2004, 2009, 2011, and 2012, while under predicting in 2003, 2005, 2006, and 2010. The separation shown in Figure 48 starting in 2011 reflects this. The average measured flow over the period shown is 33 $m^3/s$, while the average simulated flow is nearly 36 $m^3/s$.

Relevant statistics for daily values from 2003-2013 are shown in Table 29. The statistics show an overestimation of the measured flow data at S-65 over the period, but the Nash-Sutcliffe efficiency statistic, at 0.59, is considerably greater than zero, indicating a fairly good fit on the daily statistics, particularly for an uncalibrated model.

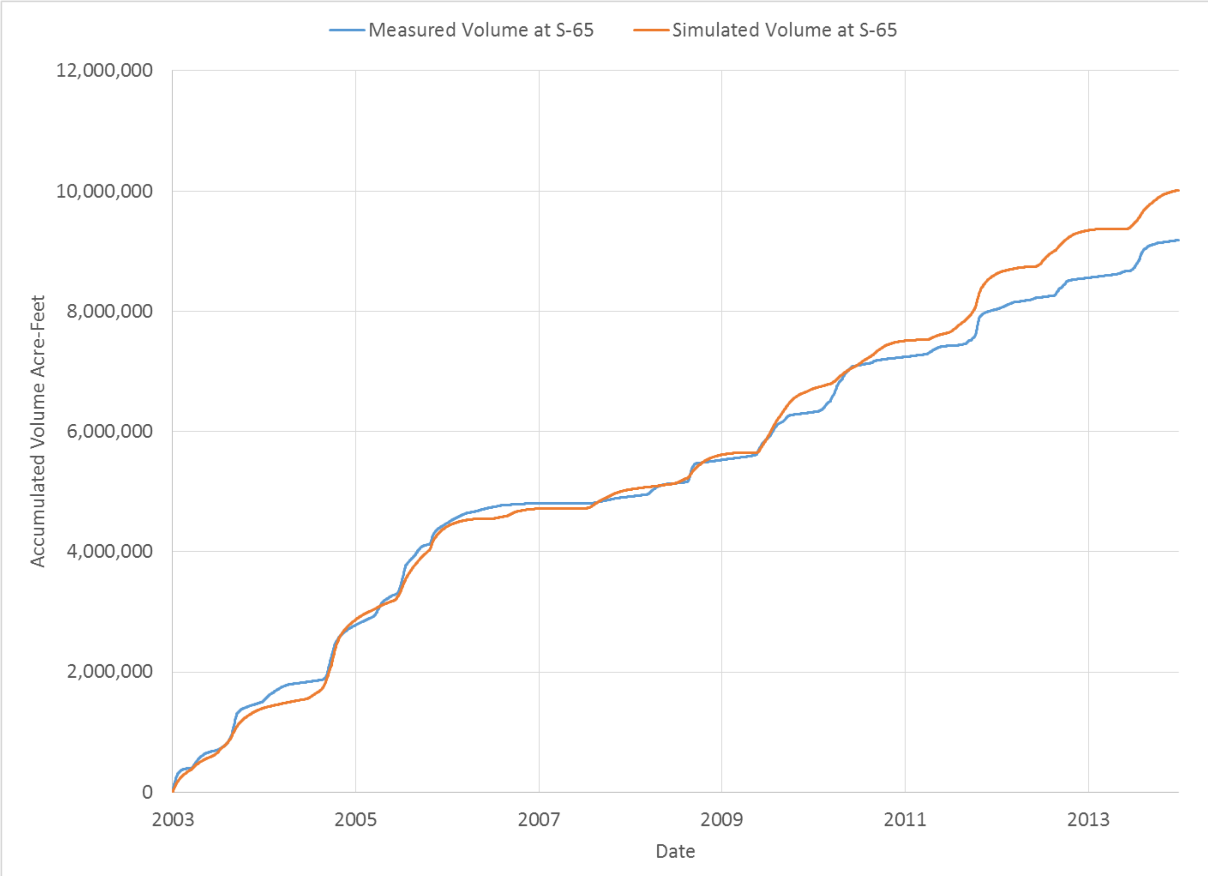


**Figure 48. Comparison of measured and simulated flow at S-65.**

**Table 28. Measured and simulated water volumes at S-65.**

| Year | Measured Volume (Acre/Feet) | Simulated Volume (Acre/Feet) | Ratio of Simulated to Measured |
|---|---|---|---|
| **2003** | 1,523,250 | 1,401,889 | 92% |
| **2004** | 1,256,369 | 1,466,791 | 117% |
| **2005** | 1,694,486 | 1,549,771 | 91% |
| **2006** | 322,308 | 296,127 | 92% |
| **2007** | 119,783 | 319,389 | 267% |
| **2008** | 608,814 | 576,924 | 95% |
| **2009** | 796,262 | 1,098,067 | 138% |
| **2010** | 916,941 | 797,248 | 87% |
| **2011** | 790,876 | 1,109,401 | 140% |
| **2012** | 524,165 | 727,475 | 139% |
| **2013** | 629,541 | 671,506 | 107% |
| **Total** | 9,182,795 | 10,014,589 | 109% |

**Table 29. Daily statistics of flow at S-65.**

| Statistic | Value | Unit |
|---|---|---|
| **Bias** | 3.0 | m^3/s |
| **Nash–Sutcliffe** | 0.59 | - |
| **RMSE** | 30.17 | m^3/s |
| **RMSE/Sigma** | 0.64 | - |

Figure 48 shows comparisons of measured and simulated total N concentrations at S-65. The measured values mostly lie in a fairly narrow range between 1 and 1.5 mg/l, with a period between 2007 and 2009 where some values were near 2 mg/l. The simulated values generally overestimate the measured values and do not match the overall pattern well.

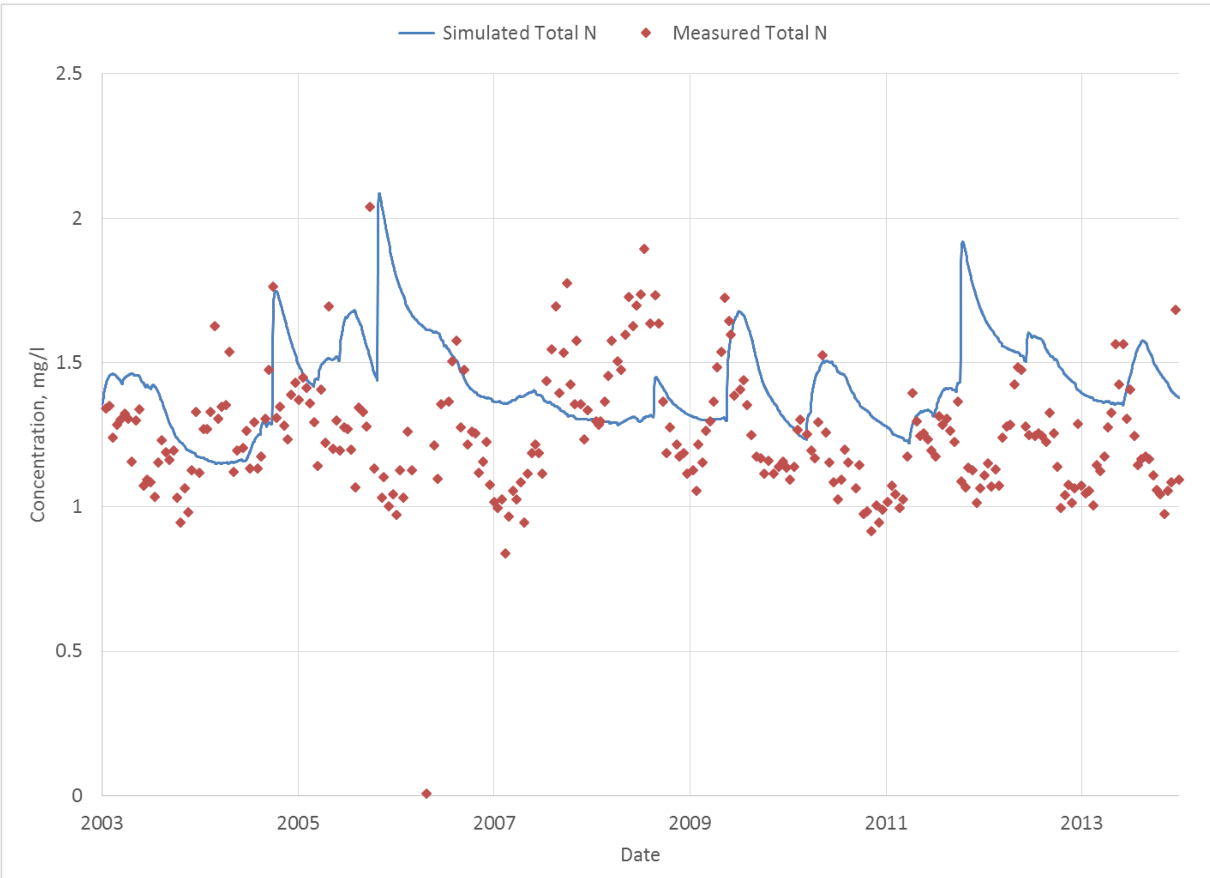


**Figure 49. Comparison of measured and simulated total N at S-65.**

Figure 50 shows the comparison between the measured total P data and the simulated total P values at S-65. It is clear that the model is underestimating total P at S-65, with the baseline simulated values around 0.01 mg/l while the lowest measured values tend to cluster around 0.05 mg/l and spike up over 0.2 mg/l. As with the case at S-68, this most likely indicates a need to pay particular attention to the attenuation parameters in Lake Kissimmee, since it acts as a significant buffer to nutrient concentrations at S-65, which is at the exit point from the lake.

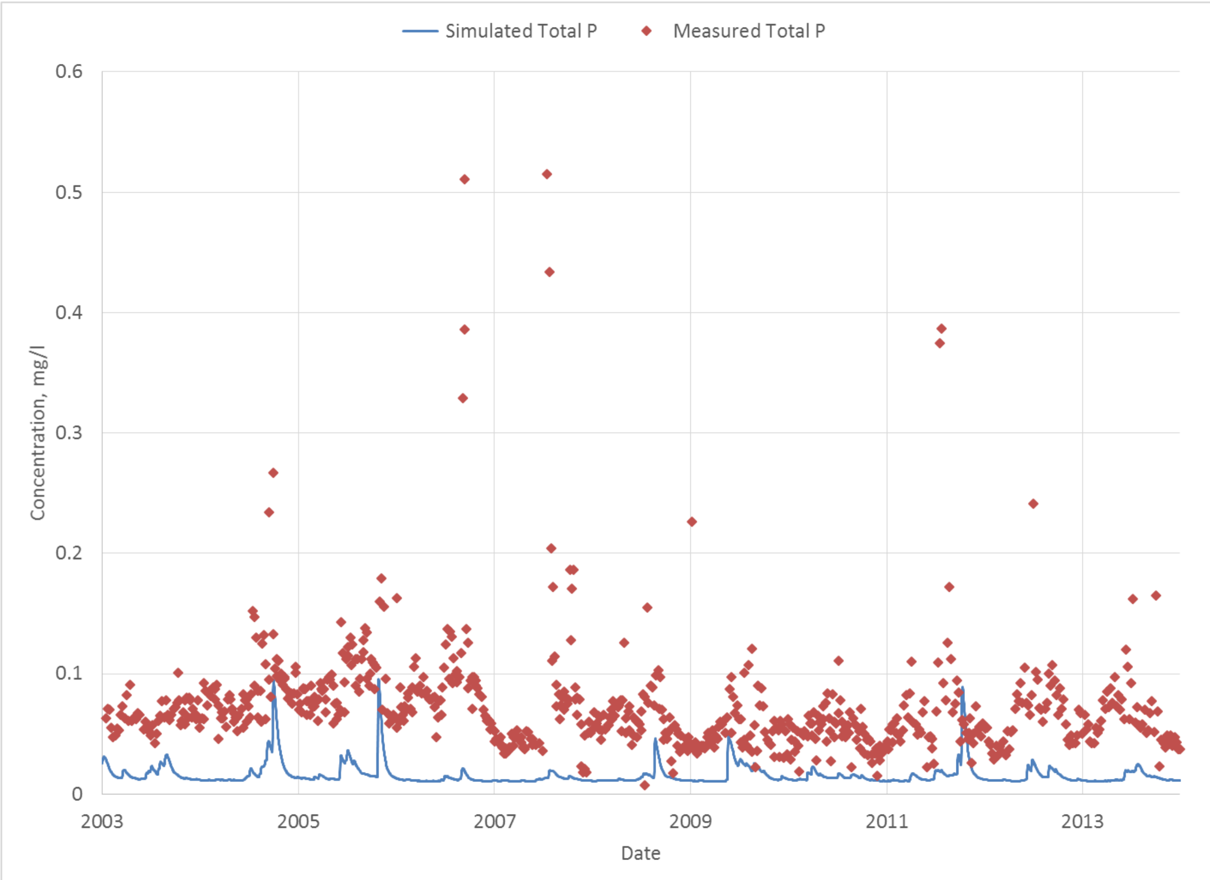


**Figure 50. Comparison of measured and simulated total P at S-65.**

# 5 Appendices

## 5.1 FLUCCS/WAM Land Use ID Correspondence

Table 30 below gives the mapping between FLUCCS codes and the WAM land use ID (LUID). This table is used when importing land use datasets with an associated FLUCCS code. To prepare a land use feature class for use in WAM, a user will add an integer field to the dataset for the WAM LUID. The feature class will then be joined to Table 30 based on the FLUCCS code, and the field calculator will be used in ArcMap to fill in values for the newly added LUID field. The joined table should then be removed before use in WAM.

**Table 30. FLUCCS codes and descriptions and associated WAM land use IDs.**

| FLUCCS | FLUCCS Description | LUID |
|---|---|---|
| **1000** | Residential | 2 |
| **1009** | RV Parks | 2 |
| **1100** | Low Density Residential, Fixed Single Family Units | 2 |
| **1110** | Low Density Residential, Fixed Single Family Units | 2 |
| **1120** | Low Density Residential, Mobile Home Units | 2 |
| **1130** | Low Density Residential, Mixed Units (Fixed and Mobile) | 2 |
| **1140** | Ranchettes - Fixed Single Units | 71 |
| **1150** | Ranchettes - Mobile Units | 71 |
| **1160** | Ranchettes - Mixed Units | 71 |
| **1180** | Low Density Residential, Under Construction | 2 |
| **1190** | Low Density Residential, Under Construction | 2 |
| **1200** | Medium Density Residential, Fixed Single Family Units | 19 |
| **1210** | Medium Density Residential, Fixed Single Family Units | 19 |
| **1220** | Medium Density Residential, Mobile Home Units | 19 |
| **1230** | Medium Density Residential, Mixed Units (Fixed and Mobile) | 19 |
| **1290** | Medium Density Residential, Under Construction | 19 |
| **1300** | High Density Residential | 20 |
| **1310** | High Density Residential, Fixed Single Family Units | 20 |
| **1320** | High Density Residential, Mobile Home Units | 20 |
| **1330** | High Density Residential, Multiple Dwelling Units (Low Rise) | 21 |
| **1340** | High Density Residential, Multiple Dwelling Units (High Rise) | 21 |
| **1350** | High Density Residential, Mixed Units (Fixed and Mobile | 20 |
| **1370** | High Density Residential, Mixed Units (Fixed and Mobile | 20 |
| **1390** | Medium Density Residential, Under Construction | 20 |
| **1400** | Commercial and Services | 3 |
| **1410** | Retail Sales and Services | 3 |
| **1411** | Shopping Centers (Plazas, Malls) | 3 |
| **1420** | Wholesale Sales and Services | 3 |
| **1423** | Junk Yards | 3 |
| **1424** | Farmers Markets | 3 |

| | | |
|---|---|---|
| **1430** | Professional Services | 3 |
| **1440** | Cultural and Entertainment | 3 |
| **1443** | Open Air Theaters | 3 |
| **1450** | Tourist Services | 3 |
| **1452** | Motels | 21 |
| **1453** | Travel Trailer Parks | 21 |
| **1454** | Campgrounds | 7 |
| **1460** | Oil and Gas Storage | 3 |
| **1470** | Mixed Commercial and Services | 3 |
| **1480** | Cemeteries | 23 |
| **1490** | Commercial and Services Under Construction | 3 |
| **1500** | Industrial | 22 |
| **1510** | Industrial | 22 |
| **1513** | Seafood Processing | 22 |
| **1514** | Meat Packaging Facilities | 22 |
| **1515** | Poultry and Egg Processing | 22 |
| **1516** | Grains and Legumes Processing | 22 |
| **1520** | Timber Processing | 22 |
| **1521** | Sawmills | 22 |
| **1522** | Plywood and Veneer Mills | 22 |
| **1523** | Pulp and Paper Mills | 22 |
| **1524** | Pole Peeler and Treatment Plants | 22 |
| **1526** | Log Home Prefabrication | 22 |
| **1527** | Woodyards | 22 |
| **1530** | Mineral Processing | 22 |
| **1532** | Phosphate Processing | 75 |
| **1533** | Limerock Processing | 22 |
| **1535** | Heavy Minerals Processing | 22 |
| **1540** | Oil and Gas Processing | 22 |
| **1542** | Jet Fuel Processing | 22 |
| **1544** | Liquefied Gases Processing | 22 |
| **1545** | Asphalt Processing | 22 |
| **1550** | Other Light Industrial | 22 |
| **1551** | Boat Building and Repair | 22 |
| **1552** | Electronics Industry | 22 |
| **1554** | Aircraft Building and Repair | 22 |
| **1555** | Container Manufacturer | 22 |
| **1556** | Mobile Home Manufacturers | 22 |
| **1560** | Other Heavy Industrial | 22 |
| **1561** | Ship Building and Repair | 22 |
| **1562** | Pre-stressed Concrete Plants | 22 |

| | | |
|---|---|---|
| **1563** | Metal Fabrication Plants | 22 |
| **1564** | Cement Plants | 22 |
| **1565** | Other Heavy Industrial | 22 |
| **1570** | Other Heavy Industrial | 22 |
| **1590** | Industrial, Under Construction | 22 |
| **1600** | Extractive | 73 |
| **1610** | Strip Mines | 73 |
| **1611** | Clay Mines | 73 |
| **1612** | Peat Mine | 17 |
| **1613** | Heavy Minerals Mine | 73 |
| **1614** | Phosphate Mines | 74 |
| **1620** | Sand and Gravel Pits | 73 |
| **1630** | Rock Quarries | 73 |
| **1631** | Limerock Quarries | 73 |
| **1632** | Dolomite Quarries | 73 |
| **1633** | Phosphate Quarries | 74 |
| **1634** | Heavy Mineral Mines | 73 |
| **1640** | Oil and gas fields | 73 |
| **1650** | Reclaimed Land (Extractives) | 5 |
| **1660** | Holding Ponds (Extractives) | 73 |
| **1670** | Inactive Strip Mines | 73 |
| **1700** | Educational Facilities | 3 |
| **1710** | Educational Facilities | 3 |
| **1720** | Religious Facilities | 3 |
| **1730** | Military | 3 |
| **1736** | National Guard Installations | 3 |
| **1740** | Medical and Health Care | 3 |
| **1741** | Hospitals | 3 |
| **1742** | Nursing Homes and/or Convalescent Centers | 21 |
| **1750** | Governmental | 3 |
| **1751** | Governmental - Wastewater Treatment Plant | 3 |
| **1756** | Maintenance Yards | 3 |
| **1758** | SRWMD Conservation Lands | 5 |
| **1759** | Other Public Conservation Lands | 5 |
| **1760** | Correctional Facilities | 72 |
| **1761** | State Prisons | 72 |
| **1763** | Correctional Facilities | 72 |
| **1765** | Municipal Prisons | 72 |
| **1770** | Other Institutional Facilities | 3 |
| **1771** | Private Conservation Lands | 5 |
| **1800** | Recreation | 3 |

| | | |
|---|---|---|
| **1810** | Swimming Beach | 3 |
| **1820** | Golf Courses | 23 |
| **1830** | Race Tracks | 24 |
| **1831** | Automobile Race Tracks | 3 |
| **1832** | Horse Race Tracks | 24 |
| **1833** | Dog Race Tracks | 24 |
| **1840** | Marinas and Fish Camps | 3 |
| **1841** | Marinas and Fish Camps - Wild Game | 5 |
| **1850** | Golf Courses | 23 |
| **1851** | City Parks | 23 |
| **1852** | Zoos | 29 |
| **1860** | Community Recreational Facilities | 3 |
| **1870** | Stadiums | 3 |
| **1880** | Historical Sites | 3 |
| **1890** | Other Recreational Facilities | 3 |
| **1900** | Undeveloped Land | 70 |
| **1910** | Undeveloped Land Within Urban Areas | 70 |
| **1920** | Inactive Land With Street Pattern but Without Structure | 70 |
| **1923** | Inactive Development Land - Nonforested | 70 |
| **1924** | Inactive Development Land - Forested | 70 |
| **1930** | Urban Land in Transition | 70 |
| **1940** | Other Open Land | 70 |
| **2100** | Pastures and Fields | 4 |
| **2110** | Improved Pasture | 26 |
| **2111** | Intensive Pasture | 85 |
| **2120** | Unimproved Pasture | 27 |
| **2130** | Woodland Pasture | 28 |
| **2140** | Row Crops | 25 |
| **2141** | Field Corn | 69 |
| **2142** | Tomatoes | 63 |
| **2143** | Potatoes | 60 |
| **2144** | Carrots, Greens & Mixed Vegetables | 50 |
| **2149** | Cabbage | 61 |
| **2150** | Field Crops | 62 |
| **2151** | Field Crops Spray Field | 86 |
| **2156** | Sugar Cane | 68 |
| **2160** | Mixed Crops | 60 |
| **2200** | Tree Crops | 84 |
| **2210** | Citrus Grove | 84 |
| **2220** | Fruit Orchards | 30 |
| **2221** | Peach Orchards | 30 |

| | | |
|---|---|---|
| **2224** | Blueberries | 31 |
| **2230** | Other Groves | 30 |
| **2231** | Pecan Groves | 30 |
| **2240** | Abandoned Tree Crops | 30 |
| **2300** | Feeding Operations | 32 |
| **2310** | Cattle Feeding Operations | 32 |
| **2320** | Poultry Feeding Operations | 33 |
| **2330** | Swine Feeding Operations | 34 |
| **2400** | Nurseries and Vineyards | 35 |
| **2410** | Tree Nurseries | 35 |
| **2420** | Sod Farms | 36 |
| **2430** | Ornamentals | 37 |
| **2450** | Floriculture | 35 |
| **2500** | Specialty Farms | 39 |
| **2510** | Horse Farms | 38 |
| **2520** | Dairies | 39 |
| **2521** | Dairy Waste Pond | 9 |
| **2522** | Dairy High Intensity Area - Untreated | 87 |
| **2523** | Dairy High Intensity Area - Treated | 88 |
| **2524** | Dairy Boundary Pastures | 90 |
| **2525** | Abandoned Dairies | 89 |
| **2530** | Kennels | 40 |
| **2540** | Aquaculture | 41 |
| **2549** | Aquaculture | 41 |
| **2550** | Tropical Fish Farms | 41 |
| **2590** | Other Specialty Farms | 25 |
| **2600** | Old Field | 5 |
| **2610** | Old Field | 5 |
| **2620** | Old Field | 5 |
| **3100** | Herbaceous | 5 |
| **3200** | Prairies | 5 |
| **3210** | Palmetto Prairies | 5 |
| **3220** | Coastal Scrub | 5 |
| **3230** | Other Shrubs and Brush | 5 |
| **3290** | Other Shrubs and Brush | 5 |
| **3300** | Other Shrubs and Brush | 5 |
| **3430** | Other Shrubs | 5 |
| **4100** | Upland Coniferous Forests | 5 |
| **4110** | Pine Flatwoods | 5 |
| **4119** | Pine Flatwoods - Melaleuca Infested | 7 |
| **4120** | Longleaf Pine - Xeric Oak | 7 |

| | | |
|---|---|---|
| **4130** | Sand Pine | 5 |
| **4140** | Pine - Mesic Oak | 7 |
| **4190** | Other Pines | 8 |
| **4200** | Upland Hardwood Forest | 7 |
| **4210** | Xeric Oak | 6 |
| **4220** | Brazilian Pepper | 7 |
| **4230** | Oak - Pine - Hickory | 7 |
| **4240** | Melaleuca | 7 |
| **4250** | Temperate Hardwoods | 6 |
| **4270** | Live Oak | 6 |
| **4271** | Live Oak | 6 |
| **4280** | Cabbage Palm | 7 |
| **4290** | Cabbage Palm - Melaleuca Infested | 7 |
| **4310** | Beech - Magnolia | 6 |
| **4320** | Sand Live Oak | 5 |
| **4330** | Western Everglades Hardwoods | 7 |
| **4340** | Hardwood - Conifer Mixed | 7 |
| **4350** | Dead trees | 7 |
| **4370** | Australian Pine | 8 |
| **4380** | Other Hardwoods | 7 |
| **4390** | Other Hardwoods | 7 |
| **4400** | Coniferous Plantations | 8 |
| **4410** | Coniferous Plantations | 8 |
| **4411** | Sand Pine Plantations | 8 |
| **4412** | Christmas Tree Plantations | 8 |
| **4420** | Tree Plantations | 8 |
| **4430** | Forest Regeneration Areas | 8 |
| **5100** | Streams and Waterways | 9 |
| **5110** | Natural River, Stream, Waterway | 9 |
| **5120** | Streams and Waterways | 9 |
| **5200** | Lakes | 9 |
| **5210** | Lakes larger than 500 acres | 9 |
| **5220** | Lakes larger than 100 acres but less than 500 acres | 9 |
| **5230** | Lakes larger than 10 acres but less than 100 acres | 9 |
| **5240** | Lakes less than 10 acres | 9 |
| **5250** | Marshy Lakes | 9 |
| **5300** | Reservoirs | 9 |
| **5310** | Reservoirs larger than 500 acres | 9 |
| **5320** | Reservoirs larger than 100 acres but less than 500 acre | 9 |
| **5330** | Reservoirs larger than 10 acres but less than 100 acres | 9 |
| **5340** | Reservoirs less than 100 acres | 9 |

| | | |
|---|---|---|
| **5400** | Bays and Swamps | 9 |
| **5410** | Embayments Opening Directly into the Gulf or the Atlantic | 9 |
| **5420** | Embayments Not Opening Directly into the Gulf or the Atlantic | 9 |
| **5430** | Enclosed salt water ponds within salt marsh | 9 |
| **5500** | Major Springs | 9 |
| **5600** | Slough Waters | 9 |
| **5710** | Atlantic Ocean | 9 |
| **6000** | Wetlands | 16 |
| **6100** | Mixed Wetland Hardwoods | 12 |
| **6110** | Bay Swamps | 10 |
| **6111** | Bay Swamps - Bayhead | 10 |
| **6120** | Mangrove Swamps | 10 |
| **6121** | Black Mangrove | 10 |
| **6130** | Gum Swamps | 10 |
| **6140** | Shrub Swamps | 10 |
| **6150** | Stream and Lake Swamps (Bottomland) | 15 |
| **6160** | Inland Ponds and Sloughs | 15 |
| **6170** | Mixed Wetland Hardwoods | 12 |
| **6171** | Mixed Wetland Hardwoods - Willows | 12 |
| **6172** | Mixed Wetland Hardwoods - Mixed Shrubs | 12 |
| **6180** | Cabbage Palm Savannah | 12 |
| **6181** | Cabbage Palm Hammock | 12 |
| **6191** | Wet Melaleuca | 12 |
| **6200** | Wetland Coniferous Forest | 15 |
| **6210** | Cypress | 14 |
| **6215** | Cypress | 14 |
| **6216** | Cypress | 14 |
| **6218** | Cypress - melaleuca infested | 14 |
| **6219** | Cypress - with wet prairies | 14 |
| **6220** | Wet Flatwoods | 15 |
| **6230** | Atlantic White Cedar | 15 |
| **6240** | Cypress - Pine - Cabbage Palm | 15 |
| **6250** | Wetland Coniferous Forest | 15 |
| **6300** | Wetland Forested Mixed | 15 |
| **6310** | Hydric Hammock | 15 |
| **6320** | Tidal Swamp | 15 |
| **6400** | Vegetated Non-Forested Wetlands | 16 |
| **6410** | Freshwater Marshes | 16 |
| **6411** | Freshwater Marshes - Sawgrass | 16 |
| **6412** | Freshwater Marshes - Cattail | 16 |
| **6420** | Saltwater Marshes | 10 |

| | | |
|---|---|---|
| **6430** | Wet Prairies | 16 |
| **6439** | Wet Prairies - with Pine | 16 |
| **6440** | Emergent Aquatic Vegetation | 16 |
| **6450** | Submergent Aquatic Vegetation | 16 |
| **6460** | Emergent Aquatic Vegetation | 16 |
| **6500** | Non Vegetated Wetlands | 42 |
| **6510** | Salt Barrens | 42 |
| **6520** | Intertidal Areas | 17 |
| **6530** | Inland Shores/Ephemeral Ponds | 17 |
| **6540** | Oyster Bars | 42 |
| **6600** | Cut-over Wetlands | 15 |
| **7100** | Beaches | 17 |
| **7200** | Sand Other Than Beaches | 17 |
| **7340** | Exposed Rocks | 17 |
| **7400** | Barren Land | 17 |
| **7410** | Rural Land in Transition | 4 |
| **7420** | Borrow Areas | 17 |
| **7430** | Spoil Areas | 17 |
| **7440** | Fill Areas | 17 |
| **7450** | Burned Areas | 17 |
| **7470** | Dikes and Levees | 17 |
| **8000** | Transportation, Communications and Utilities | 3 |
| **8100** | Transportation | 18 |
| **8110** | Airports | 3 |
| **8111** | Commercial Airports | 3 |
| **8112** | General Aviation Airports | 3 |
| **8113** | Private Airports | 3 |
| **8115** | Airports | 3 |
| **8120** | Railroads | 3 |
| **8130** | Bus and Truck Terminals | 3 |
| **8132** | Bus (Government, School, City Service) | 3 |
| **8133** | Truck Terminals | 3 |
| **8140** | Limited Access Roads (Interstate System) | 18 |
| **8141** | Limited Access Roads (Interstate System) | 18 |
| **8142** | Divided Highways (Federal - State) | 18 |
| **8143** | Two-Lane Highways (State) | 18 |
| **8147** | Transportation Corridors | 18 |
| **8150** | Port Facilities | 3 |
| **8160** | Canals and Locks | 3 |
| **8170** | Oil, Water or Gas Long Distance Transmission Lines | 5 |
| **8180** | Auto Parking Facilities | 3 |

| | | |
|---|---|---|
| **8200** | Communications | 3 |
| **8213** | Transmission Towers | 5 |
| **8220** | Communication Facilities | 22 |
| **8300** | Utilities | 22 |
| **8310** | Electrical Power Facilities | 22 |
| **8311** | Thermal Electrical Power Facilities | 22 |
| **8312** | Gas Turbine Electrical Power Plants | 22 |
| **8315** | Sub-station Electrical Power Facilities | 3 |
| **8320** | Electrical Power Transmission Lines | 5 |
| **8330** | Water Supply Plants | 22 |
| **8340** | Sewage Treatment | 43 |
| **8341** | Sewage Treatment Plants | 43 |
| **8349** | Sewage Treatment | 43 |
| **8350** | Solid Waste Disposal Facilities | 44 |
| **8370** | Surface Water Collection Basin | 9 |
| **9520** | Inactive Dairies | 89 |

# 6 References

Bottcher, A.B., N.B. Pickering, and A.B. Cooper, 1998. EAAMOD-FIELD: A flow and phosphorus model for high water tables. In Proc. 7th Annual Drainage Symposium, 599-606. St. Joseph, Mich.: ASAE.

Bottcher, A.B., B.J. Whiteley, James, A.I., and J.G. Hiscock, 2012. Watershed Assessment Model (WAM): Model use, calibration and validation. Transactions of ASABE 55(4): 1367-1383.

Earth Tech, 2006, Kissimmee Basin Hydrologic Assessment, Modeling, and Operations Planning Study Alternative Formulation/Evaluation Tool Development Technical Design Document, prepared for SFWMD.

Jensen, M.E., R.D. Burman, and R.G. Allen, 1990. Evapotranspiration and Irrigation Water Requirements. ASCE Manuals and Reports on Engineering Practice No. 70, Am. Soc. Civil Engr., New York, NY. 332 p.

Knisel, W.G. (Ed), 1993. GLEAMS: Groundwater Loading Effects of Agricultural Management Systems. Univ. of Georgia, Coastal Plain Expt. Sta, Bio. and Agri. Engr. Dept., Publ. No. 5.

Leonard, R. A., W.G. Knisel, and D. A. Still, 1987. GLEAMS: Groundwater Loading Effects of Agricultural Management Systems. Transactions of the ASAE, 30(5).

SFWMD, FDEP and FDACS, 2014. Chapter 8: Lake Okeechobee Watershed Protection Program Annual and Three-Year Update. 126p.

Soil and Water Engineering Technology, Inc., 2008. EAAMOD Technical and User Manuals. Final Reports to the Everglades Research and Education Center, University of Florida, Belle Glade, FL. Also available from www.swet.com.